Quantification and Prediction of Human Fetal (-)-Δ^9-tetrahydrocannabinol (THC)/11-OH-THC Exposure to Inform Neurodevelopmental Toxicity of Cannabis

Aditya R. Kumar

A dissertation

submitted in partial fulfillment of the

requirements for the degree of

Doctor of Philosophy

University of Washington

2023

Reading Committee:

Jashvant D. Unadkat, Chair

Kenneth E. Thummel

Allan E. Rettie

Program Authorized to Offer Degree:

Pharmaceutics

University of Washington

Abstract

Quantification and Prediction of Human Fetal (-)-Δ^9-tetrahydrocannabinol (THC)/11-OH-THC Exposure to Inform Fetal Toxicity of Cannabis

Aditya R. Kumar

Chair of the Supervisory Committee:

Jashvant D. Unadkat

Department of Pharmaceutics

Prenatal cannabis use is associated with various detrimental outcomes in the offspring, the foremost being neurodevelopmental toxicity[1-5]. Δ^9-tetrahydrocannabinol (THC) is the most abundant psychoactive compound in cannabis and is thought to be the cause of this toxicity. THC's primary *in vivo* psychoactive metabolite, 11-OH-THC, may also contribute to this toxicity[6]. It is unethical to conduct a randomized clinical trial to determine if these cannabinoids are the causative factors in producing neurodevelopmental toxicity from prenatal cannabis use. An alternative approach is to conduct preclinical fetal cannabis toxicity studies *in vivo* in animals or *in vitro* at THC/11-OH-THC concentrations that mimic human fetal THC/11-OH-THC exposure. To determine the latter, we quantified the fetal circulation and tissue cannabinoid exposure across gestation. Since these determinations provide cannabinoid exposure at only a given time, we also developed a maternal-fetal physiologically based pharmacokinetic (m-f-PBPK) model to predict the time-dependent fetal THC/11-OH-THC exposure after chronic inhalation or oral THC consumption at various gestational ages.

To accomplish the above goals, we first determined all the potential mechanisms of clearance and distribution that can affect THC/11-OH-THC fetal exposure. In Chapter 2[7], we incubated 500 nM THC and 50 nM 11-OH-THC in adult human intestine, lung, placenta, and in fetal liver microsomes with selective inhibitors for CYP (1A, 2C19, 2C9, 2D6, 3A), UGT (1A9, 2B7), and/or FMO enzymes to identify the drug metabolizing enzymes responsible for depletion of the cannabinoids. While there was no significant depletion of either cannabinoid in the human lung or placenta, in the intestine THC was significantly metabolized by CYP2C9 (89%) and CYP3A (11%) while 11-OH-THC was significantly metabolized by CYP3A (51%) and UGT2B7 (25%). In the fetal liver, both compounds were nearly completely metabolized by CYP3A7. The presence of intestinal and fetal liver metabolism, respectively, will impact bioavailability after oral THC administration and fetal exposure, relative to the maternal exposure.

Next, in Chapter 3[8], we determined the mechanism and quantified the extent of transplacental transfer of THC and its metabolites. To do so, we perfused THC alone (5 μM) or in combination (100 – 250 nM) with its metabolites (100 nM or 250 nM 11-OH-THC, 100 nM COOH-THC) in an *ex vivo* dual cotyledon, dual perfusion, term human placenta model. While 11-OH-THC and COOH-THC appeared to passively diffuse across the placenta, 5 μM THC had a significantly lower maternal-fetal vs fetal-maternal clearance, suggesting that THC is actively transported, in the fetal-maternal direction, at the placental barrier. When a P-gp/BCRP inhibitor (4 μM valspodar) was added to the perfusion, the difference in clearance remained, suggesting that THC was transported by an unknown apical efflux or basal influx transporter(s) in the syncytiotrophoblast membrane.

The estimated human fetal microsomal metabolism (Chapter 2) and the passive diffusion/active transport kinetics of THC (Chapter 3), which both reduce fetal cannabinoid exposure, were inputted in our m-f-PBPK model to predict fetal plasma and brain cannabinoid concentrations in trimester 1 (T1), 2 (T2), and 3 (T3) (Chapter 4). These predictions aligned well with the corresponding values observed *in vivo*, i.e. our model is considered verified. For

example, the predicted umbilical venous plasma (UVP)/maternal plasma (MP) at gestational week (GW) 38 and fetal brain/MP at GW15, 0.26 and 0.56 respectively, were similar to the observed values *in vivo*, 0.33 (38 %CV) and 0.39 (63 %CV) respectively.

Then, we used our m-f-PBPK model to predict the steady-state total and unbound fetal brain and plasma THC/11-OH-THC concentrations across gestational age. The maximum ($C_{max,ss}$) and average ($C_{ss,avg}$) steady concentrations in the UVP and fetal brain of both THC and 11-OH-THC were highest at the earliest GW tested, 15 weeks. For example, at GW15, after a typical daily dose of THC consumed by inhalation (100 mg), the predicted fetal brain $C_{ss,avg}$ of THC and 11-OH-THC was 37 and 70 nM, respectively. After a typical daily oral consumption of 10 mg THC, the predicted $C_{ss,avg}$ of THC and 11-OH-THC in the fetal brain was lower, 0.73 and 8.9 nM, respectively. The corresponding unbound fetal brain $C_{ss,avg,u}$ was predicted to be even lower due to extensive THC binding in the brain. Our verified m-f-PBPK model can be used to predict these fetal brain concentrations for any dose, route or frequency of consumption.

We propose that future fetal toxicity studies (*in vitro* or *in vivo* in animals) should be conducted to replicate the predicted unbound fetal UVP and fetal brain THC/11-OH-THC concentrations at the typical doses consumed by pregnant people. Such preclinical studies will provide a better understanding of the potential of THC/11-OH-THC to produce neurotoxicity in the offspring as a result of prenatal cannabis use.

Acknowledgments

First and foremost, I extend my deepest gratitude to Jashvant Unadkat for his unwavering support throughout my journey in graduate school. Your encouragement empowered me to take the lead on my project, providing the freedom to shape its direction. I am truly grateful for your trust in me and the continuous motivation to strive for perfection. Your mentorship has been invaluable, and I've learned a great deal from you through this process.

A sincere thank you to my committee members: Kenneth Thummel, Allan Rettie, Nina Isoherranen, Gabriela Patilea-Vrana, Steve White, and Qingcheng Mao. Thank you for all of your guidance and advice in my dissertation and in my career. The challenges you presented ultimately contributed to a more impactful and compelling dissertation. To my collaborators, your collective experience and knowledge were indispensable. Without your support, completing this dissertation would not have been possible. Your contributions were crucial to the success of the project.

To the past and present members of the Unadkat lab, I commend you for creating a collaborative and intellectually stimulating environment. Your teamwork facilitated a seamless integration of diverse talents, fostering a space for impactful scientific exploration. To my friends, your laughter and shared memories added immeasurable joy to this journey. Thank you for making the experience more enjoyable.

Lastly, my deepest appreciation goes to my family. To my mom and dad, you have given me more than I could ever ask for. Thank you for wholeheartedly supporting my passions and consistently providing the opportunities and resources I needed to dive headfirst into every new endeavor. To my brother, thank you for being the one whom I could share every experience with, since day one. Your encouragement means the world to me.

Without each and every one of you, none of this would have been possible. Your constant support has shaped me into the scientist and person I am today. Thank you from the bottom of my heart.

Table of Contents

Chapter 1: Introduction

1.1 Specific Aims

Cannabis is used by pregnant people for its medicinal and psychoactive properties[9]. This use is highest during the first trimester (T1)[10]. Fetal exposure to cannabis constituents is widely believed to cause neurodevelopmental toxicity. Indeed, *in vivo* human observational studies have found that prenatal cannabis use is associated with lower cognition (such as short-term memory, IQ, verbal reasoning and quantitative scores) and behavioral issues (such as hyperactivity, impulsivity, delinquency) in children between the ages of 3-14 years old[1-5]. These findings were significant even after correcting for potential confounding factors such as other substance abuse (e.g., tobacco, cocaine), differences in socioeconomic status, and varying consumption of cannabis. Nevertheless, it is impossible to correct for all confounding factors. Conducting a randomized controlled clinical trial in pregnant people of the effect of prenatal cannabis use on neurodevelopmental toxicity is unethical. However, an alternative approach is to conduct preclinical *in vitro* and *in vivo* animal studies with the constituents of cannabis plants, implicated in producing neurodevelopmental toxicity, at their relevant pharmacological concentrations.

Δ^9-Tetrahydrocannabinol (THC) is the most abundant psychoactive compound in cannabis and is thought to be the cause of its neurodevelopmental toxicity[6]. THC's primary psychoactive metabolite, 11-OH-THC, may also contribute[6]. Each of the previous preclinical cannabis toxicity studies on brain development have been conducted *in vitro* at relatively high THC concentrations (2-15 μM)[11,12] and *in vivo* at THC doses higher than typically used by humans[13] as the relevant human fetal brain concentrations are not known. To conduct informative cannabis neurodevelopmental toxicity *in vitro* or *in vivo* animal studies, one must quantify (or predict) the average and maximum concentration of the psychoactive cannabinoids, THC and 11-OH-THC, in the fetal circulation and brain at typical cannabis doses used by pregnant people. Exposing animals to suprapharmacological cannabinoid concentrations can lead to misleading experimental results and thereby result in uninterpretable effects of prenatal

toxicity of cannabis. While fetal brain and umbilical cord blood samples can be obtained at the time of pregnancy termination and delivery, respectively, such opportunistic sampling (**as in Aim 1, Chapter 2**) can only provide a "snapshot" (at a single time-point) of fetal exposure to the cannabinoids. To obtain a complete picture of fetal exposure, multiple samples, over time, from a single pregnant individual must be obtained. Because such sampling is ethically and logistically challenging, here we developed a maternal-fetal physiologically based pharmacokinetic (m-f-PBPK) model to predict maternal and fetal exposure to THC and 11-OH-THC after both inhalation and oral THC consumption (**Aim 3**). To do so, as detailed below in our Aims, such a model must be first populated with all the relevant maternal-fetal clearances (CL) and distribution parameters that determine THC/11-OH-THC fetal exposure (**Aims 1 & 2**). Parenthetically, while COOH-THC, a circulating metabolite of THC, has a long terminal half-life (>40 hours)[14], it is not psychoactive, hence it is not a focus of our investigations.

Since maternal drug exposure drives fetal drug exposure, quantifying the metabolic kinetics of THC/11-OH-THC in the adult liver[15], intestine, and lungs (**Aim 1**) is imperative because cannabis is often consumed by inhalation or orally. Second, the magnitude of placental/fetal liver metabolic CL of the cannabinoids (**Aim 1**) as well as their placental transfer (active and passive) CLs must be determined (**Aim 2**) as these will also determine fetal cannabinoid exposure. As THC is metabolized by recombinant cytochrome P450 (CYP)1A1 and CYP3A[16] it could be metabolized in the placenta and/or fetal liver (**Aim 1**). Additionally, THC could be a substrate of placental P-gp and/or BCRP[17,18] (**Aim 2**). Therefore, the goals of this dissertation are to first accomplish the above aims. Once accomplished, our current m-f-PBPK model can be populated with these THC/11-OH-THC kinetic parameters to predict their fetal exposure at multiple gestational ages (**Aim 3**). Before using, all predictive models must be verified with *in vivo* data to the extent possible. Therefore, we will collect the following samples from pregnant people who have consumed cannabis within 2 days of termination or delivery. For trimester 1 (T1) and trimester 2 (T2), fetal tissue (brain, liver, kidney), placenta and maternal

plasma (MP) will be collected at pregnancy termination. For trimester 3 (T3), umbilical venous plasma (UVP), MP and placenta will be collected at delivery (**Aim 3**). Cannabinoid concentrations (THC, 11-OH-THC, and COOH-THC) will be quantified in the collected samples. Therefore, the specific aims of this dissertation are:

Aim 1 (Chapter 2): Identify the drug metabolizing enzymes and quantify their metabolic kinetics for depleting THC/11-OH-THC in microsomes from human intestines (HIMs), lungs (HLuMs), placentas (HPMs), and fetal livers (HFLMs).

Aim 2 (Chapter 3): Quantify the transplacental transfer of THC/11-OH-THC/COOH-THC by active transport and/or by passive diffusion using the perfused human term placenta model.

Aim 3 (Chapter 4): Using our m-f-PBPK model, predict fetal plasma and tissue THC/11-OH-THC exposure at typical doses, routes and frequency of maternal THC consumption.

1.2 Cannabis Use Statistics

Cannabis (i.e., marijuana, weed, pot, etc.) is a plant that has been used by humans for more than 2500 years for its medicinal and psychoactive properties[9]. Cannabis has been used recreationally for its physiological (e.g., muscle relaxant and appetite stimulant) and psychological (analgesic, anxiolytic, euphoria, etc.) effect. Eighteen percent of all adults and 43% of young adults (19 – 30 years old) in the United States (US) report using cannabis in the past year and 3.9% and 11% report daily cannabis use, respectively[19,20]. Cannabis is primarily consumed orally (e.g., tincture, cookies, brownies, etc.) or by inhalation [e.g., smoking (joints, blunts, bongs, dabs) and vaporizing]. For inhalation use in the US, white users are more likely to use pipes/vaporizers and black users are more likely to use blunts[21]. Young adults (18 – 34 years old) use cannabis predominantly by inhalation (74%) but some use it orally (24%) or topically (2%)[22].

Cannabis is widely used by pregnant individuals; its use was confirmed by quantitative analysis of urine samples in over 22.6% of pregnancies from universal drug screening and use

increased in concordance with an increase in legalization[23]. Pregnant people report using cannabis to mitigate conditions related to pregnancy (e.g., nausea, insomnia, and weight gain) as well as continued use for pre-existing conditions (e.g., pain and anxiety) and for euphoria, stress management, and mental well-being[24]. Both the FDA and EMA recommend discontinuation of any current cannabis use during pregnancy and lactation. Also, they recommend that medical practitioners counsel patients regarding the lack of safety and efficacy data and the potential detrimental effects to the developing fetus/newborn from prenatal cannabis use[25].

The psychological effects of cannabis arise from its constituent THC and its *in vivo* metabolite, 11-OH-THC[6]. In the US, cannabis is legalized for medicinal use in 13 states and fully legalized for both recreational and medicinal use in 23 states and 3 territories[26]. Eight countries have legalized cannabis use for recreational and medicinal use at the federal level: Uruguay, Georgia, South Africa, Canada, Mexico, Malta, Thailand, and Luxembourg. For medicinal use, THC-containing therapies have been approved by the FDA and EMA as an analgesic and antispasmodic for multiple sclerosis, antiemetic for chemotherapy-induced nausea, and orexigenic for AIDS-induced anorexia[27]. Each of these therapies are theorized to be mediated by THC and 11-OH-THC binding to the cannabinoid receptors[28-31].

1.3 Mechanism of Psychoactive Effect of THC/11-OH-THC

To produce their psychoactive effect, THC and 11-OH-THC bind to cannabinoid receptor type 1 (CB1), a G-protein coupled receptor that is part of the endocannabinoid receptor signaling pathway. They also bind to cannabinoid receptor type 2 (CB2) to produce anti-inflammatory and analgesic effects[32-34]. CB1 is located predominantly within the hippocampus, hypothalamus, basal ganglia, cerebellum, frontal cortex, spinal cord and the peripheral nervous system (PNS)[32]. In contrast, CB2 is localized primarily in the immune system (e.g., spleen), glial cells, and hematopoietic stem cells. While both THC and 11-OH-THC have psychoactive

effects, 11-OH-THC has a more potent analgesic and anticonvulsant effect in mice, as assessed by a hot-plate test/acetic acid-induced writhing test and latency of clonic and tonic seizures, respectively[33,35,36]. In humans, 11-OH-THC elicits a larger peak psychological high and a greater change in the Cornell Medical Index questionnaire value, a psychodiagnostics test, for the same dose (1 mg) of either THC or 11-OH-THC administered intravenously (IV)[6]. As detailed below, the effect of cannabis use during pregnancy on fetal development has also been investigated.

1.4 Effect of Prenatal Cannabis Use on Fetal Development

Prenatal cannabis use is associated with neurodevelopmental deficits and growth restriction. An *in vivo* observational study enrolled pregnant individuals and stratified them into four groups: no cannabis use (n=5,540), cannabis use before pregnancy (n=245), cannabis use in early pregnancy (<18 weeks gestation; n=173), and continued cannabis use (n=41). Birth weight and head circumference were measured *in utero* and at the time of birth. Individuals who used cannabis in early pregnancy and those who had continued use had offspring with a lower birth weight compared to non-users. There was no clear trend for change in head circumference[37]. Effect of prenatal cannabis use on birth weight and head circumference has also been investigated in 9 other studies where mixed results were seen. In total, 4 studies showed lower birth weight and head circumference while 6 studies showed no change.[38] As the results were inconsistent, we do not know the true effect of prenatal cannabis on fetal growth outcomes, however the differences could be due to random effects in the study populations. More importantly, effect of prenatal cannabis use on the neurodevelopment of the offspring has been evaluated. Like the previous study, this observational study grouped pregnant individuals into non-users (n=10,834), early-users (n=413), and continued-users (n=242). The offspring were evaluated between 9-11 years of age using the Child Behavior Checklist and the Prodromal Questionnaire–Brief Child Version. Prenatal cannabis use was associated with an

increase in behavioral issues (such as inattention, elevated externalizing, more social and thought problems)[5]. Lastly, another set of studies found that prenatal cannabis is associated with additional behavioral issues (e.g., hyperactivity, impulsivity, delinquency) and lower cognition (e.g., short-term memory, IQ, verbal reasoning and quantitative scores) in children between ages 3-14 years[1-4]. These studies were opportunistic and attempted to correct for potential confounding factors (such as maternal age, BMI, height, education, nationality, parity, gravidity, fetal sex, and maternal psychopathology) between individuals who did and did not use cannabis during pregnancy and other concomitant drug use (e.g., alcohol, tobacco, cocaine). However, it is impossible to parse out the effect of all potential confounders and therefore delineate the effect of prenatal cannabis use on neurodevelopmental toxicity.

An alternative approach to the above observational studies must be pursued to delineate the neurodevelopmental toxicity of cannabis since a randomized controlled study in pregnant people is unethical. Such an approach would be to perform *in vitro* and *in vivo* animal studies that replicate THC and 11-OH-THC concentrations in the fetal circulation and tissues (e.g., the brain) at usual cannabis doses and frequency used prenatally. Fetal plasma and tissue cannabinoid concentrations may be lower than the respective maternal plasma concentrations as the placenta may restrict fetal exposure through active efflux transport (see section 1.5 below). The few studies *in vitro* and *in vivo* in animals that have been conducted have used concentrations that may not be relevant to those observed in adult human plasma (typically <1 μM) or have used doses much greater than those used by adults (typically <100 mg for inhalation and <20 mg for oral consumption). For example, THC stimulates the degradation of microtubule-binding protein in growing axons of cortical tissue at 2 and 10 μM THC[11,12]. In pregnant mice, dosed with 3 mg/kg THC, long-lasting impact on embryonic neurodevelopment such as decreased fine-motor performance and cerebellum axonal growth was observed[12,13]. THC, 5 mg/kg, also inhibits the proliferation and differentiation capacity of neural stem cells in fetal mice, leading to reduced hippocampal development[11]. The hippocampus is a structure,

near the temporal lobe, responsible for long-term memory formation and memory retrieval. Unfortunately, these mouse study designs did not include measurement of the fetal brain concentrations. However, one study reported ~40 nmol/kg (equivalent to nM concentrations if brain tissue density is assumed to be 1 g/mL) in fetal brain 2 hours after 3 mg/kg THC was dosed subcutaneously[39]. Another study reported ~460 nmol/kg in fetal brain 15 minutes after 5 mg/kg was dosed subcutaneously[40]. Lastly, THC inhibits BeWo cell proliferation at 3 – 30 μM THC[41], which is a marker for placental tissue development. Since human fetal brain THC concentrations have never been measured, these concentrations may not be representative of those obtained after a typical dose of prenatal cannabis use. Therefore, human fetal plasma and brain concentrations must be either directly measured or accurately predicted. A limited set of fetal brain and plasma samples can be obtained at pregnancy termination and time of delivery, respectively. However, these limited "snapshot" samples at only a few time points, cannot provide an accurate measure of fetal drug exposure. **Specific Aim 3** (**Chapter 4**) will address this gap in knowledge where we will predict, using our m-f-PBPK model, fetal tissue exposure to these cannabinoids. To do so, in the narrative below, we describe the pharmacokinetic parameters of cannabinoids that must be quantified and populated into our m-f-PBPK model.

1.5 Factors that Determine Fetal Cannabis Exposure

Unbound THC/11-OH-THC fetal circulating plasma concentration ($C_{avg,ss,f,u}$) is driven by the unbound maternal steady-state plasma concentration ($C_{avg,ss,m,u}$) and multiple clearance pathways (Figure 1.1): 1) unbound (or intrinsic) placental passive diffusion clearance (CL_{PD}); 2) unbound active placental apical efflux (CL_{PM}) and influx (CL_{MP}) clearance; 3) unbound active placental basal efflux (CL_{PF}) and influx (CL_{FP}) clearance; 4) unbound placental metabolic clearance (CL_{p0}); and 5) unbound fetal metabolic clearance (CL_{f0}) (Eq. 1). The $C_{avg,ss,f,u}$ can also be expressed relative to the $C_{avg,ss,m,u}$ known as $K_{p,uu}$ (Eq. 2). Assuming linear kinetics, $K_{p,uu}$ is also equivalent to the ratio of unbound fetal to maternal area under the plasma concentration-

time curve to infinity ($AUC_{inf,u}$). The total fetal steady-state circulating plasma concentration ($C_{avg,ss,f}$) is the ratio of the $C_{avg,ss,f,u}$ and the protein binding in the fetal plasma ($f_{u,p,fetus}$) (Eq. 3).

$$C_{avg,ss,f,u} = C_{avg.ss.m.u} * \frac{(CL_{MP}+CL_{PD})*(CL_{PF}+CL_{PD})}{(CL_{FP}+CL_{PD}+CL_{f0})*(2CL_{PD}+CL_{PM}+CL_{PF}+CL_{p0})-(CL_{FP}+CL_{PD})*(CL_{PF}+CL_{PD})} \quad \text{(Eq. 1)}$$

$$K_{p,uu} = \frac{C_{avg,ss,f,u}}{C_{avg.ss.m.u}} = \frac{AUC_{inf,f,u}}{AUC_{inf,m,u}} = \frac{(CL_{MP}+C_{PD})*(CL_{PF}+CL_{PD})}{(CL_{FP}+CL_{PD}+CL_{f0})*(2CL_{PD}+CL_{PM}+CL_{PF}+C_{p0})-(CL_{FP}+C_{PD})*(CL_{PF}+CL_{PD})}$$

(Eq. 2)

$$C_{avg,ss,f} = \frac{C_{avg.ss.f,u}}{f_{u,p,fetus}} \quad \text{(Eq. 3)}$$

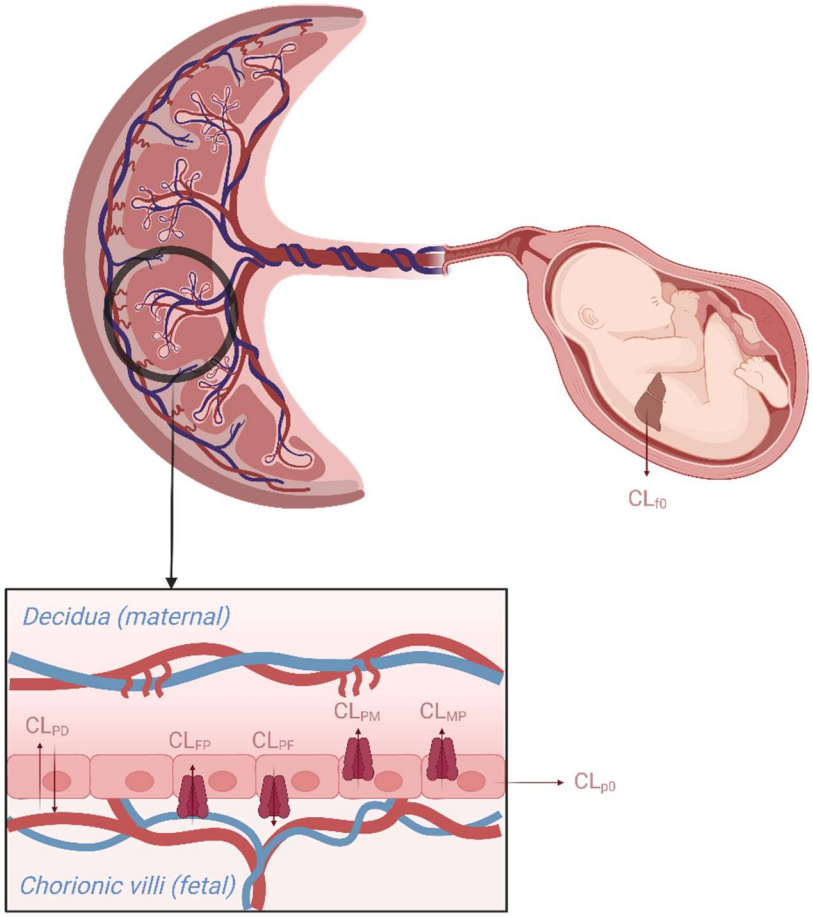

Figure 1.1: Fetal plasma concentration is driven by multiple clearance pathways in addition to the maternal plasma concentration. Unbound (or intrinsic) placental passive diffusion clearance (CL_{PD}) transfers drug across the syncytiotrophoblast layer. Unbound placental metabolic clearance (CL_{p0}), unbound fetal metabolic clearance (CL_{f0}), and unbound active placental apical efflux (CL_{PM}) and basal influx (CL_{FP}) clearance can reduce fetal plasma concentrations. While unbound active placental apical influx (CL_{MP}) and basal efflux (CL_{PF}) clearance can increase fetal plasma concentrations.

Based on the above equations, active placental transport CL (mediated by CL_{PM} or CL_{FP}) could result in $K_{p,uu}$ and K_p of <1. Indeed, such a possibility is suggested by studies in macaques where the total THC fetal plasma AUC was reduced in comparison to maternal plasma AUC

(Figure 1.2[42]). Three near term (gestational days 146-151) rhesus macaques were administered 0.3 mg/kg THC intravenously (IV) and blood was simultaneously sampled from the uterine vein and intraplacental artery cannula to represent maternal and fetal circulating blood/plasma concentrations, respectively. Plasma was sampled for 96 hours but was quantifiable in fetal plasma up to only 3 hours. THC fetal/maternal plasma AUC_{inf} ratio was 0.30 ± 0.17. This reduction in fetal THC exposure (relative to maternal exposure) has also been seen in humans[43]. After daily cannabis consumption by inhalation, data from three maternal-fetal pairs showed that the fetal THC and COOH-THC plasma concentration at a single timepoint were 0.26 ± 0.10 and 0.24 ± 0.15 of their corresponding maternal concentration, respectively. Similarly, in rats given THC by vapor inhalation, at 15 minutes and 6 hours after dosing, not only plasma but also fetal brain THC and 11-OH-THC concentrations were less than that in the corresponding maternal plasma, with a fetal brain/MP of ~0.3 and 3, respectively[40]. Since THC exhibits a fetal/maternal plasma $K_p < 1$[42,43], it is likely that THC is actively transported across the syncytiotrophoblast membrane in the placenta through CL_{PM} or CL_{FP} or extensively metabolized in the placenta and/or fetus. If the placental transport is due only to CL_{PM} or CL_{FP}, the $C_{avg,ss,f,u}$ can be simplified to Eq. 4 and 5, respectively.

$$C_{avg,ss,f,u} = C_{avg.ss.m.u} * \frac{CL_{PD}}{CL_{PD}+C_{PM}+CL_{p0}+2CL_{f0}+CL_{f0}*\frac{(CL_{PM}+CL_{p0})}{CL_{PD}}} \quad \text{(Eq. 4)}$$

$$C_{avg,ss,f,u} = C_{avg.ss.m.u} * \frac{CL_{PD}}{CL_{PD}+CL_{FP}+C_{p0}+2CL_{f0}+CL_{p0}*\frac{(CL_{FP}+CL_{f0})}{CL_{PD}}} \quad \text{(Eq. 5)}$$

If THC is effluxed by the human placenta, its CL_{PM} could be mediated by efflux transporters at the apical membrane of the syncytiotrophoblast (e.g., P-glycoprotein (P-gp), breast cancer resistance protein (BCRP), multidrug resistance protein 2 (MRP2), MRP4). Alternatively, THC could be transported into the placenta (CL_{FP}) by influx transporters at the respective basal membrane (e.g., organic anion transporting polypeptide 2B1 (OATP2B1), organic cation transporter 3 (OCT3), organic anion transporter 4 (OAT4), OATP1A2,

OATP1B1). Whether THC or 11-OH-THC is a substrate of any of these transporters (e.g., P-gp and BCRP) is discussed in section 1.8.

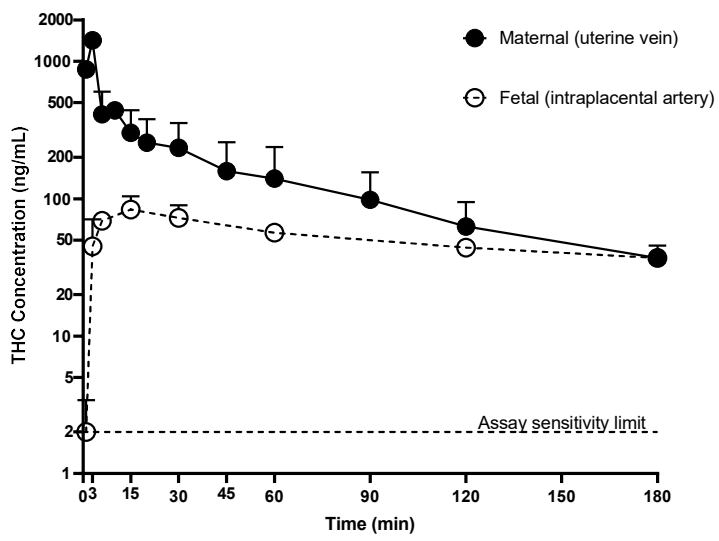

Figure 1.2: THC concentrations are lower in fetal vs. maternal circulation after 0.3 mg/kg THC dosed intravenously (IV) to three late-term rhesus macaques. Maternal plasma concentrations (solid circle and line) and fetal plasma concentrations (open circles and dashed line) were sampled from the uterine vein and the intraplacental artery, respectively. Maternal plasma concentration was also quantified at a 24-hour timepoint (data not shown). All concentrations are shown as mean ± SE. The data were digitized from Bailey 1987[42] and replotted here.

To understand how fetal exposure changes relative to maternal exposure, one must quantify the placenta and fetal liver metabolism and the placental passive diffusion and active transport. Placenta and fetal liver metabolism of THC/11-OH-THC was evaluated in **Aim 1** (**Chapter 2**) by incubating THC and 11-OH-THC in T1, T2 and term human placental microsomes (HPM) and T2 human fetal liver microsomes (HFLM; first trimester livers are too small to make microsomes). Placenta passive diffusion and active transport was evaluated in **Aim 2** (**Chapter 3**) by perfusing THC and 11-OH-THC in human term placentas (early gestation placentas cannot be perfused). As detailed below, to predict absolute fetal plasma/tissue concentrations one must first accurately predict plasma concentrations after inhalation and oral cannabis consumption in both the non-pregnant and pregnant individuals.

1.6 Factors that Determine THC and 11-OH-THC Exposure in the Healthy Non-pregnant Population

THC is a neutral, highly lipophilic molecule at physiological pH with an alcohol and ether group, an acid dissociation constant (pKa) of 10.6, and an octanol-water partition coefficient (logP) of 6.97[44] (Table 1.1; Figure 1.3). 11-OH-THC is also neutral molecule at physiological pH with two alcohols and one ether group, a pKa of 9.34, and a logP of 5.33[44]. Lastly, the major circulating metabolite, COOH-THC is an acidic molecule with one carboxyl, alcohol, and ether group, a pKa of 4.02, and an octanol-water partition coefficient (logD) of 3.07 at pH=7.4 (ALOGPS, ChemAxon).

Table 1.1: Physicochemical Properties of THC, 11-OH-THC, and COOH-THC

Parameter	THC	11-OH-THC	COOH-THC	Reference
Molecular Weight (g/mol)	314.45	330.47	344.45	ChEMBL
LogP	6.97	5.33	---	[44]
LogD at pH=7.4	---	---	3.07	ALOGPS
Ionization Type	Neutral	Neutral	Acid	ChEMBL
pKa	10.6	9.34	4.02	ChemAxon
B/P	0.667	0.625	0.588	[45]
$f_{u,p}$	0.011	0.012	---	[15]

LogP: octanol-water partition coefficient; LogD: octanol-water distribution coefficient; pKa: acid dissociation constant; B/P: blood to plasma ratio; $f_{u,p}$: fraction unbound in the adult non-pregnant plasma

THC, 11-OH-THC, and COOH-THC pharmacokinetics in adults have been investigated after IV, inhalation, and oral administration. Changes in THC/11-OH-THC exposure during pregnancy have not been quantified but can be estimated from the non-pregnant exposure using the gestational age dependent changes in the relevant drug metabolizing enzymes and transporters. THC pharmacokinetics after IV, inhalation, and oral administration are reported to be highly variable. In the literature, after IV administration of THC, only two studies[46,47] had rich sampling ($\geq$24 hours) and used a rigorous quantitative method (with liquid or gas chromatography) (Table 1.2). The first study[47] dosed 9 subjects with 5 mg THC IV and the plasma $AUC_{0\text{-}48h}$ and C_{max} for THC was 281 nM*h and 208 nM, respectively. The second study[46]

dosed 6 subjects with 2 mg THC IV and the plasma $AUC_{0\text{-}24h}$ and C_{max} for THC were 85.1 nM*h and 368 nM, respectively. Upon extrapolating to time infinity, the dose normalized plasma AUC_{inf} and C_{max} for THC were 53.7 ± 3.52 nM*h/mg and 113 ± 100 nM/mg, respectively. This yields a systemic THC plasma CL of 62.1 L/h and a V_{ss} of 11.6 L/kg via tri-phasic decay. Neither study quantified 11-OH-THC exposure.

1.6.1 Absorption

Due to a rapid absorption phase, the THC concentration vs time profile after inhalation is similar to that after IV administration. After inhalational administration of THC, only two studies[47,48] had rich sampling (>20 hours) and used a rigorous quantitative method, gas chromatography tandem mass spectrometry (GC-MS) (Table 1.3). The first study[47] dosed 9 subjects by inhalation with 9.47 mg THC and the plasma $AUC_{0\text{-}48h}$ and C_{max} for THC were 106 nM*h and 79.8 nM, respectively. The second study[48] dosed 10 subjects by inhalation with 10.5 mg THC and the plasma $AUC_{0\text{-}6h}$ and C_{max} for THC were 235 nM*h and 271 nM, respectively, and the plasma $AUC_{0\text{-}22h}$ and C_{max} for 11-OH-THC were 192 nM*h and 57.3 nM, respectively. Upon extrapolating to time infinity, the dose normalized plasma AUC_{inf} and C_{max} for THC were 17.1 nM*h/mg and 17.1 nM/mg, respectively. THC bioavailability after inhalation consumption is variable with a range of 13-39%, depending on the smoking technique. Experienced users, who have a superior smoking technique (e.g., larger puff volume and increased duration in lungs), have increased bioavailability (27%) compared to the inexperienced user (14%)[47].

Unlike inhalation, the THC plasma concentration vs time profile after oral consumption is quite different compared to IV administration. After oral consumption of THC, only three studies[49-51] had rich sampling ($\geq$24 hours), a large number of subjects (>25), and used a rigorous quantitative method, liquid chromatography tandem mass spectrometry (LC-MS/MS) (Table 1.4). The first study[51] dosed 51 subjects orally in the fasted state with either 4.25 mg THC solution or 5 mg THC in capsule. The second study[50] dosed 52-54 subjects orally in both the fed and fasted state with either 4.25 mg THC solution or 5 mg THC in capsule. The third

study[49] dosed 27-28 subjects orally in both the fed and fasted state with either 5 or 10 mg THC in capsule. Upon extrapolating to time infinity, in the fasted state the dose normalized plasma THC AUC_{inf} and C_{max} were 2.52 ± 0.39 nM*h/mg and 1.15 ± 0.43 nM/mg, respectively and for 11-OH-THC these values were 6.57 ± 1.80 nM*h/mg and 1.61 ± 0.57 nM/mg, respectively. In the fasted condition, the oral systemic bioavailability was ~6 ± 3%. There was a considerable food effect on both THC and 11-OH-THC pharmacokinetics. When given a high fat meal prior to dosing and compared to the fasted state, THC and 11-OH-THC plasma AUC_{inf} increased by 2.4 and 1.30-fold, respectively while mean C_{max} increased by 19% and decreased by 31%, respectively (the change in mean C_{max} was not statistically significant)[50]. Both cannabinoids had a delay in plasma t_{max} by ~4 hours. We postulate that this food effect caused an increase in plasma AUC_{inf} through an increase in bioavailability, primarily by increasing the fraction of THC absorbed across the gut lumen (f_a). As THC is highly lipophilic, the f_a likely increases with a high fat diet by increasing the solubility of THC in the intestinal fluid. However, THC solubility was similar in the fed state simulated intestinal fluid (FeSSIF; 36 ± 3.6 μM) compared to the fasted state simulated intestinal fluid (FaSSIF; 28 ± 5.9 μM)[52]. In addition, the difference in rate of dissolution between the fasted and fed states may result in lower absorption of THC in the fasted state. Due to the lipophilicity of THC, its f_a is likely not permeability-limited.

1.6.2 Distribution

After absorption, as a result of the high lipophilicity (logP) of THC (6.97[44]) and 11-OH-THC (5.33[44]), the cannabinoids rapidly sequester to adipose tissue in humans and animals. The observed THC tissue distribution in human postmortem samples expressed as tissue/plasma concentration are: lung (10.9), liver (6.78), heart (5.05), kidney (1.88), muscle (1.56), brain (1.38) and spleen (0.78)[53-56]. The corresponding values for 11-OH-THC are: liver (5.09), brain (3.45), heart (3.36), spleen (2.81), muscle (1.98), kidney (1.43) and lung (1.21). Extensive partitioning into each of these organs indicates that both compounds have a large volume of distribution. Interestingly, the brain distribution is higher for 11-OH-THC than THC, which could

potentially explain the observed higher psychoactivity of 11-OH-THC, discussed in section 1.3. Of note, these tissues were not cleared of blood and therefore the tissue/plasma concentration ratios (or their AUC ratios) cannot be interpreted as tissue K_p. The THC tissue concentration data are highly variable between animal species (rat, mice, pigs) but distribution into the adipose tissue is substantially higher than that in the liver, lung, kidney, which is generally higher than in brain, heart, muscle, and spleen[57-61].

Each cannabinoid is also highly protein bound. About 62-65% of THC is bound to lipoproteins in human plasma with the majority bound to low-density lipoproteins (34%)[62,63]. Data are not available on lipoprotein binding for the metabolites. THC and 11-OH-THC are also bound to human serum albumin[15,62,64]. All three cannabinoids, THC, 11-OH-THC, and COOH-THC are bound to fatty-acid binding proteins (FABPs)[65-67]. THC has the highest affinity to FABPs, compared to the metabolites, with binding to FABP1, 3, 5, and 7. 11-OH-THC and COOH-THC have only been shown to bind to FABP1. With the combined binding to lipoproteins, albumin, and FABPs, THC and 11-OH-THC have a fraction unbound in plasma ($f_{u,p}$) of 0.011 and 0.012, respectively, as measured by ultracentrifugation[15]. There is no reported $f_{u,p}$ for COOH-THC. THC has a large V_{ss} (11.6 L/kg[46,47]), likely a result of the high lipophilicity despite its high plasma protein binding. COOH-THC also has a high V_{ss} (1.28 ± 0.42[68]), but it is markedly smaller than THC, likely as it is ionized at pH=7.4. Neither THC nor 11-OH-THC exhibit high partitioning into the erythrocytes with a blood to plasma (B/P) ratio of 0.667 and 0.625, respectively[45]. After dosing, the rapid decrease in plasma cannabinoid concentrations is due to not only rapid distribution but also elimination via metabolism and excretion (see below).

1.6.3 Elimination

Following IV administration of THC to humans, 80-90% of the drug is recovered in the urine (20%) and feces (65%) within 5 days after dosing[46]. Most of the urinary excretion is from conjugated COOH-THC[69,70]. However, most of the excretion in the feces is non-conjugated COOH-THC (28%), polar acids (26%), and non-conjugated 11-OH-THC (20%)[69,71]. THC is

primarily metabolized with less than 5% being excreted unchanged in the urine and feces (mostly feces) after IV administration. THC forms many metabolites but is primarily metabolized by hydroxylation at the C11 position to form 11-OH-THC and secondarily at the C8 position to form 8β-OH-THC[69,72]. In the liver, CYP2C9 is responsible for the formation of 11-OH-THC, while CYP3A is responsible for the formation of 8β-OH-THC[73,74]. The hepatic CYP2C9 pathway, forming 11-OH-THC, is the major pathway for THC metabolism with a predicted fraction metabolized (f_m) of 0.91 *in vitro* using human liver microsomal incubations[15]. This f_m is higher than that estimated from an *in vivo* human CYP2C9 polymorphism study where clearance was compared in CYP2C9 *3/*3 poor metabolizers and *1/*1 extensive metabolizers (f_m = 0.68)[75]. However, if you correct for the percent of metabolic activity remaining in CYP2C9 *3/*3 poor metabolizers[74], the adjusted CYP2C9 f_m *in vivo* (0.92) is in concordance with the *in vitro* value[15]. The remaining metabolism can be attributed to either CYP3A, CYP2C19, or CYP2D6[16,76].

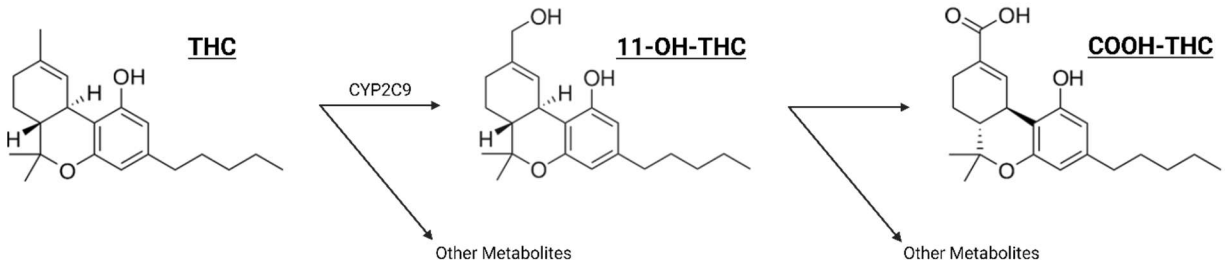

Figure 1.3: THC is primarily hydroxylated *in vivo,* by CYP2C9, to a psychoactive metabolite, 11-OH-THC. 11-OH-THC is then further oxidized to a non-psychoactive metabolite, COOH-THC, which is the major circulating metabolite in blood.

11-OH-THC is metabolized by microsomal enzymes (CYP2C9, CYP3A, UDP-glucuronosyltransferase (UGTs)[15]) and cytosolic enzymes (aldehyde dehydrogenases (ALDH) and aldehyde oxidase (AOX)[77]). The UGT mediated metabolism of 11-OH-THC is likely catalyzed by UGT1A9, UGT2B7, or UGT1A10[15,78]. The CYP2C9 pathway as well as the cytosolic enzymes are responsible for formation of the major circulating metabolite, COOH-THC[15,77]. Other than COOH-THC, 11-OH-THC is also converted to 8β-11-di-OH-THC. Following IV 11-OH-THC administration, 70-75% of the radiolabeled dose is excreted in the urine (20-

25%) and feces (50%) within 7 days[6]. Less than 5% of the dose is excreted as unchanged 11-OH-THC in urine. In the feces, 20% of the dose is excreted as unchanged 11-OH-THC, 18% as 8β-11-di-OH-THC, and 10% as conjugated 11-OH-THC[6]. Unchanged 11-OH-THC excreted in the feces after IV administration indicates potential biliary excretion of 11-OH-THC which could lead to enterohepatic recirculation. Other than the aforementioned urinary and fecal excretion, COOH-THC also undergoes glucuronidation to COOH-glucuronide by UGT1A1 and 1A3[15,78].

The placenta tissue expresses numerous drug metabolizing enzymes such as CYPs, UGTs, monoamine oxidase (MAO), xanthine oxidase (XO), sulfotransferases (SULTs), and glutathione-S-transferases (GSTs). CYP19A1 and CYP1A1 activity is present across trimesters while UGT1A, UGT2B, MAO and XO activities are present in the third trimester[79]. CYP19A1, also known as aromatase, is responsible for the conversion of androgens (e.g. testosterone) to estrogens (e.g. estradiol)[80] and metabolism of numerous drugs (e.g. methadone[81] and glyburide[82]). CYP1A is responsible for metabolism of a series of xenobiotics, including the drugs caffeine, phenacetin, tizanidine, granistetron, riociguat. Interestingly, placental activity of CYP19A1 decreases in individuals who smoke tobacco/cannabis, but CYP1A activity increases. Among the fetal organs, the fetal liver is the major xenobiotic metabolizing organ. Within the fetal liver, the most abundant enzyme is CYP3A7 and other enzymes with activity across trimesters are CYP2C9 and XO[79]. CYP3A7 activity and abundance (per gram of tissue) does not change across gestational age[83]. Though we have estimates of the magnitude of metabolism in the adult human liver and contribution by different enzymes[15], we do not have these estimates for the adult intestines or lungs. Intestinal and lung metabolism of THC could lead to a significant first-pass effect after oral and inhalation consumption, respectively. Additionally, as there is substrate overlap between adult CYP3A4/5 and fetal liver CYP3A7, there is high potential for metabolism of THC and 11-OH-THC in the fetal liver. Therefore, in **Aim 1** (**Chapter 2**), we will determine if these cannabinoids are depleted in microsomes made

from these tissues, and if depleted, we will determine their depletion kinetics and identify the enzymes involved.

1.7 Changes in Maternal Metabolic Activity During Pregnancy

Changes in enzyme abundance across gestational age of pregnancy and the subsequent change in enzyme activity will impact the clearance of THC and its metabolites. Since THC and its metabolites are metabolized primarily by CYP2C9, CYP3A, and UGTs, any induction of these enzymes will decrease maternal-fetal exposure.

Hepatic CYP2C9 activity is increased by 16% during the third trimester compared to non-pregnancy, estimated from *in vivo* observed steady-state unbound phenytoin (primarily metabolized in the liver via CYP2C9) concentrations in pregnant people and postpartum[84]. Estrogens are a potential inducer of CYP2C9 activity, as shown by HepG2 cell studies[85]. This induction was confirmed where 4-hydroxylation of diclofenac and tolbutamide increased by 1.4 to 2-fold when human hepatocytes were incubated with the pregnancy hormone, estradiol (1 μM)[86]. However, another study showed no change in CYP2C9 activity (4-hydroxylation of diclofenac) when human hepatocytes were incubated with high concentrations of pregnancy-related hormones (20 μM progesterone, 3 μM estradiol, etc.)[87]. THC and 11-OH-THC are extensively metabolized by CYP2C9 thus the generally observed pregnancy-related induction of CYP2C9 is expected to increase the clearance of both cannabinoids in a gestational age-dependent manner leading to an overall decrease in maternal-fetal exposure.

Intestinal and/or hepatic CYP3A is induced by 1.99-fold in the third trimester (28-32 weeks gestation), estimated from *in vivo* observed unbound formation clearance of 1-OH-midazolam (primarily by CYP3A) compared to postpartum[88]. Analyses of the pharmacokinetics of midazolam in addition to other CYP3A substrates (indinavir and nifedipine), in pregnancy, with different intestinal and hepatic extraction ratios, led to the conclusion that this induction is primarily hepatic and not intestinal[89]. However, indinavir is saturated in the intestine and when

only midazolam and nifedipine are considered, either sole hepatic CYP3A induction or mixed hepatic and intestinal CYP3A induction could explain the observed AUC ratios during pregnancy and postpartum. The magnitude of CYP3A induction appears to be consistent across trimesters when comparing the dextromethorphan/dextrorphan ratio in trimester 1 (14-18 weeks), trimester 2 (24-28 weeks), and trimester 3 (36-40 weeks) pregnancy versus the postpartum period[90]. This consistent CYP3A induction was confirmed *in vitro,* in human hepatocytes*,* where maximum CYP3A induction by cortisol was achieved at the relevant trimester 1, 2, 3 plasma cortisol concentrations[91]. Others, using much higher concentrations than those observed in plasma during pregnancy, have found that CYP3A is induced in human hepatocytes by 1 μM estradiol resulting in a 0 to 2.5-fold increase in 1'-hydroxylation of midazolam depending on the donor[86]. Another study found that CYP3A abundance and activity (6β-hydroxylation of testosterone) increases in human hepatocytes by 1.25-fold with high concentrations of pregnancy hormones (20 μM progesterone, 3 μM estradiol, etc.)[87]. However, when pregnancy hormones were administered as a cocktail (estradiol, estriol, cortisol, progesterone, testosterone, pituitary growth hormone, and placental growth hormone) or individually at their relevant trimester 3 pregnancy plasma concentrations, cortisol was the only hormone to induce CYP3A activity in each condition[92]. Therefore, cortisol is likely responsible for the pregnancy related induction of CYP3A. THC has minor hepatic metabolism by CYP3A so while CYP3A-mediated metabolism will be induced during pregnancy it should not have a large change on hepatic THC clearance. On the other hand, 11-OH-THC is extensively metabolized by CYP3A, so, as before, the pregnancy-related induction should increase its hepatic clearance. But any induction of the cannabinoid clearance by CYP3A enzymes will not be gestational age-dependent as such induction appears to be constant across the trimesters.

UGT1A4 activity increases by ~1.5-fold in trimester 2 and 3 pregnancies compared to postpartum, as evaluated by the *in vivo* lamotrigine 2-N-glucuronide/lamotrigine plasma concentration ratio[93]. UGT2B7 activity does not change between pregnancy and postpartum, as

evaluated by the *in vivo* zidovudine-glucuronide/zidovudine concentration ratio[94]. The *in vivo* data are supported by studies using human hepatocytes, where UGT1A4 and 1A1 protein abundance is increased by 1.5 to 2-fold with 10 μM estradiol, but not by other pregnancy hormones (estriol, estetrol, progesterone, and cortisol)[95]. Also, UGT2B7, 1A3, 1A6, and 1A9 protein abundance was not changed by any pregnancy hormones. Of note, these estradiol concentrations are much higher than those present in the plasma during pregnancy. 11-OH-THC is metabolized by UGT1A9, 1A10, and 2B7 and COOH-THC by UGT1A1 and 1A3. Therefore UGT-mediated 11-OH-THC metabolism will likely not change during pregnancy but COOH-THC metabolism by UGT1A1 could be increased.

1.8 Is THC and/or 11-OH-THC Transported across the Placenta and the BBB and How Does this Transport Change across Gestational Age?

Whether THC and its metabolites are transported by P-gp and/or BCRP at the blood-brain barrier (BBB) or gut lumen is controversial. In mice, THC appears to be efflux transported by either P-gp or BCRP. Mice, naturally deficient in P-gp, dosed with 25 mg/kg THC orally, had a 2.2-fold increase in systemic plasma THC AUC compared with wild-type mice[17]. This suggests that P-gp is involved in the transport of THC at the gut lumen preventing THC absorption. With regard to brain disposition, P-gp and Bcrp knock-out mice dosed intraperitoneally with 3 mg/kg THC had up to 3.2- and 4.7-fold increase in the brain/blood THC ratio compared with wild-type mice, respectively[18]. However, the brain/blood THC ratio was higher at only certain timepoints and neither the P-gp nor Bcrp knock-out mice data were significantly different than wild-type when all timepoints were included. Thus, it is uncertain whether P-gp and/or Bcrp effluxes THC at the BBB and modulates its brain distribution. There is no corresponding information on 11-OH-THC transport in mice. However, with P-gp or BCRP-overexpressing cells using the Transwell or the cell accumulation assay, presence or absence of THC, 11-OH-THC, and COOH-THC transport was undetectable[96]. In the Transwell assay, THC could not be quantified

in the receiver compartment due to extensive intracellular binding. Similarly, THC efflux was not discernible in the cell accumulation assay perhaps due to its high lipophilicity.

For the blood-placental barrier (BPB), as stated before, P-gp and BCRP are expressed on the apical membrane of the syncytiotrophoblast in the placenta. Active THC/11-OH-THC transport by either of these efflux transporters could decrease their overall fetal exposure. P-gp and BCRP are two of the highest expressed apical efflux transporters in the human placenta[79]. As gestational age increases, while the amount of P-gp and BCRP in the human placenta decreases per gram of tissue, because of increase in size, the overall abundance of both transporters in the placenta is highest at term[97]. Additionally, the fetal brain undergoes rapid maturation, and the fetal BBB develops between 8-18 weeks gestation. P-gp and BCRP are also highly expressed in the fetal BBB and P-gp reaches the highest abundance in the third trimester[98]. If THC is a substrate of either transporter, fetal brain exposure to THC would be reduced relative to fetal circulating plasma exposure.

As for the highest expressed influx transporters on the basal membrane of the syncytiotrophoblast, these are OATP2B1, OCT3, and OAT4. Of note, because THC and 11-OH-THC are neutral molecules at physiological pH, they do not fit the profile of molecules that are likely to be transported by OATPs, OATs or OCTs. While there are no data to contradict this assumption, if they are involved in THC/11-OH-THC active transport at the BPB, their induction or lack thereof could impact the magnitude of transport across gestational age. Unlike the efflux transporters on the apical membrane, OATP2B1 and OAT4 placental abundance per gram of tissue does not change across gestational age and OCT3 abundance increases with gestational age[97]. However, due to steady growth of the placenta with gestational age, the overall abundance of each transporter in the placenta is highest at term.

As noted above, data in both macaques and humans suggest that THC may be effluxed by the human placenta. To determine if this is the case, in **Aim 2** (**Chapter 3**) we will perfuse THC, 11-OH-THC and COOH-THC with and without a P-gp/BCRP inhibitor, valspodar, in

cotyledons from human term placenta, in the maternal-fetal and fetal-maternal direction. Through these studies, we will estimate the CL_{PD} and CL_T at term and identify if the cannabinoids are a substrate of P-gp/BCRP and if so, quantify the fraction transported by each. Upon identifying the fraction transported, we can scale the magnitude of transport at term to earlier gestational ages using changes in their placenta transporter abundance[97].

Pregnancy-induced changes in transporter activity could affect the extent of absorption of THC across the gut lumen and therefore the extent of distribution of the cannabinoids to fetus and the fetal brain. Limited data exist on the effect of pregnancy on hepatic, intestinal or renal transporters. The *in vivo* observed unbound clearance of glyburide (likely hepatic) is increased by 2.05-fold in the third trimester (28-32 weeks gestation) compared to postpartum, which could be due to induction of hepatic BCRP, OATP1B1, CYP3A4 and/or CYP2C9[99]. Renal P-gp activity is increased 2.07-fold in the third trimester (28-32 weeks gestation), as estimated from *in vivo* observed unbound renal secretory clearance of digoxin compared to postpartum[88]. Based on the measurement of metformin secretory renal clearance, renal OCT2 activity is increased in the second and third trimester but doesn't change in trimester 1[100]. Renal OAT1/2/3 activity is increased across gestational age[101]. However, given that very little THC or 11-OH-THC is excreted unchanged in the urine, any increased activity of renal transporters during pregnancy would be irrelevant to the clearance of these cannabinoids.

The estimated metabolic (**Aim 1**) and placenta transfer kinetics (**Aim 2**) will be inputted into our m-f-PBPK model to predict the THC/11-OH-THC fetal exposure (e.g., fetal brain) across gestational age (**Aim 3**). This predicted exposure is vital to conducting informative studies *in vitro* and *in vivo* in animals to assess the impact of prenatal cannabis use on neurodevelopmental toxicity.

1.9 Specific Aims

To predict fetal THC/11-OH-THC exposure at various gestational ages, after maternal inhalation and oral cannabis use, we will pursue the following aims:

Aim 1 (Chapter 2): Identify the drug metabolizing enzymes and quantify their metabolic kinetics for depleting THC/11-OH-THC in microsomes from human intestines (HIMs), lungs (HLuMs), placentas (HPMs), and fetal livers (HFLMs).

1.1. Use selective enzyme inhibitors to identify the relevant drug metabolizing enzymes mediating the depletion of THC/11-OH-THC in these microsomes.

1.2. Through the above depletion studied, quantify the intrinsic metabolic clearance (CL_{int}) and fraction metabolized (f_m) by each identified enzyme.

1.3. Populate the m-f-PBPK model in Aim 3 with the above *in vitro* enzyme kinetics to predict fetal exposure to THC/11-OH-THC at various gestational ages.

Aim 2 (Chapter 3): Quantify the transplacental transfer of THC/11-OH-THC/COOH-THC by active transport and/or by passive diffusion using the perfused human term placenta model.

2.1. Perfuse the human placenta with THC/11-OH-THC/COOH-THC, in a single-pass mode, to determine their maternal-fetal and fetal-maternal transplacental transfer in the presence and absence of the dual P-gp/BCRP inhibitor, valspodar.

2.2. Through Aim 2.1, determine if THC/11-OH-THC/COOH-THC is effluxed by P-gp/BCRP. If yes, determine the fraction transported (f_t) by each relevant transporter.

2.3 Populate our m-f-PBPK model (Aim 3) with the estimated placenta and fetal liver metabolic clearances from Aim 1.2 and transplacental transfer kinetics from Aim 2.1, to predict the fetal exposure to THC/11-OH-THC.

Aim 3 (Chapter 4): Using our m-f-PBPK model, predict fetal plasma and tissue THC/11-OH-THC exposure at typical doses, route and frequency of maternal THC consumption.

3.1. Quantify the THC/11-OH-THC concentration in 1st and 2nd trimester human fetal brain, liver, kidney, placenta and MP and in term UVP, MP and placenta from pregnant individuals who have recreationally consumed cannabis prior to pregnancy termination or term delivery.

3.2. Populate our current m-f-PBPK model with the various THC/11-OH-THC maternal-fetal disposition parameters from Aims 1 and 2. Then, using our m-f-PBPK model, predict fetal plasma and/or fetal tissue exposure to THC/11-OH-THC, at 1^{st}, 2^{nd}, and 3^{rd} trimester. Verify our m-f-PBPK model predictions, to the extent possible, by data collected in Aim 3.1.

3.3 Using our verified m-f-PBPK model, predict at steady-state the dynamic (time-dependent) changes in the unbound and total fetal plasma and tissue THC/11-OH-THC concentrations at different gestational ages for typical routes, doses and frequency of prenatal cannabis use.

Table 1.2: Total and maximum exposure of THC and its metabolites following intravenous administration of THC

				THC		11-OH-THC		COOH-THC		Reference
Dose (mg)	**Sampling duration (h)**	**Number of Subjects**	**Method of Quantification**	**AUC (nM*h)**	**C_{max} (nM)**	**AUC (nM*h)**	**C_{max} (nM)**	**AUC (nM*h)**	**C_{max} (nM)**	
5	48	9	GC-MS	281	208	_	_	_	_	[47]
2	24	6	HPLC and Liquid Scintillation	85.1	368	_	_	_	_	[46]
0.5	72	6	Liquid Scintillation	113	20.0	_	_	_	_	[102]
0.5	30	12	Liquid Scintillation	60.8	19.8	_	_	_	_	[103]
2.5	2	22	GC-MS	109	562	_	_	_	_	[104]
2.5	2	11	GC-MS	104	485	_	_	_	_	[105]
3.1	72	12	Thin-layer Chromatography	828	231	33.4	10.9	110	2125	[71]
3.71	8	8	GC-MS	294	874	41.3	28.1	606	107	[106]
4.5	72	12	Thin-layer Chromatography	421	29.6	391	26.6	2498	189	[69]
5	4	11	GLC-MS	230	629	_	_	_	_	[107]
5	4	18	GLC-MS	274	938	_	_	_	_	[108]
5	10	8	GC-MS	406	1310	_	_	623	112	[70]

AUC: area under the plasma concentration-time curve from time=0 to the last timepoint; C_{max}: maximum concentration; GC-MS: gas chromatography tandem mass spectrometry; GLC-MS: gas-liquid chromatography tandem mass spectrometry; underlined studies that used selective assays and spanned at least 24 hours were used for pharmacokinetic data.

Table 1.3: Total and maximum exposure of THC and its metabolites following inhalation administration of THC

				THC		11-OH-THC		COOH-THC		Reference
Dose (mg)	Sampling duration (h)	Number of Subjects	Method of Quantification	AUC (nM*h)	C_{max} (nM)	AUC (nM*h)	C_{max} (nM)	AUC (nM*h)	C_{max} (nM)	
9.47	48	9	GC-MS	106	79.8	_	_	_	_	47
10.5	22	10	GC-MS	235	271	192	57.3	350	103	48
8.94	2	6	Radioimmunoassay	84.4	313	_	_	_	_	109
9.7	6	6	GLC-MS	219	300	_	_	302	91.5	110
12.8				246	342			378	125	
16.0				321	493			422	132	
10	24	12	Liquid Scintillation	12.8	8.16	_	_	_	_	103
13.1	4	18	GLC-MS	95.0	262	_	_	_	_	108
19	4	11	GLC-MS	104	194	_	_	_	_	107
15.8	168	6	GC-MS	141	251	33.6	17.3	1453	60.0	111
33.8				250	483	94.9	21.9	3484	147	
18.2	6	10	GC-MS	71.6	152	13.9	7.56	_	_	112
36.5				128	252	24.2	10.9			
25.6	4	19	GC-MS	280	356	94.1	51.1	_	_	113
22.5	8	11	GC-MS	111	156	42.4	20.3	_	_	114
47.5		12		273	384	93.8	37.2			
29.3	8	18	LC-MS	243	430	73.2	27.8	262	88.3	115
49.1		20		360	645	111	49.6	435	173	
69.4		20		478	735	122	47.8	467	158	
54	10	22	LC-MS/MS	350	242	57.5	30.3	610	195	116
54	30	14	LC-MS/MS	331	109	98.3	20.3	2001	153	117
45	8	12	GC-MS	15.6	66.7	10.0	5.45	132	21.8	118
23	5.4	96	Radioimmunoassay	392	447	_	_	543	158	119
15.2	8	8	GC-MS	34.7	42.6	23.0	8.17	516	84.8	120
26.9				82.0	107	49.9	25.1	795	142	
15.8	12	6	GC-MS	117	344	_	_	_	_	121
33.8				159	699					
3.71	8	8	GC-MS	64.8	60.9	13.9	4.25	180	28.7	106
15.3	6	18	Not listed	146	219	_	_	_	_	122
30.6				222	358					
61.2				308	595					

3.08	0.5	8	GC-MS	1173	107	_	_	_	_	[123]
53.1	11	11	GC-MS	284	90.0	49.9	11.8	1022	136	[124]
20	24	14	GC-MS	64.6	82.0	3.09	8.17	119	53.1	[125]
14.5	8.3	19	LC-MS/MS	142	148	17.6	12.4	_	_	[126]
33.5				179	197	29.7	21.2			
1.6	4	6	LC-MS/MS	19.9	11.7	_	_	_	_	[127]

AUC: area under the plasma concentration-time curve from time=0 to the last timepoint; C_{max}: maximum concentration; GC-MS: gas chromatography tandem mass spectrometry; GLC-MS: gas-liquid chromatography tandem mass spectrometry; LC-MS: liquid chromatography tandem mass spectrometry; underlined studies that used selective assays and spanned at least 20 hours were used for pharmacokinetic data.

Table 1.4: Total and maximum exposure of THC and its metabolites following oral administration of THC

				THC		11-OH-THC		COOH-THC		Reference
Dose (mg)	**Sampling duration (h)**	**Number of Subjects**	**Method of Quantification**	**AUC (nM*h)**	**C_{max} (nM)**	**AUC (nM*h)**	**C_{max} (nM)**	**AUC (nM*h)**	**C_{max} (nM)**	
4.25[1,$]	48	51	LC-MS/MS	11.2	6.19	32.1	8.38	_	_	[51]
5[2,$]				12.7	7.65	38.9	11.0			
4.25[1,#]	48	52	LC-MS/MS	28.9	4.83	38.2	3.72	_	_	[50]
5[2,#]		54		33.3	8.27	44.9	6.54			
5[2,$]		53		14.1	6.96	33.8	9.44			
5[11,$]	24	28	LC-MS/MS	9.95	3.16	21.7	5.14	_	_	[49]
5[11,#]		28		27.8	5.35	28.4	3.63			
10[11,$]		28		27.7	7.44	44.5	9.69			
10[11,#]		27		56.0	9.34	53.7	6.98			
21[3]	6	12	Liquid Scintillation	1.10	0.36	_	_	_	_	[103]
5[4]	8	13	LC-MS/MS	9.30	7.25	22.5	12.0	_	_	[128]
6.5[4]		9		13.5	11.2	27.1	16.3			
8[4]		9		18.3	11.2	34.9	15.9			
5[2,#]	10.5	9	GC-MS	97.3	14.9	44.8	9.08	_	_	[129]
15[2,#]				160	45.5	128	33.6			
10[2,$]	24	24	GC-MS	1138	10.1	2808	13.6	42375	96.0	[130]
17.5[5]	72	12	Thin-layer Chromatography	666	35.6	207	18.0	4608	228	[71]
15[2,$]	12	7	LC-MS/MS	51.0	13.0	22.4	5.48	_	_	[131]
30[2,$]				82.8	21.7	35.9	11.6			
45[2,$]				154	39.5	100	17.2			
60[2,$]				286	113	169	30.2			
75[2,$]				441	93.0	203	30.6			
90[2,$]				693	160	334	58.2			
20[5]	24	12	Thin-layer Chromatography	791	197	82.9	10.3	453	40.6	[69]
20[6]	6	11	GLC-MS	54.3	17.5	_	_	_	_	[107]
20[6]	10	12	GC-MS	62.6	16.4	_	_	_	_	[132]
20[2,$]	24	9	LC-MS/MS	8.43	3.26	9.51	2.99	121.94	20.71	[133]
10.8[7,#]	24	12	GC-MS	104	20.6	107	11.3	_	_	[134]
10.8[7,$]				37.0	12.7	86.9	14.1			
5.4[7,$]	24	6	GC-MS	11.0	4.71	32.0	6.90	_	_	[135]

10.8[7,$]		12		38.9	12.7	87.2	14.1			
21.6[7,$]		7		73.1	17.2	184	25.1			
10.8[7,$]	24	36	GC-MS	27.6	8.58	62.4	10.5	_	_	[136]
3[8]	2	11	LC-MS/MS	6.53	4.96	8.52	5.64	67.8	57.7	[137]
5[8]				10.3	7.65	11.8	7.58	94.2	92.1	
6.5[8]				13.7	9.91	15.6	10.5	130	114	
0.75[8]	6	9	LC-MS/MS	2.80	1.30	4.15	1.69	_	_	[138]
1.5[8]		10		6.39	3.21	10.1	3.66			
8[8,$]	6	12	LC-MS/MS	1422	11.4	2276.2	12.9	_	_	[139]
10.8[7,$]	24	9	LC-MS/MS	25.4	5.72	_	_	_	_	[140]
10.8[5,$]	24	14	LC-MS/MS	64.8	24.1	97.0	19.9	_	_	[141]
10.8[7,$]				55.8	16.6	85.6	14.3			
0.36[9]	24	12	LC-MS/MS	15.9	3.18	20.6	3.63	267	49.6	[142]
0.95[10]				5.72	1.59	5.75	2.12	40.6	12.5	

#fed, $fasted, 1: Syndros; 2:Marinol; 3: cherry syrup; 4: tablet; 5: sesame oil in gelatin capsule; 6: chocolate cookie 7: Sativex; 8: namisol; 9: decoction; 10: cannabis oil; 11: sunflower oil in gelatin capsule; AUC: area under the plasma concentration-time curve from time=0 to the last timepoint; C_{max}: maximum concentration; GC-MS: gas chromatography tandem mass spectrometry; GLC-MS: gas-liquid chromatography tandem mass spectrometry; LC-MS: liquid chromatography tandem mass spectrometry; underlined studies that used selective assays, spanned at least 24 hours, and had a high subject number (n>25) were used for pharmacokinetic data.

Chapter 2: Characterizing and Quantifying Extrahepatic Metabolism of (-)-Δ^9-Tetrahydrocannabinol (THC) and Its Psychoactive Metabolite, 11-OH-THC

The work presented in this chapter was previously published in Drug Metabolism and Disposition 50(6):734-740(2022)

2.1 Abstract

(-)-Δ^9-tetrahydrocannabinol (THC) is the psychoactive constituent of cannabis, a drug recreationally consumed by inhalation and orally. Physiologically based pharmacokinetic (PBPK) modeling can be used to predict systemic and tissue exposure to THC and its psychoactive metabolite, 11-OH-THC. To populate a THC/11-OH-THC PBPK model, we previously characterized the depletion clearance of THC (by CYP2C9) and 11-OH-THC (by UGT, CYP3A, and CYP2C9) in adult human liver microsomes. Here we focused on quantifying extrahepatic depletion clearance of THC/11-OH-THC, important after oral (intestine) and inhalational (lung) consumption of THC as well as prenatal THC use (placenta and fetal liver). THC (500 nM) was metabolized in adult human intestinal microsomes (n = 3-5) by CYP2C9 (V_{max}: 2.0 ± 0.72 nmol/min/mg; K_m: 70 nM; CL_{int}: 29 ± 10 mL/min/mg and f_m: 0.89 ± 0.038 at concentration << 70 nM) and CYP3A (CL_{int}: 3.8 ± 1.7 mL/min/mg; f_m: 0.11 ± 0.038). 11-OH-THC (50 nM) was metabolized by CYP3A (CL_{int}: 0.41 ± 0.092 mL/min/mg; f_m: 0.51 ± 0.11) and UGT2B7 (CL_{int}: 0.20 ± 0.043 mL/min/mg; f_m: 0.25 ± 0.053). THC at 500 nM (CL_{int}: 7.6 ± 0.36 mL/min/mg) and 11-OH-THC at 50 nM (CL_{int}: 1.1 ± 0.062 mL/min/mg) were predominately (f_m: 0.99 and 0.80, respectively) metabolized by CYP3A in human fetal liver microsomes (n = 3). However, we did not observe significant depletion of THC/11-OH-THC in adult lung, 1st, 2nd trimester or term placenta microsomes. Using PBPK modeling and simulations, these data could be used in the future to predict systemic and tissue THC/11-OH-THC exposure in healthy and special populations.

2.2 Introduction

Cannabis is the most frequently used recreational drug in the United States. It is primarily consumed orally or by inhalation and with increased legalization, its use has also increased. Currently 17.9% of the United States adult population (age 12 or older) uses

cannabis[143]. Due to the psychoactive effects of (-)-Δ^9-tetrahydrocannabinol (THC)[144] and its active metabolite, (±)-11-hydroxy-Δ^9-THC (11-OH-THC), changes in exposure to these cannabinoids could cause possible negative outcomes (e.g. anxiety and panic attacks[145]) when their clearance (CL) is altered by drug-drug interactions (DDIs), pathophysiological changes (e.g. hepatic impairment), or other sources of inter-individual variability.

Physiologically based pharmacokinetic (PBPK) modeling is a useful mechanistic tool to predict human THC and 11-OH-THC exposure *in silico*. PBPK modeling integrates physiological processes, drug specific physicochemical properties and *in vitro* metabolism and transport parameters to predict a drug's disposition in the body. In addition to using a healthy adult PBPK model to estimate THC/11-OH-THC exposure in different genetic populations or in the presence of DDIs, such a model can be extended to predict the disposition of these cannabinoids in special populations that are difficult to study, for example, people with hepatic impairment or pregnant women. A pregnancy PBPK model could help predict fetal THC/11-OH-THC exposure throughout gestation following maternal cannabis consumption. Such predictions are important due to the potential deleterious effects of cannabis to the fetus/infant[1-5]).

To build a THC PBPK model, we first need to quantify and then populate the model with the intrinsic metabolic and transport clearance (CL_{int}) of THC and 11-OH-THC. Because THC and 11-OH-THC are cleared predominantly from the body by metabolism (and do not appear to be significantly transported[96]), here we focused on quantifying the metabolic depletion CL of THC and 11-OH-THC in tissues that could potentially contribute to the overall CL and bioavailability (F) of THC and 11-OH-THC from the body after inhalation or oral cannabis consumption. Because THC is cleared from the body primarily by metabolism [146], we previously characterized and quantified the hepatic depletion CL of THC and 11-OH-THC where we found that THC was predominately metabolized by cytochrome P450 (CYP)2C9 while 11-OH-THC was metabolized by CYP2C9, CYP3A, and uridine 5'-diphospho-glucuronosyltransferase (UGT) enzymes [15]. In addition, through these studies and those with recombinant CYP enzymes, we

found that THC could be metabolized by CYP enzymes present in the lung (CYP1A1 [147]) and in the intestine (CYP3A4/5, CYP2C9, CYP2C19, CYP2D6, UGTs [148]). Therefore, the tissues of interest here were the intestine and the lung since THC is primarily consumed orally and by inhalation and these organs could lead to both first pass and systemic CL of THC. In addition, to populate our maternal-fetal (m-f) PBPK model [149], we also characterized the metabolism of THC and 11-OH-THC in the human placenta and fetal liver. Indeed, our studies with recombinant CYP enzymes showed that THC/11-OH-THC can be metabolized by CYPs that are present in the fetal liver (CYP3A7 [83]) or the placenta (CYP1A1 [150]).

2.3 Materials and Methods

2.3.1 Chemical and Reagents

THC (1 mg/ml), 11-OH-THC (1 mg/ml), and (±)-11-nor-9-carboxy-Δ^9-THC (11-COOH-THC) (1 mg/ml) DEA-exempt methanol stocks and deuterated internal standards [IS; (-)-Δ^9-THC-D_3, (±)-11-OH-THC-D_3, (±)-11-COOH-THC-D_3] were purchased from Cerilliant (Round Rock, TX). Low-binding (LB) microcentrifuge tubes (composed of chemical-resistant polypropylene) were purchased from Genesee Scientific (San Diego, CA). Bovine serum albumin (BSA) (Fraction V - heat-shock treated), sodium phosphate, sucrose, acetonitrile, formic acid (liquid chromatography-mass spectrometry (LC-MS/MS grade), LC glass inserts, and LC pre-split snap caps were purchased from Fisher Scientific (Hampton, NH). Alamethicin, midazolam (MDZ), 1-hydroxymidazolam (1-OH-MDZ), resorufin (RES), and 7-ethoxyresorufin (7-ER) were purchased from Cayman Chemicals (Ann Arbor, MI). Uridine 5'-diphosphoglucuronic acid (UDPGA), ethylenediaminetetraacetic acid (EDTA), β-nicotinamide adenine dinucleotide phosphate (NADP+), D-glucose 6-phosphate (G6P), glucose-6-phosphate dehydrogenase (G6PDH), phenylmethylsulfonyl fluoride (PMSF), itraconazole (ITZ), sulfaphenazole (SFZ), omeprazole (OMPZ), alpha-naphthoflavone (ANF), quinidine (QND),

methimazole (MMI), fluconazole (FLZ), and niflumic acid (NFA) were purchased from Sigma-Aldrich (St. Louis, MO). Azamulin (AZA) was purchased from Toronto Research Chemicals (Toronto, ON).

2.3.2 Biological Materials

Pooled adult, mixed gender human intestinal microsomes (HIM) (Lot 1610314: n=15, 10 mg/mL) and human lung microsomes from cigarette smokers (HLuM) (Lot 1910176: n=5, 10 mg/mL; Lot 1310176: n=4, 10 mg/mL) were purchased from Xenotech (Lenexa, KS). HLuM from cigarette smokers were chosen because smoking induces CYP1A activity[151]. Human placentas and fetal liver tissues were acquired from the Birth Defects Research Laboratory (Seattle, WA). Human placental microsomes (HPM) (2 mg/mL) were prepared as described before from trimester 1 (T1), trimester 2 (T2), and term placentas[97] and the demographics are shown in Table S2.1. Human fetal liver microsomes (HFLM) (18.6 mg/mL) were prepared from six T2 pooled livers (Table S2.2) as follows. Approximately 1 g of tissue was weighed and homogenized in buffer containing 20 mM sucrose, 50 mM Kpi, 10 mM EDTA and a protease inhibitor (0.2 mM PMSF) with an Omni Bead Ruptor Homogenizer. The homogenate was then centrifuged at 9,000 x g and 4°C for 20 minutes in Optima L-90K Ultracentrifuge (Beckman Coulter, Brea, CA). The resulting S9 fraction was immediately centrifuged at 100,000 x g and 4°C for 1 hour to yield both the cytosolic and microsomal fractions. Microsomal fractions were resuspended in 300 µL of storage buffer (50 mM Kpi, 20 mM sucrose, 10 mM EDTA) and protein content was quantified by a Pierce bicinchoninic acid (BCA) assay. T2 livers were used as they were available to us in quantity and size needed to prepare microsomes.

2.3.3 Cannabinoid Incubations

HIM (0.25 and 0.75 mg/mL for THC and 11-OH-THC incubations, respectively), HFLM (1 mg/mL), HLuM (1 and 2 mg/mL), and HPM (0.5 mg/mL) were incubated in LB tubes with either 500 nM THC or 50 nM 11-OH-THC, at pharmacologically relevant systemic concentrations[16].

Incubations were performed in 0.1 M potassium phosphate buffer (pH 7.4) containing 0.2 g/dL BSA to reduce nonspecific binding to plastic and maximize cannabinoid solubility (300 µL final volume). When depletion in the microsomes was observed, to identify the enzymes involved, THC or 11-OH-THC was incubated in the presence and absence of selective enzyme inhibitors: 10 µM SFZ (CYP2C9), 2 µM ITZ (CYP3A), 1 µM QND (CYP2D6), 30 µM OMPZ (CYP2C19), 3 µM ANF (CYP1A), 25 µM MMI (flavin-containing monooxygenase (FMO)), 2.5 mM FLZ (UGT2B), and 2.5 µM NFA (UGT1A9). Although FLZ and NFA are generally not selective for the enzymes listed, for our purposes they were (see reasons provided in the discussion). The same inhibitors were used for all microsomes with the exception of HFLM. Due to presence of CYP3A7 in the HFLM (vs. CYP3A4/5 in adults), and an increased selectivity of AZA for CYP3A7 compared to ITZ, 5 µM AZA was used as the CYP3A-selective inhibitor for the HFLM incubations. To confirm CYP activity in the HFLM, HLuM, and HPM incubations, 1-OH-MDZ formation from MDZ (CYP3A), RES formation from 7-ER (CYP1A), and β-estradiol formation from testosterone (CYP19), were quantified as positive controls, respectively. CYP and FMO incubations were pre-incubated at 37°C for 10 minutes in a heated shaking block and CYP-mediated depletion of the cannabinoids was initiated with a NADPH regenerating system (1.3 mM NADP+, 3.3 mM G6P, 3.3 mM $MgCl_2$, 0.4 unit/mL G6PDH). For UGT-mediated depletions, the microsomes were pre-incubated with alamethicin (25 µg/mL) for 15 minutes on ice to allow for pore formation then pre-incubated as described above (with the addition of 3.3 mM $MgCl_2$). Then, the reaction was initiated with 2.5 mM UDPGA (as NADPH was not included, no CYP metabolism was present). The incubation period (30 – 60 minutes) for each set of experiments was optimized to achieve extensive substrate depletion in order to estimate the depletion kinetic parameters with confidence. Depletion of the cannabinoids was terminated by adding 100 µL ice-cold acetonitrile containing the internal standards (250 nM THC-D_3, 250 nM 11-OH-THC-D_3, 250 nM 11-COOH-THC-D_3) to a 50 µL aliquot of the reaction mixture in LB tubes and then mixing using a vortex. Samples were centrifuged at 18,000 x g and 4°C for 10 minutes, and 70

µL of the supernatant was stored at -20°C in LC glass inserts until analysis by LC-MS/MS. Three to five independent experiments were conducted, each in duplicate or triplicate.

2.3.4 LC-MS/MS Analysis

Samples (10 µL injection) were analyzed with an Acquity ultra-performance liquid chromatography (UPLC) system (Waters Corporation, Milford, MA) coupled to an AB Sciex Triple Quad 6500 (SCIEX, Framingham, MA). Acquity UPLC ethylene bridged hybrid (BEH) C18 column (1.7 µM 2.1 x 50 mm) attached to a BEH C18 5 mm guard column (Waters Corporation, Milford, MA) was used for chromatographic separation with a mobile phase flow rate of 0.3 mL/min. The mobile phase consisted of acetonitrile and water containing 0.1% formic acid as the organic and aqueous phases, respectively. The chromatographic LC-MS/MS conditions used are provided in Table S2.3. Integration of the chromatographic peaks was performed using Analyst v1.6.2 (Framingham, MA). This method was used for all samples other than placental metabolism for which a previously published method was used[15].

2.3.5 Estimation of THC and 11-OH-THC Depletion Kinetic Parameters

Depletion data were first corrected for any substrate loss observed in "no NADPH" incubations (mean = 3.68%). Then, for data from each set of experiments, a THC (Eq. 1) or 11-OH-THC (Eq. 2) depletion model was simultaneously fitted to the time course of depletion in HIM, in the absence and presence of CYP inhibitors, using nonlinear regression (Phoenix 8.1, Certara (Princeton, NJ). This allowed us to estimate CL via the different CYP pathways. To avoid identifiability issues, the THC CYP2C9 Michaelis-Menten constant (K_m) value was fixed to 70 nM based on our previous estimate of this parameter in human adult liver microsomes obtained under identical incubation conditions[15].

$$\frac{dA_{THC,intestinal}}{dt} = -\left(\frac{V_{max,CYP2C9} * C_{THC}}{K_{m,CYP2C9} + C_{THC}} + CL_{CYP3A} * C_{THC}\right) \quad \text{(Eq. 1)}$$

$$\frac{dA_{11-OH-THC,intestinal,CYP}}{dt} = -(CL_{CYP3A} + CL_{Other\ CYP}) * C_{11-OH-THC} \quad \text{(Eq. 2)}$$

$$\frac{dA_{11-OH-THC,intestinal,UGT}}{dt} = -(CL_{UGT2B7} + CL_{Other\ UGT}) * C_{11-OH-TH} \quad \text{(Eq. 3)}$$

For 11-OH-THC, Eq. 2 was fitted to the CYP-mediated depletion data and Eq. 3 was fitted to the UGT-mediated depletion data. In the above models, CL via CYP2C9, CYP3A, or UGT2B7 was assumed to be completely inhibited (i.e. zero) in the presence of their respective inhibitors[152-155]. This allowed us to estimate CL via the different enzymatic pathways. Then, CL_{int} was estimated using the model predicted CL, fraction unbound in the incubation ($f_{u,inc}$) and microsomal protein amount as shown in Eq. 4. For THC and 11-OH-THC HIM incubations, $f_{u,inc}$ was measured via ultracentrifugation (0.021 and 0.039) and microsomal protein amount was 0.075 mg and 0.225 mg, respectively.

$$CL_{int} = \frac{CL}{f_{u,inc} * \text{mirosomal protein amount}} \quad \text{(Eq. 4)}$$

Unlike the HIM models, the data from all HFLM experiments were simultaneously fitted to the THC depletion (Eq. 5 & 6), 11-OH-THC depletion (Eq. 7 & 8) and 1-OH-MDZ formation (Eq. 9 & 10) in the absence and presence of AZA. This was done to account for incomplete CYP3A inhibition by AZA in HFLM which was estimated as shown in Eq. 11. Then, CL_{int} was estimated using Eq. 4, where the microsomal protein amount was 0.3 mg for both THC and 11-OH-THC incubations. For THC and 11-OH-THC HFLM incubations, $f_{u,inc}$ was measured via ultracentrifugation (0.0024 and 0.013, respectively).

$$\frac{dA_{THC,fetal\ liver}}{dt} = -(CL_{CYP3A} + CL_{Other\ CYP}) * C_{THC} \quad \text{(Eq. 5)}$$

$$\frac{dA_{THC+A\_\_,fetal\ liver}}{dt} = -(CL_{CYP3A} * \text{inhibition correction} + CL_{Other\ CYP}) * C_{THC} \quad \text{(Eq. 6)}$$

$$\frac{dA_{11-OH-THC,fetal\ liver}}{dt} = -(CL_{CYP3A} + CL_{Other\ CYP}) * C_{11-OH-THC} \quad \text{(Eq. 7)}$$

$$\frac{dA_{11-OH-THC+AZ\_\_,fetal\ liver}}{dt} = -(CL_{CYP3A} * \text{inhibition correction} + CL_{Other\ CYP}) * C_{11-OH-THC} \quad \text{(Eq. 8)}$$

$$\frac{dA_{1-OH-MDZ,fetal\ liver}}{dt} = CL_{CYP3A} * C_{MDZ} \quad \text{(Eq. 9)}$$

$$\frac{dA_{1-OH-MDZ+AZA,fetal\ liver}}{dt} = CL_{CYP3A,remaining} * C_{MDZ} \quad \text{(Eq. 10)}$$

$$\text{Fetal liver CYP3A inhibition correction} = \frac{\text{CL}_{\text{CYP3A,remaining}}}{\text{CL}_{\text{CYP3A}}} \quad \text{(Eq. 11)}$$

Goodness of model fits was assessed by evaluating the residual plots and %CV of the estimates (which ranged 14 – 44% indicating excellent to good confidence in the estimates). Data were weighted using iterative reweighted least squares, where weight = $1/(y_{hat}^2)$, to obtain homoscedasticity in the weighted residual plots.

2.3.6 *In Vitro* to *In Vivo* Extrapolation of Kinetic Data

Kinetic parameters estimated from the mathematical models were extrapolated to *in vivo* whole organ clearance values to ascertain the importance of the estimated *in vitro* values. Intestinal (CL_{GI}) and fetal liver (CL_{FH}) clearance were calculated using the well-stirred model (Eq. 12 & 13, respectively).

$$CL_{GI} = \frac{f_{u,b} * CLint * MPPI * Q_{GI}}{f_{u,b} * CLint * MPPI + \ _{GI}} \quad \text{(Eq. 12)}$$

$$CL_{FH} = \frac{f_{u,b} * CLint * MPPGFL * FLW * Q_{FH}}{f_{u,b} * CLint * MPPGFL * FLW + Q_{FH}} \quad \text{(Eq. 13)}$$

Where fraction unbound in blood ($f_{u,b}$) was calculated using the previously reported fraction unbound in plasma ($f_{u,p}$) and blood to plasma ratio (B/P)[15,45]. The calculated $f_{u,b}$ for THC and 11-OH-THCs were 0.016 and 0.019, respectively. Intestinal blood flow (Q_{GI}) is 625 mL/min[156] and total microsomal protein per intestine (MPPI) is 3000 mg protein[157]. It is important to note that we used blood flow for the entire gut, but the actual flow to the mucosa would be much lower resulting in an overall lower CL in the enterocytes than what is estimated here. Fetal liver blood flow (Q_{FH}), 56.1 mL/min, was estimated using the average gestational age of the pooled HFLM as previously described[149]. A microsomal protein per gram fetal liver value (MPPGFL) of 10.1 mg protein/g liver, was calculated using the protein concentrations estimated with the BCA assay and the measured weight of the fetal liver tissue from which the microsomes were isolated. Fetal liver weight (FLW), 8.19 g, was estimated based on gestational

age as previously described[149]. The metabolic fraction that escapes the gut (F_g) and the fraction that escapes the fetal liver (F_{fh}) were calculated using Eq. 14 and the respective CL parameter.

$$F = 1 - \frac{CL}{Q} \quad \text{(Eq. 14)}$$

2.4 Results

2.4.1 THC or 11-OH-THC Depletion Kinetics in Pooled Adult Intestinal Microsomes

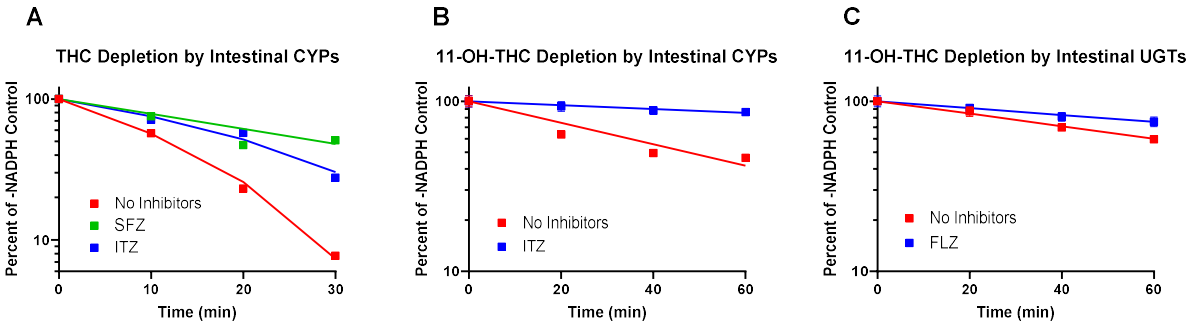

Figure 2.1: Depletion of A) THC (500 nM), and 11-OH-THC (50 nM) by B) CYP and C) UGT enzymes in a representative experiment conducted with pooled human adult intestinal microsomes. Lines indicate model fit to the data normalized to data obtained without NADPH. As demonstrated by CYP-selective inhibitors, extensive metabolism of THC by CYP3A (inhibitor: 2 μM ITZ) and CYP2C9 (inhibitor: 10 μM SFZ) was observed as well as extensive metabolism of 11-OH-THC by CYP3A (inhibitor: 2 μM ITZ) and UGT2B7 (inhibitor: 2.5 mM FLZ). Data shown in B and C are mean ± SD of triplicates. Points that do not have error bars have a small SD that is within the datapoint. Data shown in A are mean of duplicates and therefore do not have error bars. No depletion by CYP1A, CYP2C19, CYP2D6, or FMO enzymes was observed (depletion was not inhibited by inhibitors of these enzymes; data not shown).

At the inhibitor concentrations used, based on published data, we assumed selective and complete inhibition of the respective enzyme[152-155]. Based on these selective inhibitors, HIM extensively metabolized THC via CYP2C9 (SFZ) and CYP3A (ITZ) (Figure 2.1A, Table 2.1) with no involvement by CYP1A, CYP2C19, CYP2D6, FMO, or UGT enzymes (depletion was not inhibited by inhibitors of these enzymes; data not shown). In contrast, HIM extensively metabolized 11-OH-THC via CYP3A (ITZ) and UGT2B7 (FLZ) (Figure 2.1B & 2.1C, Table 2.1) with no involvement by CYP1A, CYP2C9, CYP2C19, CYP2D6, or FMO enzymes (data not

shown). The unsaturated (THC concentration < CYP2C9 K_m) and saturated (THC concentration = 32 µM, maximum solubility in intestinal fed and fasted fluid) CL_{GI} of THC were 442 ± 48 mL/min and 142 ± 53 mL/min, respectively, yielding an F_g of 0.29 ± 0.078 and 0.77 ± 0.085, respectively. Also, the CL_{GI} of 11-OH-THC was 45 ± 6.9 mL/min yielding an F_g of 0.93 ± 0.14.

Table 2.1: Depletion Kinetics of THC and 11-OH-THC in Pooled Human Intestinal Microsomes

	THC				11-OH-THC	
	V_{max} (nmol/min/mg)	**K_m (nM)**	**CL_{int}* (mL/min/mg)**	**f_m**	**CL_{int} (mL/min/mg)**	**f_m**
CYP2C9	2.0 ± 0.72	70 (fixed)	29 ± 10	0.89 ± 0.038	---	---
CYP3A	---	---	3.8 ± 1.7	0.11 ± 0.038	0.41 ± 0.092	0.51 ± 0.11
Total CYP	---	---	33 ± 12	**1.0 ± 0.053**	0.54 ± 0.13	**0.67 ± 0.16**
UGT2B7	---	---	NS	NS	0.20 ± 0.043	0.25 ± 0.053
Total UGT	---	---	NS	NS	0.27 ± 0.037	**0.33 ± 0.046**

Data presented are mean ± SD of independent experiments (n = 3-5), each conducted in duplicate or triplicate. NS = not significant.
*- when CYP2C9 is not saturated; CL_{int} was calculated as depletion $CL/f_{u,inc}$.

2.4.2 THC and 11-OH-THC Depletion Kinetics in Pooled Adult Lung Microsomes

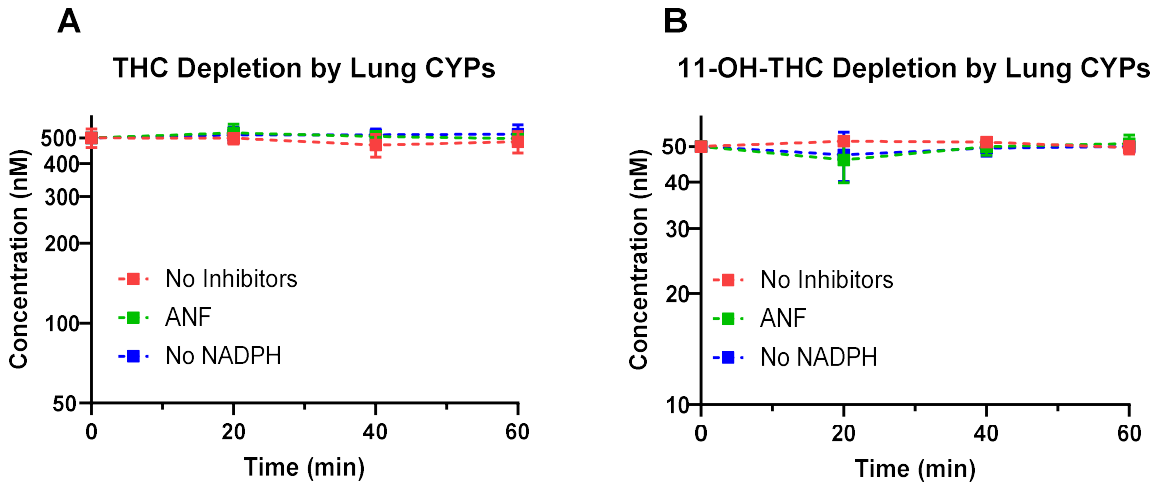

Figure 2.2: Depletion of A) THC (500 nM) or B) 11-OH-THC (50 nM) by CYP enzymes in pooled human adult lung microsomes (cigarette smokers). No significant depletion of THC

or 11-OH-THC was observed in lung microsomes. Data shown are mean ± SD of independent experiments (n = 3), each conducted in duplicate. ANF (3 uM): CYP1A inhibitor.

HLuM did not significantly deplete either THC or 11-OH-THC via CYP metabolism (Figure 2.2). These microsomes demonstrated CYP1A activity as measured by the NADPH-dependent formation of RES from 7-ER which was inhibitable by ANF (Figure S2.1).

2.4.3 THC and 11-OH-THC Depletion Kinetics in Placenta Microsomes

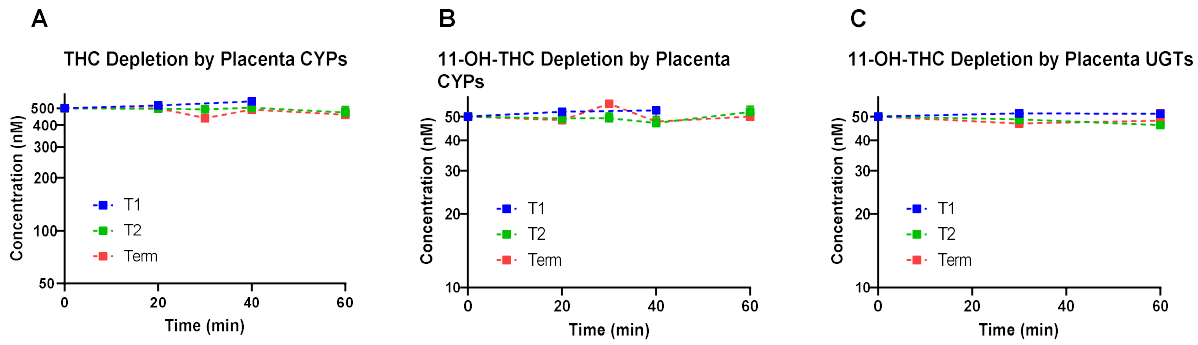

Figure 2.3: Depletion of A) THC (500 nM) or 11-OH-THC (50 nM) by B) CYP or C) UGT enzymes in human T1, T2 and term placental microsomes. No significant depletion of THC or 11-OH-THC was observed in the placental microsomes. Data shown are mean ± SD (where applicable) of 1-4 independent experiments, each conducted in single or duplicate. Microsomes were isolated from T1 placentas (blue, no SD shown) at gestational ages 79 and 96 days, T2 (green, no SD shown for 11-OH-THC UGT depletion) at gestational ages 134, 135 and 137 days, and Term (red, 2 placentas for CYP and 3 for UGT depletion).

HPM (T1, T2 or term placentas) did not significantly deplete either THC or 11-OH-THC via CYP or UGT metabolism (Figure 2.3). As expected, these microsomes demonstrated CYP19 activity as measured by the NADPH-dependent formation of β-estradiol from testosterone (Figure S2.2).

2.4.4 THC and 11-OH-THC Depletion Kinetics in Pooled Fetal Liver Microsomes

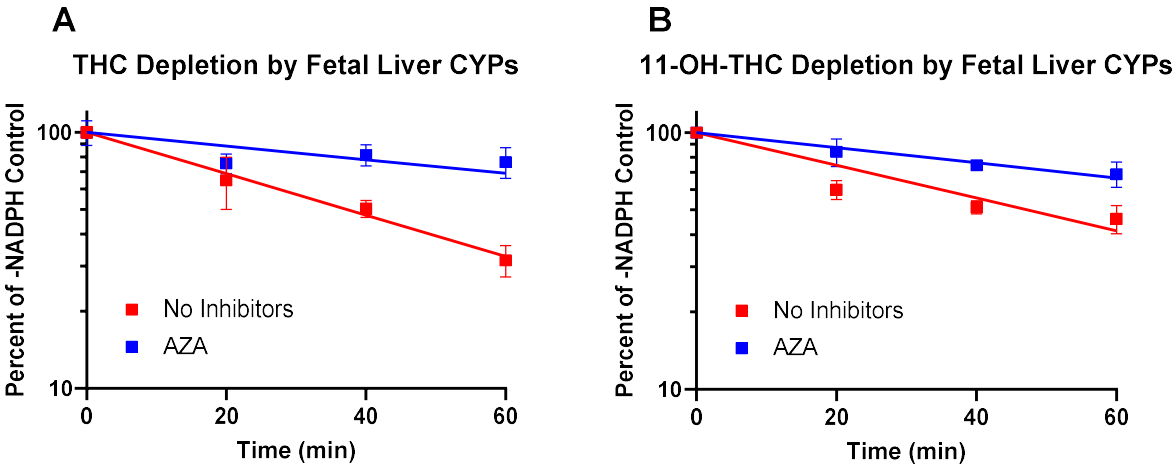

Figure 2.4: Depletion of A) THC (500 nM) or B) 11-OH-THC (50 nM) by CYP enzymes in pooled human fetal liver microsomes. Lines indicate model fit to the data normalized to those obtained without NADPH. Extensive metabolism of THC and 11-OH-THC by CYP3A was observed in the fetal liver microsomes as evidenced by inhibition by AZA (5 μM). Data shown are mean ± SD of 3 independent experiments, each conducted in duplicate. Points that do not have error bars have a small SD that is within the datapoint. No depletion by CYP2C9 or UGT enzymes was observed (depletion was not inhibited by inhibitors of these enzymes; data not shown).

CYP3A was ~67% inhibited by 5 μM AZA based on inhibition of formation of 1-OH-MDZ, from MDZ (Figure S2.3). Similarly, THC depletion in HFLM was not completely inhibited by AZA. Therefore, when estimating the fraction metabolized (f_m) via CYP3A-mediated metabolism of THC and 11-OH-THC, the lack of complete inhibition of CYP3A by AZA was taken into account (see Eq 6, 8, 11). Based on these and other selective inhibitors, HFLM were found to extensively metabolize both THC and 11-OH-THC via CYP3A enzymes (Figure 2.4, Table 2.2) with no involvement by CYP2C9 or UGT enzymes (data not shown). While THC (f_m = 0.99) was predominately metabolized by CYP3A, 11-OH-THC (f_m = 0.80) was extensively metabolized by other unidentified NADPH-mediated (likely CYP) enzyme(s). The CL_{FH} of THC and 11-OH-THC were 8.8 ± 0.49 mL/min and 1.7 ± 0.10 mL/min, respectively, yielding an F_{fh} of 0.84 and 0.97, respectively.

Table 2.2: Depletion Kinetics of THC and 11-OH-THC in Pooled Human Fetal Liver Microsomes

	THC		11-OH-THC	
	CL_{int} (mL/min/mg)	**f_m**	**CL_{int} (mL/min/mg)**	**f_m**
CYP3A	7.6 ± 0.28	0.99 ± 0.06	3.5 ± 0.20	0.80 ± 0.06
Total CYP	7.6 ± 0.36	1	4.4 ± 0.24	1

Data presented are mean ± SD of 4 independent experiments. CL_{int} was calculated as depletion $CL/f_{u,inc}$.

2.5 Discussion

THC and 11-OH-THC were incubated with microsomes at 500 and 50 nM respectively to reflect their maximum circulating plasma concentrations[16] after inhalation (29.3 mg[115]) and oral administration (90 mg[131]) of THC. In the intestine, THC concentrations are likely to be considerably higher than 500 nM as the maximum fed-state simulated intestinal fluid solubility of THC is 36 μM[52]. In the microsomal incubations with THC, formation of 11-OH-THC was not observed. This could be due to either little 11-OH-THC being formed during the short incubation period or rapid sequential metabolism of 11-OH-THC or both. Formation of 11-COOH-THC, a metabolite of 11-OH-THC, was also not observed in any of the THC or 11-OH-THC CYP microsomal incubations, possibly due to limited experimental timeframe employed or the lower abundance of CYP2C9 in intestinal microsomes or both.

In the absence of CYP2C9 inhibition, the depletion of THC in HIM was not log-linear since the slope of the depletion curve increased with time (Figure 2.1A). This was not the case in the presence of CYP2C9 inhibition. These observations are typical of saturable metabolism and consistent with our previous data in human liver microsomes[15], where saturation of CYP2C9 was observed (THC K_m of 70 nM, $K_{m,u}$ of 2.91 nM). Consistent with these data, when THC was incubated at 50 nM, depletion in HIM was found to be log-linear (data not shown). However, further experiments at this concentration were not conducted due to lack of analytical

sensitivity that limited our ability to determine THC depletion with confidence. CYP2C9 is the second most abundant CYP enzyme, after CYP3A, in the human intestine and it has previously been shown to metabolize drugs in HIM[148,158,159]. Therefore, saturable kinetics of CYP2C9 was built into the kinetic model used to fit to the THC depletion data in HIM. When CYP2C9 is partially saturated (e.g. at 10 min in Figure 2.1A), the estimated f_m of CYP2C9 is 0.84 ± 0.081 vs. 0.89 ± 0.038 when unsaturated, and the corresponding estimated f_m of CYP3A is 0.16 ± 0.081 vs. 0.11 ± 0.038.

The slope of 11-OH-THC depletion appears to decrease with time in both the intestinal and the fetal liver microsomes, in each individual experiment as well as the mean data (Figure 2.1B and Figure 2.4B). The basis for this phenomenon is unknown but could be due to declining enzyme activity over time, either from product inhibition or enzyme instability in the incubations. The latter is unlikely, but not impossible, as this has not been observed for other CYP3A substrates[160]. UGTs (f_m = 0.33) also depleted 11-OH-THC in HIM. We have previously shown that recombinant UGT2B7 and UGT1A9, metabolize 11-OH-THC[16]. Here we observed no significant inhibition of 11-OH-THC depletion by NFA, a semi-selective UGT1A9 inhibitor (data not shown). Therefore, we concluded that inhibition of 11-OH-THC metabolism by FLZ (a semi-selective UGT2B7 inhibitor), was entirely due to UGT2B7, an enzyme found in the human intestines[161]. In addition, the CYP inhibitors are not fully selective and there is some cross-inhibition of other CYPs. However, since there was no inhibition seen with any of the inhibitors except ITZ and SFZ, it is unlikely that other CYPs beside CYP3A and CYP2C9 are responsible for THC or 11-OH-THC intestinal depletion. Any cross inhibition between CYP2C9 and CYP3A was corrected for.

Although there was extensive metabolism observed in the HIM, the whole organ CL of THC and 11-OH-THC was approximately 1/3rd and 1/30th of their respective hepatic CL (THC: 1500 mL/min; 11-OH-THC: 1350 mL/min[15]). This is consistent with the lower abundance of CYP2C9 and CYP3A in the intestine (0.0084 and 0.059 nmol/mg protein, respectively) vs. the

liver (0.060 and 0.096 nmol/mg protein, respectively)[158,162] and a lower abundance of intestinal UGTs[148]. Nevertheless, intestinal metabolism could still contribute to the low oral bioavailability of THC by first-pass gut metabolism. Indeed, the estimated F_g of THC (from observed IV and oral administration data), assuming fraction absorbed (F_a) = 1, is 0.17[47,107]. Using a common 20 mg THC oral dose and an average intestinal volume of 250 mL, the THC concentration in the gut would be ~250 μM which exceeds the maximum solubility in fed-state simulated intestinal fluid (~36 μM[52]). The latter would far exceed the CYP2C9 Km (70 nM) and saturate the enzyme resulting in a predicted F_g of THC of 0.77 ± 0.085 due to CYP3A first-pass effect metabolism. This discrepancy, between *in vivo* and *in vitro* estimate of F_g is likely due to F_a of THC being <1 (estimated from these data as ~0.2). We speculate that after oral administration of THC, THC is incompletely absorbed and experiences limited first pass metabolism in the intestine, predominately by CYP3A. Thus, we predict mostly CYP2C9-based DDI at the hepatic level (first pass and systemic) after oral administration of THC. Indeed, CYP2C9 genetic polymorphism (with homozygous *3 alleles) increases oral THC plasma exposure (area under the curve (AUC))[75].

Of the many recombinant enzymes tested, CYP1A1 turnover of THC and 11-OH-THC was the highest per pmol of the CYP enzymes evaluated[16]. Since human lungs (and placentas) express CYP1A1 at relatively high levels[147,163], we speculated that THC would be metabolized in microsomes from these organs. However, no significant THC depletion was observed in lung (from cigarette smokers) and placenta microsomes despite the fact that these microsomes exhibited functional CYP activity. While CYP1A is expressed and active in human lung tissue, its role in *in vivo* lung CYP1A metabolism has never been confirmed[147,164]. Therefore, we conclude that inhaled THC will not undergo first-pass CYP1A metabolism in the lungs.

Data in fetal-catheterized rhesus macaques show that fetal THC plasma AUC is 0.30 of the corresponding maternal plasma AUC[42]. Theoretically, assuming that the plasma protein binding of THC is the same or similar in the maternal and fetal compartment, and if THC is not

effluxed by the placental transporters (P-glycoprotein (P-gp) and breast cancer resistance protein (BCRP)) or metabolized in the placenta or fetal liver, the fetal-maternal unbound plasma AUC ratio (K_p) should be unity[149]. Thus, a ratio of 0.30 suggests possible placental or fetal liver metabolism or placental efflux of the drug. However, data from our laboratory were inconclusive as to whether THC is a substrate of human P-gp or BCRP[96]. Therefore, we speculated that THC is metabolized by either the placenta or the fetal liver or both.

Placentas from women who smoke cigarettes demonstrate increased CYP1A1 enzyme activity and mRNA expression[151,163]. CYP19 is also highly expressed in the placenta[150]. Nevertheless, consistent with our HLuM data and no turnover by recombinant CYP19[16], we found no depletion of THC or 11-OH-THC in human placentas at any gestational age. In contrast, extensive CYP3A-mediated depletion of THC and 11-OH-THC was observed in pooled HFLM. The previously mentioned decreasing slope of 11-OH-THC depletion over time is what likely caused the lower estimated CYP3A f_m of 0.80. If the rate of depletion throughout the experimental run was consistent with the elimination rate within the first 20 minutes (Figure 2.4B), the f_m of CYP3A would have been closer to 0.95. Due to the smaller fetal liver size (compared with maternal liver), we estimated that the fetal hepatic CL of THC and 11-OH-THC was approximately 1/270th and 1/240th of their respective adult hepatic CL, thereby contributing very little to the overall maternal THC CL. Nevertheless, such metabolism could explain a fetal THC K_p of less than unity (observed in macaques) provided the fetal THC CL is significant relative to its transplacental CL (all unbound)[149]. Therefore, it is imperative that we determine the transplacental CL of THC. Such studies are ongoing in our laboratory using the perfused human placenta.

In conclusion, we quantified the enzyme kinetics of THC and 11-OH-THC in extrahepatic tissues (intestine, fetal liver, lung, and placenta). In the intestine, THC (at sub-saturating concentrations) was extensively metabolized by CYP2C9 and CYP3A while 11-OH-THC was extensively metabolized by CYP3A and UGT2B7. In the fetal liver, both compounds were

extensively metabolized by CYP3A. There was no significant metabolism of either cannabinoid in the human lung or placenta. Populating a THC/11-OH-THC PBPK model with the enzyme kinetics estimated here is necessary to predict THC and 11-OH-THC disposition in healthy adults. Once such a PBPK model is verified in healthy adults, it can be used to predict the disposition of these drugs in special populations where enzyme abundances and activities are altered by genetic polymorphism (e.g. CYP2C9 [165]), or physiological changes (e.g. hepatic impairment and pregnancy). The kinetic parameters calculated here and from our ongoing perfused human placenta studies will be used to populate our m-f-PBPK model to predict maternal-fetal exposure to THC and 11-OH-THC PK following both oral and inhalational cannabis use. Such predictions will help assess risk to the fetus after maternal cannabis consumption.

Collaborations: Olena Anoshchenko created the placenta microsomes and Gabriela Patilea-Vrana conducted the placenta microsomal incubations.

2.6 Supplemental Information

Table S2.1: Demographics of the Human Placentas

Subject ID	Gestational Age (days)	Trimester	Fetal Sex (M/F)	Maternal Age (years)	Maternal Ethnicity
PL040	96	T1	M	26	White
PL987	79	T1	Unknown	18	Hispanic
PL037	135	T2	F	33	White
PL041	137	T2	F	Unknown	Unknown
PL946	134	T2	F	21	White/Hispanic
PL1	---	Term	Unknown	Unknown	Unknown
PL5	----	Term	Unknown	Unknown	Unknown
PL6	---	Term	Unknown	Unknown	Unknown

T1: 1 – 97 days; T2: 98 – 195 days; Term: at delivery

Table S2.2: Demographics of Human Fetal Livers

Subject ID	Gestational Age (days)	Trimester	Fetal Sex (M/F)	Maternal Age (years)	Maternal Ethnicity	Alcohol Use (Y/N)
H26872	113	T2	F	32	Black	N
H27078	119	T2	M	26	White	N
H27164	127	T2	F	22	White	N
H27257	113	T2	Unknown	22	Mixed	Y
H27360	115	T2	M	Unknown	Unknown	Unknown
H27723	125	T2	F	Unknown	Unknown	Unknown

T2: 98 – 195 days

Table S2.3: LC-MS/MS parameters of drug quantification

A. LC gradient program

Time (min)	Flow Rate (mL/min)	A (water with 0.1% formic acid, %)	B (acetonitrile with 0.1% formic acid, %)
0	0.3	90	10
0.5	0.3	90	10
2	0.3	5	95
4	0.3	5	95
4.1	0.3	90	10
4.5	0.3	90	10

B. MS/MS parameters

Compound	Parent Ion (m/z)	Product Ion (m/z)	Declustering Potential (V)	Collision Energy (V)	Collision Cell Exit Potential (V)
THC	315.2	193.3	100	33	10
d3-THC	318.3	196.3	100	33	10
11-OH-THC	331.4	193.3	150	35	15
d3-11-OH-THC	334.4	196.3	150	35	15
COOH-THC	345.3	327.3	150	23	15
d3-COOH-THC	348.3	330.3	150	23	15
1-OH-MDZ	342.1	324.0	170	30	20
d4-OH-MDZ	346.1	328.1	170	30	20
RES	214.0	186.0	120	40	10
TOL	271.3	155.0	60	30	6
β-estradiol	255.0	159.1	80	30	9
d4-β-estradiol	259.0	161.0	80	40	9

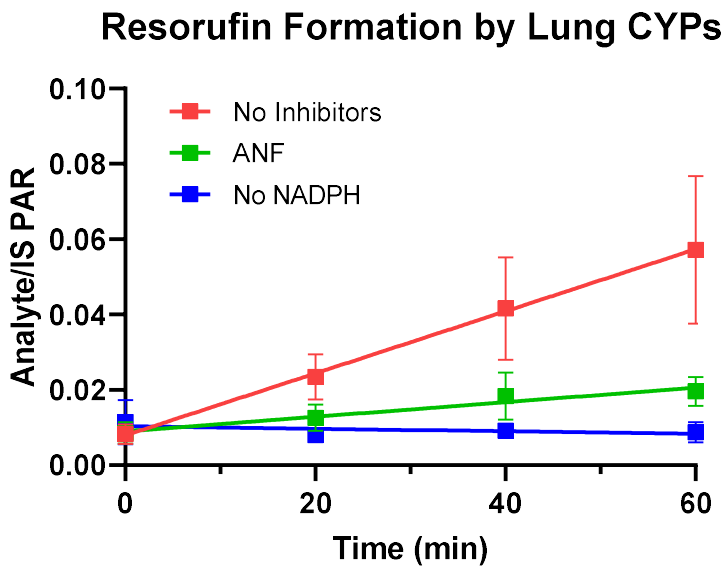

Figure S2.1: Formation of resorufin from 7-ethoxyresorufin in pooled human adult lung microsomes (cigarette smokers). Lines indicate linear regression fit to the data. Formation of resorufin was inhibited by the CYP1A inhibitor, ANF (3 μM), indicating that the HluM demonstrate CYP1A activity. Data shown (peak area ratio of the analyte to the internal standard) are mean of 2 independent experiments, each conducted in duplicate.

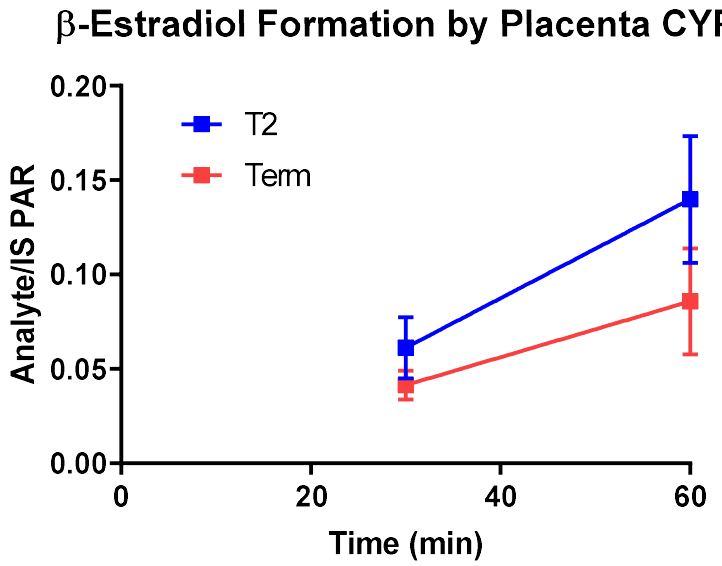

Figure S2.2: Formation of β-Estradiol (CYP19) from testosterone in human T2 and term placental microsomes. Lines indicate linear regression fit to the data. Data shown (as peak area ratio of the analyte to the internal standard) are mean of triplicate incubations from one experiment. Microsomes were isolated from T2 placentas (blue; gestational ages 134 and 135 days), and term (red, one donor).

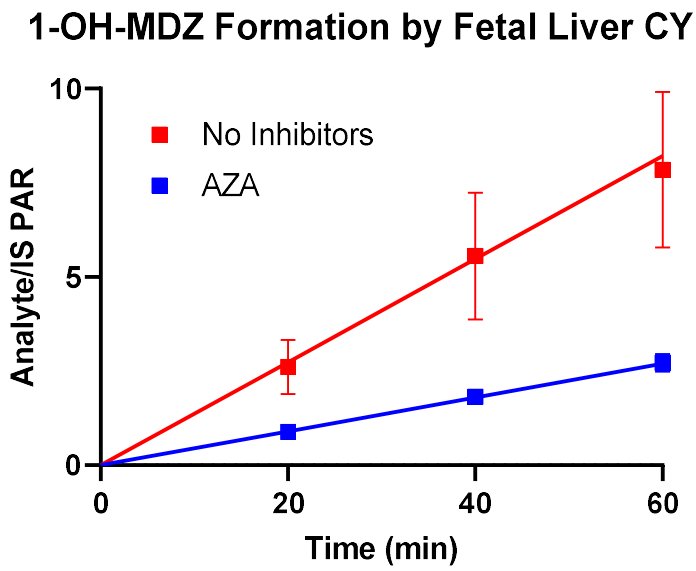

Figure S2.3: Formation of 1-OH-MDZ from MDZ in pooled human fetal liver microsomes. Lines indicate model fit to the data normalized to those obtained without NADPH. Formation of 1-OH-MDZ was inhibited by the CYP3A inhibitor, AZA (5 μM). Data shown (as peak area ratio of the analyte to the internal standard) are mean ± SD of 3 independent experiments, each conducted in duplicate.

Chapter 3: Understanding the Mechanism and Extent of Transplacental Transfer of (-)-Δ^9-Tetrahydrocannabinol (THC) in the Perfused Human Placenta to Predict In Vivo Fetal THC Exposure

The work presented in this chapter was previously published in Clinical Pharmacology and Therapeutics 114(2):446-458(2023)

3.1 Abstract

Cannabis use during pregnancy may cause fetal toxicity driven by in utero exposure to (-)-Δ^9-tetrahydrocannabinol (THC) and its psychoactive metabolite, (±)-11-hydroxy-Δ^9-THC (11-OH-THC). THC concentrations in the human term fetal plasma appear to be lower than the corresponding maternal concentrations. Therefore, we investigated if THC and its metabolites are effluxed by placental transporters using the dual cotyledon, dual perfusion, term human placenta. The perfusates contained THC alone (5 μM) or in combination (100 – 250 nM) with its metabolites (100 nM or 250 nM 11-OH-THC, 100 nM COOH-THC), plus a marker of P-gp efflux (1 or 10 μM saquinavir), and a passive diffusion marker (106 μM antipyrine, AP). All perfusions were conducted with (n = 7) or without (n = 16) a P-gp/BCRP inhibitor, 4 μM valspodar (VSP). Unbound cotyledon clearance indexes (m-f-$CL_{u,c,i}$ and f-m-$CL_{u,c,i}$) were normalized for transplacental AP clearance. At 5 μM THC, the m-f-$CL_{u,c,i}$, 5.1 ± 2.1, was significantly lower than the f-m-$CL_{u,c,i}$, 13 ± 6.1 ($p = 0.004$). This difference remained in the presence of VSP or when the lower THC concentrations were perfused. In contrast, neither metabolite, 11-OH-THC/COOH-THC, had significantly different m-f-$CL_{u,c,i}$ vs. f-m-$CL_{u,c,i}$. Therefore, THC appears to be effluxed by placental transporter(s) other than P-gp/BCRP, while 11-OH-THC and COOH-THC appear to passively diffuse across the placenta. These findings plus our previously quantified human fetal liver clearance, extrapolated to *in vivo,* yielded a THC fetal/maternal steady-state plasma concentration ratio of 0.28 ± 0.09, comparable to that observed *in vivo,* 0.26 ± 0.10.

3.2 Introduction

With expanded legalization, cannabis consumption during pregnancy is rising. Universal drug screening suggests cannabis use and/or exposure in over 22.6% of pregnancies[23], and since 2019 more states have fully legalized cannabis[26] so this value is likely higher today. In utero exposure to (-)-Δ^9-tetrahydrocannabinol (THC), the primary psychoactive compound in the

cannabis plant, and its psychoactive metabolite, (±)-11-hydroxy-Δ^9-THC (11-OH-THC) raises concern with respect to fetal neurodevelopmental risks following cannabis consumption. Studies have associated cannabis use with adverse fetal outcomes including neurodevelopmental deficits, lower birth weight and growth restriction[5,37,166]. For example, observational studies[1-5] have found decreased cognition (e.g. lower verbal or quantitative scores) and increased behavioral issues (e.g. increased hyperactivity) in children whose mothers used cannabis during pregnancy. Although such studies correct for confounding variables including concomitant use of alcohol or tobacco and socioeconomic factors, it is impossible to account for all potential confounders. Additionally, substance use with pregnancy is often self-reported and may not reflect the true amount and potency of cannabis or other illicit drugs utilized by study participants. Therefore, it remains challenging to estimate the actual risks of cannabis use during pregnancy on fetal development, especially because a randomized, controlled, prospective study of THC/11-OH-THC use during pregnancy is unethical[38].

To parse out the actual fetal risks of cannabis use, alternative (though imperfect) options are available to evaluate the potential of THC/11-OH-THC to produce short-term or long-term developmental toxicity through *in vivo* animal and/or *in vitro* experiments[12,41,167]. However, most of these studies are conducted without regard to THC/11-OH-THC concentrations in humans. To inform *in vivo* animal and *in vitro* studies, it is important to first ascertain maternal and fetal exposure to THC/11-OH-THC throughout pregnancy at recreational doses used by pregnant people.

Interestingly, fetal exposure to THC and its secondary metabolite (±)-11-nor-9-carboxy-Δ^9-THC (COOH-THC) is much lower than the corresponding maternal exposure, in both non-human primates and humans. The THC fetal/maternal plasma area under the curve ($AUC_{0\text{-inf}}$) ratio (K_p) is 0.30 ± 0.17 in a catheterized maternal-fetal macaque model[42] and is consistent with the sparse (n = 3) human umbilical vein/maternal plasma concentration ratio data at term, THC: 0.26 ± 0.10 and COOH-THC: 0.24 ± 0.15[43]. Theoretically, for drugs that passively diffuse across

the placenta, this ratio for the unbound drug ($K_{p,uu}$) should be one. Provided that the binding of the drug to maternal and fetal plasma proteins does not differ by much, the corresponding bound plus unbound (i.e. total) K_p value should also equal one. Therefore, the decreased K_p observed in non-human primates and humans could be due to efflux transport at the placenta barrier or metabolism in the placenta or fetal organs (e.g. liver) or all of the above. Indeed, data in mice which are naturally deficient of P-glycoprotein (P-gp), an efflux transporter, suggest that THC is a substrate of P-gp[17]. P-gp, along with other efflux transporters such as breast cancer resistance protein (BCRP), is expressed in the apical membrane of the syncytiotrophoblasts at the human placental barrier[97]. To confirm if THC is a substrate of the human P-gp, BCRP or both, we conducted *in vitro* experiments in our laboratory using P-gp or BCRP-overexpressing cells using the Transwell or the cell accumulation assay. However, the results were not definitive. With the Transwell assay, due to THC's extensive intracellular binding, we could not quantify THC in the receiver compartment. Similarly, due to its high lipophilicity, we could not discern any efflux of THC in the cell accumulation assay[96]. Therefore, here we used the dual-cotyledon, dual perfusion term human placenta model to determine if THC, 11-OH-THC, and/or COOH-THC are effluxed by P-gp/BCRP and, if they are, to quantify their efflux clearance and predict their *in vivo* K_p.

3.3 Materials and Methods

3.3.1 Chemicals and Reagents

THC, d3-THC, 11-OH-THC, COOH-THC, SAQ, and d9-SAQ were purchased from Cayman Chemicals (Ann Arbor, MI). AP, tolbutamide (TOL), VSP, d3-11-OH-THC, d3-COOH-THC, and ethylenediaminetetraacetic acid (EDTA) were purchased from Sigma-Aldrich (St. Louis, MO). Low-binding microcentrifuge tubes were purchased from Genesee Scientific (San Diego, CA). BSA (Fraction V - heat-shock treated), sodium phosphate, sucrose, acetonitrile, hexanes, ethyl acetate, formic acid (liquid chromatography-mass spectrometry (LC-MS/MS

grade)), acetic acid (LC-MS/MS grade), polycarbonate ultracentrifuge tubes, silanized glass culture tubes, LC glass inserts, and LC pre-split snap caps were purchased from Fisher Scientific (Hampton, NH).

3.3.2 Cotyledon Perfusions

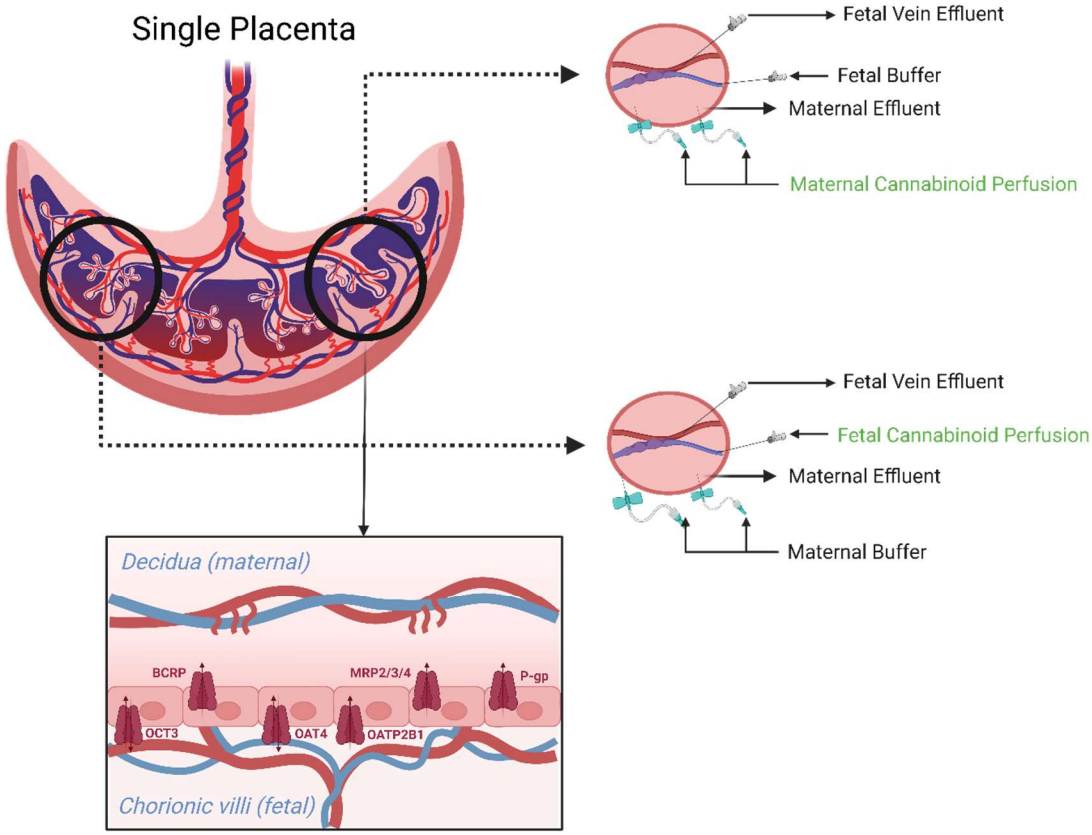

Figure 3.1: THC (Arms 1 and 2) or THC + 11-OH-THC + COOH-THC (Arm 3), saquinavir (SAQ) and antipyrine (AP) were perfused in a single-pass mode through two cotyledons isolated from each placenta. One cotyledon was perfused with drugs via the intervillous space (A) while the second cotyledon was perfused with the drugs via the fetal artery (B). Arm 2 perfusates also contained valspodar (VSP). Effluent (maternal and fetal) samples were collected at multiple timepoints throughout the perfusion and placental tissue was sampled at the end of the perfusion from the intervillous space, medial between the chorionic plate to decidua, to measure drug concentrations. Figure Inset: Efflux transporters expressed on the apical membrane (P-gp, BCRP, MRP2/3/4, etc.) and influx transporters expressed on the basal membrane (OCT3, OAT4, OATP2B1, etc.) can actively transport drugs out of and into the syncytiotrophoblast, respectively, thereby reducing fetal drug exposure.

Placentas were acquired following IRB approval and written informed consent at Madigan Army Medical Center (WA). Placentas (n = 23) from term donors with no known history of tobacco or drug use, were collected within 30 minutes of cesarean delivery (see Table S3.1 for demographics). The perfusion system and procedure were as previously described with some modification to the experimental design[168-170]. Briefly, two cotyledons were excised from each placenta and cannulated for simultaneous single pass perfusion for 2-4 hours in both the intervillous space (maternal side) and the fetal main artery at rates of 10 and 4 mL/min, respectively. The perfusate consisted of oxygenated HBSS buffer containing 0.2 g/dL bovine serum albumin (BSA), 2000 U/L sodium heparin and 5 mg/mL gentamicin, buffered to pH 7.4 and maintained at 37°C. In each experiment, cotyledons were acclimated for 1 hour then randomized to receive perfusate containing the mixture of drugs via the intervillous space or fetal main artery in order to assess passage from maternal to fetal (m-f) and fetal to maternal (f-m) compartments, respectively (Figure 3.1). The study was split into three arms and the drug mixture was as follows for each arm. Arm 1 (n = 8): 5 μM THC, a P-gp transporter marker (1 or 10 μM saquinavir (SAQ))[171,172], and a passive diffusion marker (106 μM antipyrine (AP))[173]; Arm 2 (n = 7): 5 μM THC, 1 μM SAQ, 106 μM AP, and a P-gp/BCRP/MRP4 inhibitor (4 μM valspodar (VSP)); Arm 3 (n = 8): 100 or 250 nM THC/11-OH-THC, 100 nM COOH-THC, 1 μM SAQ, and 106 μM AP. At the 4 μM concentration, VSP is predicted to completely inhibit P-gp (IC_{50} = 0.016 μM) and BCRP (IC_{50} = 1.4 μM), and partially inhibit MRP4 (IC_{50} = 6.2 μM)[174].

Effluents were collected at multiple timepoints (0, 15, 30, 45, 60, 90, 120, 150, 180, 240 min) depending on the duration of each experiment. At the end of each experiment, biopsies from the intervillous space, medial between the chorionic plate to decidua, (~1 cm x 0.5 cm x 0.5 cm) were flash frozen in liquid nitrogen along with tissue samples collected from fresh cotyledons. Tissue samples were homogenized in buffer (1:9) containing 20 mM sucrose, 50 mM Kpi, and 10 mM EDTA with a Bead Ruptor Homogenizer (Omni International, Kennesaw, GA). In Arms 1 and 2, effluent and tissue homogenate samples (100 μL) were processed by

adding 300 µL of acetonitrile containing 100 nM internal standard (d3-THC, d3-11-OH-THC, d3-COOHTHC, d9-SAQ, and TOL) and were centrifuged at 18,000 x g and 4°C for 10 minutes. 100 µL of the supernatant was stored at -20°C in LC glass inserts until analysis by LC-MS/MS. The drug concentration in tissue samples was normalized to the measured perfusate concentration. In Arm 3, where drug concentrations were below the limit of quantification using the above protein precipitation method, a liquid-liquid extraction/concentration method was used, where 1 mL of effluent samples, in 20 mL silanized glass culture tubes, was spiked with 10 µL of acetonitrile containing 2 µM internal standard, 100 µL of 1.68% formic acid in water, and 5 mL of 5:1 hexane:ethyl acetate. Samples were vortexed at each spiking step for 5 seconds and placed on a shaker for 30 min after the addition of hexane:ethyl acetate. Samples were removed from the shaker and centrifuged at 200 x g at room temperature for 10 minutes. The organic supernatant (5 mL) was pipetted into another silanized glass culture tube and evaporated under nitrogen at 40°C. Then, the samples were reconstituted with 100 µL acetonitrile, vortexed for 20 seconds and then transferred to LC glass inserts and stored at -20°C until analysis by LC-MS/MS.

3.3.3 Estimation of the Transplacental Kinetics of the Drugs

Transplacental clearances were estimated from drug concentrations in the fetal vein (CL_{mf}) and intervillous space (CL_{fm}) effluents opposite to the respective maternal and fetal compartments receiving the drugs. The area under the drug concentration-time curve from time 0 to the last measured time point (AUC_{last}) was estimated using the trapezoidal rule (Phoenix 8.1, Certara (Princeton, NJ)). The amount of drug “excreted” (A_e) into the “receiver” side (i.e. fetal or maternal effluent for m-f and f-m perfusions, respectively), was calculated using Eq. 1 where Q_r is the flow rate on the receiver side (4 or 10 mL/min for m-f and f-m perfusions, respectively).

$$A_e = AUC_{last} * Q_r \quad \text{(Eq. 1)}$$

Then, the unbound cotyledon clearances, $CL_{u,mf,c}$ and $CL_{u,fm,c}$, were calculated (Eq. 2 & 3).

$$CL_{u,mf,c} = \frac{A_{e,f}}{AUC_{last,m} * f_{u,perf,m}} \quad \text{(Eq. 2)}$$

$$CL_{u,fm,c} = \frac{A_{e,m}}{AUC_{last,f} * f_{u,perf,f}} \quad \text{(Eq. 3)}$$

AP passively diffuses across the placenta and therefore should have the same unbound CL in both directions. However, we observed that these CLs were not equal, suggesting difference in perfused surface area between the cotyledon where the m-f-CL and the cotyledon where f-m-CL was measured. To account for this difference and to reduce inter-cotyledon CL variability of the test drugs, their estimated unbound CLs were normalized to that of AP to obtain their $CL_{u,c}$ indexes ($CL_{u,c,i}$) (Eq. 4).

$$CL_{u,c,i} = \frac{THC,\ 11\text{-}OH\text{-}THC,\ COOH\text{-}THC\ or\ SAQ\ CL_{u,c}}{AP\ CL_{u,c}} \quad \text{(Eq. 4)}$$

Lastly, the $CL_{u,c,i}$ ratio was calculated (Eq. 5) to determine if it deviated from unity.

$$CL_{u,c,i}\ ratio = \frac{CL_{u,mf,c,i}}{CL_{u,fm,c,i}} \quad \text{(Eq. 5)}$$

3.3.4 Prediction of *In Vivo* K_p of THC

Whole placenta clearances were calculated in both the m-f ($CL_{mf,placenta}$; Eq. 6) and f-m ($CL_{fm,placenta}$; Eq. 7) directions by multiplying the $CL_{u,c}$ by the fraction unbound in plasma ($f_{u,p}$; THC: 0.011[15] & SAQ: 0.02[175]) and adjusting for the relative weight of the cotyledon and average weight of the term placenta (reported 590 g[176]). Cotyledon weight was measured and where it was not, the average cotyledon weight in our experiments was used.

$$CL_{mf,placenta} = \left(f_{u,p} * CL_{u,mf,c}\right) * \frac{placenta\ weight}{cotyledon\ weight} \quad \text{(Eq. 6)}$$

$$CL_{fm,placenta} = \left(f_{u,p} * CL_{u,fm,c}\right) * \frac{placenta\ weigh}{cotyledon\ weigh} \quad \text{(Eq. 7)}$$

$CL_{mf,placenta}$ was assumed to represent passive diffusion CL minus efflux transport CL of the drug (if any) while $CL_{fm,placenta}$ was assumed to represent only passive diffusion CL of the

drug, which is supported by the SAQ data where $CL_{fm,placenta}$ did not change with and without VSP. Since the AP transplacental CL was not the same in the m-f and f-m directions, when calculating the efflux transport ($CL_{T,placenta}$) and passive diffusion ($CL_{PD,placenta}$) of the drugs (Eq. 10 and 11), we accounted for this difference in passive diffusion CL of AP (Eq. 8 and 9).

$$AP_{mf}\ correction\ factor = \frac{AP\ CL_{u,mf.c}}{(AP\ CL_{u,mf,c}+AP\ CL_{u,fm,c})/2} \quad \text{(Eq. 8)}$$

$$AP_{fm}\ correction\ factor = \frac{AP\ CL_{u,fm.c}}{(AP\ CL_{u,mf,c}+AP\ CL_{u,fm,c})/2} \quad \text{(Eq. 9)}$$

$$CL_{T,placenta} = \frac{CL_{fm,placenta}}{AP_{fm}\ correction\ factor} - \frac{CL_{mf,placenta}}{AP_{mf}\ correction\ factor} \quad \text{(Eq. 10)}$$

$$CL_{PD,placenta} = \frac{CL_{mf,placenta}}{AP_{mf}\ correction\ factor} + CL_{T,placenta} = \frac{CL_{fm,placenta}}{AP_{fm}\ correction\ factor} \quad \text{(Eq. 11)}$$

The *in vivo* K_p can be calculated using the estimated $CL_{T,placenta}$ and $CL_{PD,placenta}$, the previously published *in vivo* estimated fetal hepatic CL (CL_{FH})[7], placenta metabolic CL ($CL_{m,placenta}$) and the potential placenta influx CL ($CL_{influx,placenta}$) of THC (Eq. 12). Due to a lack of significant $CL_{m,placenta}$[7] and no data to suggest $CL_{influx,placenta}$, the *in vivo* K_p of THC was then calculated with a simplified equation (Eq. 13) using the estimated $CL_{T,placenta}$ and $CL_{PD,placenta}$, and the previously published *in vivo* estimated fetal hepatic CL (CL_{FH})[7] of THC as follows:

$$K_p = \frac{CL_{PD,placenta}+C\ _{influx,placenta}}{CL_{PD,placenta}+2*CL_{FH}+CL_{T,placenta}+CL_{m,placenta}+C\ _{FH}*\left(\frac{CL_{T,placenta}+CL_{m,placenta}}{CL_{PD,placenta}}\right)} \quad \text{(Eq. 12)}$$

$$K_p = \frac{CL_{PD,placenta}}{CL_{PD,placenta}+2*CL_{FH}+CL_{T,placenta}+\left(\frac{CL_{T,placenta}*\ CL_{FH}}{CL_{PD,placenta}}\right)} \quad \text{(Eq. 13)}$$

Finally, the fraction of THC and SAQ effluxed (f_t) by the placenta was then calculated using the resulting $CL_{T,placenta}$ and $CL_{PD,placenta}$. (Eq. 14)

$$f_t = CL_{T,placenta}/(CL_{T,placenta} + CL_{PD,placenta}) \quad \text{(Eq. 14)}$$

3.3.5 Protein Binding of the Drugs in the Effluent Samples

For Arms 1 and 2, to determine the unbound drug concentration in representative maternal effluent and fetal vein effluent containing BSA, samples at the beginning (30 min) and

end (90 min) of each experiment were analyzed. For Arm 3, only 90 min effluent samples were quantified, and they were spiked with 1 μM THC, 11-OH-THC, and COOH-THC to ensure quantifiability in the fraction containing the unbound drug. Samples (180 μL) were ultracentrifuged in duplicate using a Sorval Discovery M150 SE centrifuge and a S100-AT3 rotor (Thermo Scientific) at 435,000 x g (100,000 rpm) for 90 min at 37°C. An identical second set of samples was incubated in the ultracentrifuge tubes for 90 min at 37°C without centrifugation to determine the total drug concentration and to account for any non-specific drug binding. The supernatant (50 μL) from ultracentrifuged samples and an aliquot (50 μL) from non-centrifuged samples was added to internal standard (100 μL) and centrifuged at 18,000 x g and 4°C for 10 minutes. The supernatant (60 μL) was stored at -20°C in LC glass inserts until analyzed by LC-MS/MS. Fraction unbound in perfusion ($f_{u,perf}$) was calculated as the ratio of drug concentration in the supernatant of ultracentrifuged sample (unbound concentration) and the aliquot in the non-centrifuged sample (total concentration).

3.3.6 LC-MS/MS Analysis

The concentration of all the drugs in the effluent and tissue samples were determined by injecting 10 μL of the processed samples onto an Acquity ultra-performance liquid chromatography (UPLC) system (Waters Corporation, Milford, MA) coupled to an AB Sciex Triple Quadrupole 6500 in ESI mode (SCIEX, Framingham, MA) or Waters Xevo Triple Quadrupole XS in APCI mode (Waters Corporation, Milford, MA), for Arms 1 and 2 or 3, respectively. Acquity UPLC ethylene bridged hybrid (BEH) C18 column (1.7 μM 2.1 x 50 mm) attached to a BEH C18 5 mm guard column (Waters Corporation, Milford, MA) was used for chromatographic separation with a mobile phase flow rate of 0.3 mL/min. The mobile phase consisted of acetonitrile and water containing 0.1% formic acid (Arms 1 and 2) or 0.2% acetic acid (Arm 3) as the organic and aqueous phases, respectively. The chromatographic LC-MS/MS conditions used are provided in Table S3.2. Integration of the chromatographic peaks was performed using Analyst v1.6.2 (SCIEX, Framingham, MA) for Arms 1 and 2 and

TargetLynx v4.2 (Waters Corporation, Milford, MA) for Arm 3. Buffer and placenta homogenate quality control samples at low, medium and high concentrations within the calibration curve were used to ensure reproducible results. The calibration curves were fitted with a linear regression and using a $1/x^2$ weighting scheme. For Arms 1 and 2 where protein precipitation was used, quality control samples at concentrations of 9.8, 156 and 5000 nM THC/SAQ (calibration curve range 9.8 – 5000 nM) and 3.1, 12.5 and 100 μM AP (calibration curve range 3.1 – 100 μM) were within ± 20% of the expected values. For Arm 3 where LLE was used, quality control samples at concentrations of 0.5, 12.5 and 250 nM THC (calibration curve range 0.25 – 250 nM), 2.5, 12.5 and 250 nM 11-OH-THC (calibration curve range 2.5 – 250 nM), 1, 5 and 100 nM COOH-THC (calibration curve range 0.05 – 10 nM), 10, 50 and 1000 nM SAQ (calibration curve range 10 – 1000 nM), and 0.5, 5 and 100 μM AP (calibration curve range 0.5 – 100 μM) were within ± 20% of the expected values.

3.3.7 Data Analyses

Pairwise comparison of $CL_{u,c,i}$ and cotyledon tissue concentrations between m-f and f-m perfusions in each placenta were conducted using the one-tailed, Wilcoxon signed rank test. A one-tailed test was used as our *a priori* hypothesis was that the maternal-to-fetal cannabinoid $CL_{u,c,i}$ will be significantly less than the fetal-to-maternal $CL_{u,c,i}$. When evaluating non-paired samples such as assessing $CL_{u,c,i}$ between 1 vs. 10 μM SAQ perfusions or with and without VSP or comparing cotyledon tissue concentrations with and without a 10 minute washout period post-perfusion, a two-tailed, Mann-Whitney test was used. For comparisons across all three arms of the study, such as comparison of THC $CL_{u,c,i}$ ratio and f_t, a Kruskal-Wallis test was utilized. Lastly, when comparing the fetal arteriole pressures across time, for the duration of the perfusion, for m and f perfusions in each arm, a Friedman test was used. An alpha value of 0.05 was used as a cutoff for significance for all aforementioned tests. All data are presented as mean ± SD.

3.4 Results

3.4.1 THC and SAQ Transplacental Kinetics with and without VSP

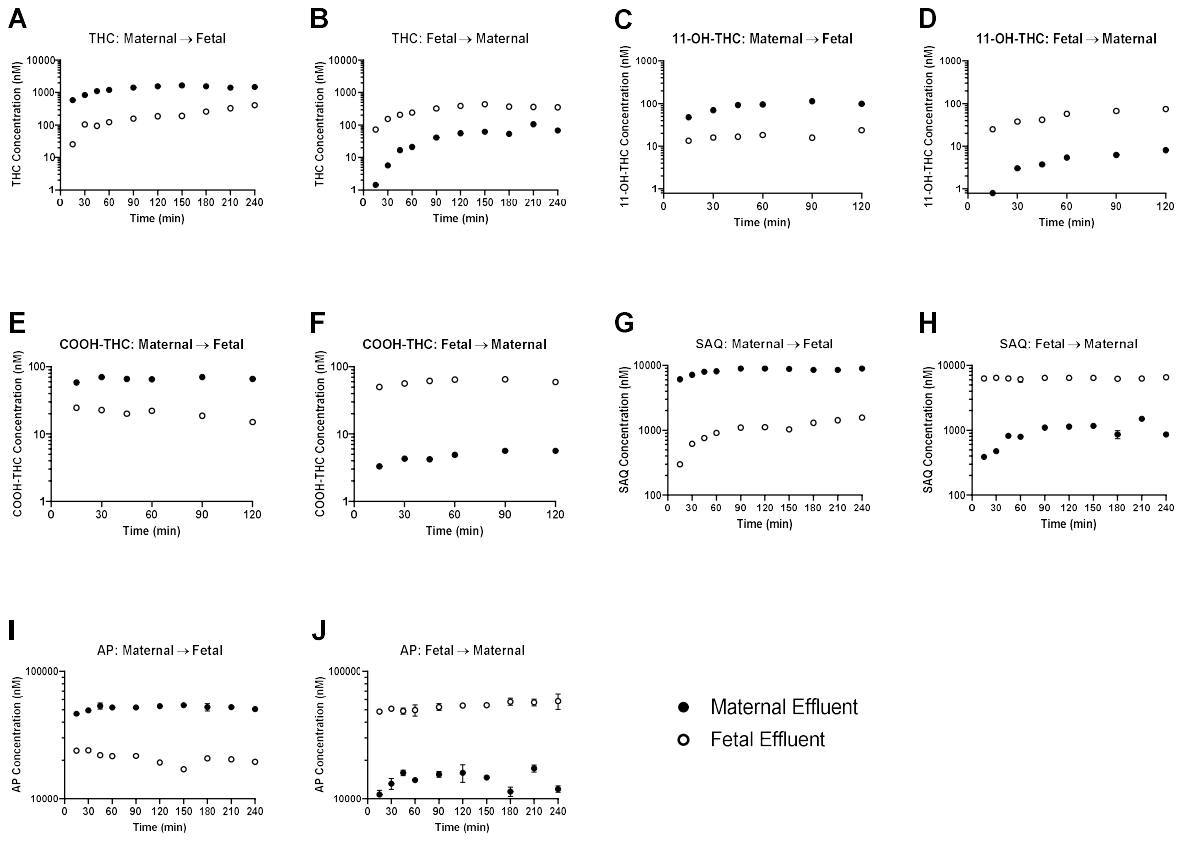

Figure 3.2: Representative maternal and fetal effluent concentration vs. time profiles for 5 µM THC (A and B), 250 nM 11-OH-THC (C and D), 100 nM COOH-THC (E and F), 10 µM SAQ (G and H), and 106 µM AP (I and J) in the maternal-fetal and fetal-maternal direction, respectively. THC, SAQ, and AP data shown are mean ± SD of quadruplicate LC-MS/MS determinations (in some case the SD are within the symbol) from placenta 5 while 11-OH-THC and COOH-THC data shown are mean of duplicate LC-MS/MS determinations from placenta 21 over their respective duration of perfusions.

No pressure changes in the fetal artery were observed during any of the experimental arms, indicating that direct drug exposure or transfer from the maternal space does not alter fetal vascular tone within 240 minutes of exposure (Table S3.3). THC (Figure 3.2A & 3.2B), 11-OH-THC (Figure 3.2C & 3.2D), COOH-THC (Figure 3.2E & 3.2F), SAQ (Figure 3.2G & 3.2H), and AP (Figure 3.2I & 3.2J) concentrations on the donor side reached steady-state within the

first hour of perfusion. The concentrations on the receiver side approached or reached steady-state rapidly for AP or much later for THC, 11-OH-THC, COOH-THC, and SAQ. The initial five perfusions of Arm 1 revealed that steady-state was reached for all the drugs within 120 min and therefore all subsequent experiments and analyses were limited to this timeframe. In addition, neither 11-OH-THC nor COOH-THC was detected in the effluents or placental tissue samples from Arms 1 and 2 perfusions, consistent with our previous finding of lack of THC metabolism in the placenta[7].

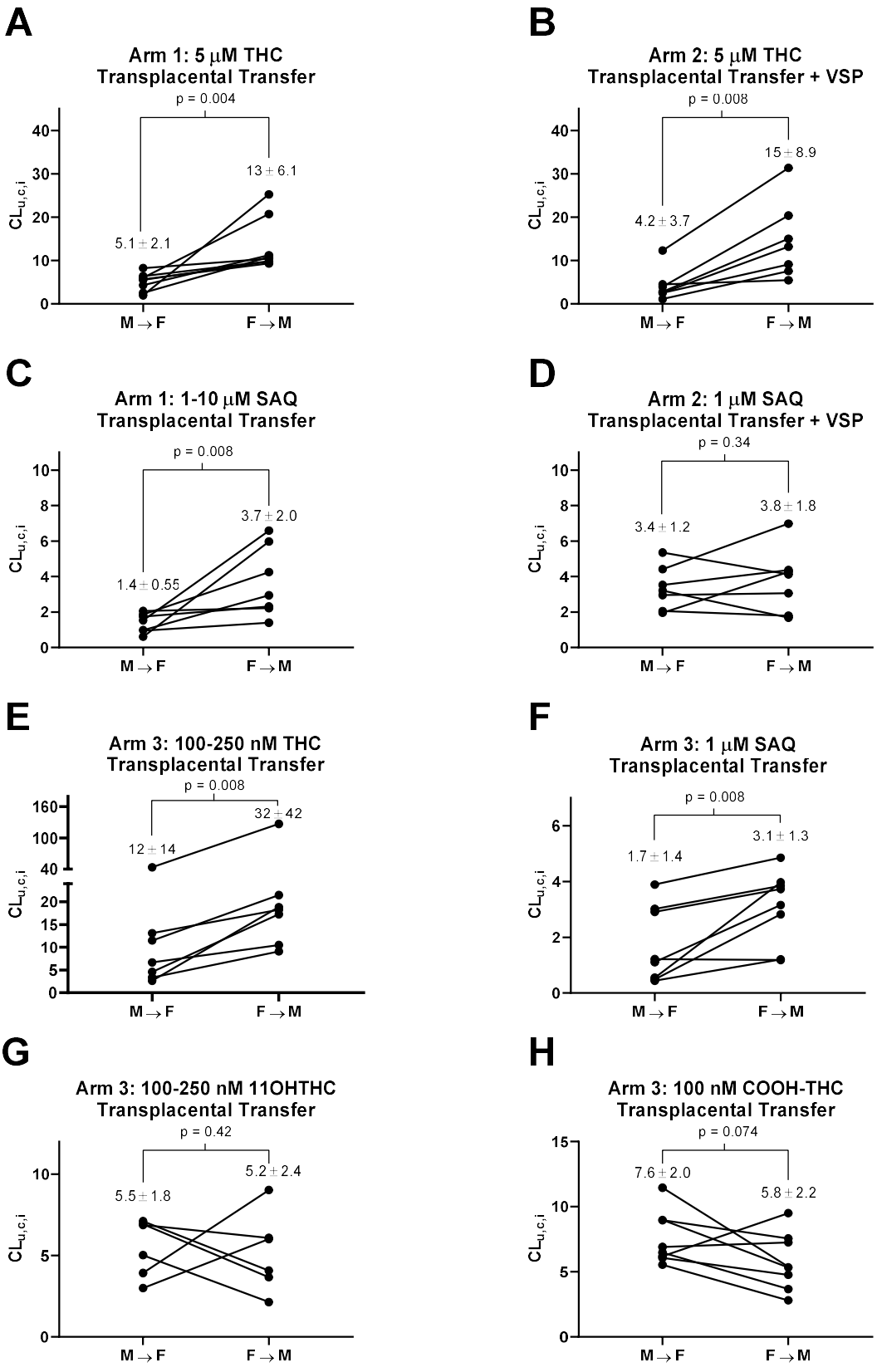
A
Arm 1: 5 μM THC
Transplacental Transfer
p = 0.004
13 ± 6.1
5.1 ± 2.1
B
Arm 2: 5 μM THC
Transplacental Transfer + VSP
p = 0.008
15 ± 8.9
4.2 ± 3.7
C
Arm 1: 1-10 μM SAQ
Transplacental Transfer
p = 0.008
3.7 ± 2.0
1.4 ± 0.55
D
Arm 2: 1 μM SAQ
Transplacental Transfer + VSP
p = 0.34
3.8 ± 1.8
3.4 ± 1.2
E
Arm 3: 100-250 nM THC
Transplacental Transfer
p = 0.008
32 ± 42
12 ± 14
F
Arm 3: 1 μM SAQ
Transplacental Transfer
p = 0.008
3.1 ± 1.3
1.7 ± 1.4
G
Arm 3: 100-250 nM 11OHTHC
Transplacental Transfer
p = 0.42
5.2 ± 2.4
5.5 ± 1.8
H
Arm 3: 100 nM COOH-THC
Transplacental Transfer
p = 0.074
5.8 ± 2.2
7.6 ± 2.0
CLu,c,i
M → F
F → M

Figure 3.3: $CL_{u,mf,c,i}$ for high (A) and low (E) THC concentration as well as SAQ (C & F) were significantly lower than their corresponding $CL_{u,fm,c,i}$. With inhibition of P-gp, BCRP, MRP4 by VSP, THC's $CL_{u,mf,c,i}$ remained significantly lower than its $CL_{u,fm,c,i}$ (B) while, as expected, SAQ $CL_{u,c,i}$ equalized (i.e. no longer significantly different (D)). 11-OH-THC (G) and COOH-THC (H) $CL_{u,mf,c,i}$ was not significantly different than its $CL_{u,fm,c,i}$. The $CL_{u,c,i}$ values were compared with a one-tailed, Wilcoxon signed rank test. Data shown are mean ± SD (n = 6 – 8; individual values listed in Tables 3.1 – 3.3).

Arms 1 & 2: In the absence of VSP, both THC (5 μM perfusions) and SAQ had a significantly lower $CL_{u,mf,c,i}$ relative to $CL_{u,fm,c,i}$ (Figure 3.3A & 3.3C, Table 3.1 & 3.2), with a $CL_{u,c,i}$ ratio for THC and SAQ of 0.45 ± 0.24 (Table 3.1) and 0.49 ± 0.30 (Table 3.2), respectively. In the presence of VSP, THC's $CL_{u,mf,c,i}$ remained significantly lower than the $CL_{u,fm,c,i}$ (Figure 3.3B) and the $CL_{u,c,i}$ ratio remained less than 1 (0.32 ± 0.24; Table 3.1). In contrast, in the presence of VSP, SAQ's $CL_{u,mf,c,i}$ and $CL_{u,fm,c,i}$ were no longer significantly different (Figure 3.3D) and its $CL_{u,c,i}$ ratio equalized (1.0 ± 0.48; Table 3.2).

Arm 3: At the reduced perfusate drug concentration (100 – 250 nM), THC had a significantly lower $CL_{u,mf,c,i}$ relative to $CL_{u,fm,c,i}$ (Figure 3.3E, Table 3.1), with a $CL_{u,c,i}$ ratio of 0.43 ± 0.21 (Table 3.1). 11-OH-THC's (100 – 250 nM) and COOH-THC's (100 nM) $CL_{u,mf,c,i}$ and $CL_{u,fm,c,i}$ were not significantly different (Figure 3.3G and 3.3H, Table 3.3) with a $CL_{u,c,i}$ ratio of 1.3 ± 0.78 and 1.5 ± 0.52 (Table 3.3), respectively.

For all the above perfusions, as anticipated, AP's $CL_{u,mf,c}$ was not significantly different from $CL_{u,fm,c}$ with or without VSP (Table S3.7).

Table 3.1: Estimates of THC $CL_{u,mf,c,i}$, $CL_{u,fm,c,i}$, the ratio of these indexes as well as CL associated with transport ($CL_{T,placenta}$) and passive diffusion ($CL_{PD,placenta}$) across the placentas in the absence (Arms 1 and 3) and presence of VSP (Arm 2)

Placenta ID	$CL_{u,mf,c}$ (mL/min)	$CL_{u,fm,c}$ (mL/min)	$CL_{u,mf,c,i}$	$CL_{u,fm,c,i}$	$CL_{u,c,i}$ ratio	$CL_{T,placenta}$ (mL/min)	$CL_{PD,placenta}$ (mL/min)	f_t
Arm 1: 5 μM THC Concentration Without VSP								
1	4.9	17	5.6	9.8	0.57	1.5	3.5	0.30
2	12	55	6.1	21	0.29	9.5	13	0.41
3	17	30	6.4	9.8	0.66	2.7	7.7	0.26
4	21	21	8.3	10	0.79	1.3	6.5	0.17
5	8.7	24	5.7	9.3	0.61	2.1	5.4	0.28
6	5.3	18	4.3	11	0.38	1.9	3.3	0.37
7	5.9	12	2.6	11	0.24	2.8	3.9	0.41
8	3.1	29	2.0	25	0.078	15	16	0.49

Mean ± SD	**9.7 ± 6.3**	**26 ± 13**	**5.1 ± 2.1[*]**	**13 ± 6.1[*]**	**0.45 ± 0.24[&]**	**4.6 ± 5.0**	**7.5 ± 4.7**	**0.34 ± 0.10[$]**
Arm 2: 5 μM THC Concentration With VSP (4 μM)								
9	2.0	15	1.1	7.6	0.15	3.5	4.1	0.46
10	4.0	42	3.9	20	0.19	9.1	12	0.43
11	12	4.9	4.5	5.5	0.83	2.0	3.6	0.36
12	22	49	12	31	0.39	16	25	0.40
13	4.9	13	2.5	13	0.19	5.9	7.2	0.45
14	8.2	7.7	2.6	9.1	0.28	5.7	6.8	0.45
15	2.5	18	2.8	15	0.19	2.6	5.2	0.34
Mean ± SD	**8.0 ± 7.0**	**21 ± 17**	**4.2 ± 3.7[^]**	**15 ± 8.9[^]**	**0.32 ± 0.24[&]**	**6.4 ± 4.9**	**9.1 ± 7.4**	**0.41 ± 0.050[$]**
Arm 3: 100 – 250 nM THC[**] Concentration Without VSP								
16	48	127	43	127	0.34	31	40	0.43
17	25	43	13	18	0.72	5.6	14	0.29
18	3.6	46	2.6	19	0.14	9.0	10	0.46
19	18	30	6.7	10	0.64	2.4	6.1	0.28
20	32	63	12	21	0.54	14	22	0.39
21	6.8	15	4.6	17	0.27	3.4	5.0	0.41
22	1.8	19	3.4	9.1	0.37	4.4	6.0	0.43
23[&&]	NA	NA	NA	NA	NA	NA	NA	NA
Mean ± SD	**19 ± 17**	**49 ± 38**	**12 ± 14[#]**	**32 ± 42[#]**	**0.43 ± 0.21[&]**	**10 ± 10**	**15 ± 13**	**0.38 ± 0.072[$]**

[**]All placentas were perfused with 250 nM THC except 16 and 17 which were perfused with 100 nM; m-f and f-m $CL_{u,c,i}$ were compared with a one-tailed Wilcoxon signed rank test: [*]p-value = 0.004, [^]p-value = 0.008, [#]p-value = 0.008; $CL_{u,c,i}$ ratio and f_t were compared across all three arms with a Kruskal-Wallis test: [&]p-value = 0.47, [$]p-value = 0.27; [&&]data for placenta 23 were not available because THC was inadvertently omitted from this experiment

Table 3.2: Estimates of SAQ $CL_{u,mf,c,i}$, $CL_{u,fm,c,i}$, the ratio of these indexes as well as CL associated with transport ($CL_{T,placenta}$) and passive diffusion ($CL_{PD,placenta}$) across the placentas in the absence (Arm 1) and presence of VSP (Arm 2)

Placenta ID	$CL_{u,mf,c}$ (mL/min)	$CL_{u,fm,c}$ (mL/min)	$CL_{u,mf,c,i}$	$CL_{u,fm,c,i}$	$CL_{u,c,i}$ ratio	$CL_{T,placenta}$ (mL/min)	$CL_{PD,placenta}$ (mL/min)	f_t
Arm 1: 1 – 10 μM SAQ[**] Concentration Without VSP								
1	0.87	5.0	0.98	2.9	0.33	1.3	1.9	0.40
2	1.9	3.7	0.94	1.4	0.67	0.54	1.6	0.25
3[&]	NA	NA	NA	NA	NA	NA	NA	NA
4	4.3	4.6	1.7	2.3	0.75	0.65	2.6	0.20
5	3.2	5.8	2.1	2.2	0.93	0.16	2.3	0.065
6	0.74	9.5	0.61	6.0	0.10	2.8	3.2	0.47
7	4.3	4.8	1.9	4.3	0.44	1.3	2.8	0.31
8	2.4	7.6	1.5	6.6	0.23	6.6	7.5	0.47
Mean ± SD	**2.5 ± 1.5**	**5.9 ± 2.0**	**1.4 ± 0.55[*]**	**3.7 ± 2.0[*]**	**0.49 ± 0.30**	**1.9 ± 2.2**	**3.1 ± 2.0**	**0.31 ± 0.15**
Arm 2: 1 μM SAQ Concentration With VSP (4 μM)								
9	3.7	3.6	2.1	1.8	1.1	N/A	1.7	N/A
10	2.0	8.7	2.0	4.3	0.46	N/A	4.6	N/A
11	15	3.7	5.4	4.1	1.3	N/A	5.0	N/A
12	7.7	11	4.4	7.0	0.63	N/A	9.9	N/A
13	5.7	2.9	3.0	3.1	0.97	N/A	3.0	N/A
14	10	1.4	3.2	1.7	1.9	N/A	2.3	N/A
15	3.2	5.3	3.5	4.4	0.81	N/A	2.8	N/A
Mean ± SD	**6.8 ± 4.5**	**5.2 ± 3.4**	**3.4 ± 1.2[^]**	**3.8 ± 1.8[^]**	**1.0 ± 0.48**	**N/A[$]**	**4.2 ± 2.8**	**N/A[$]**
Arm 3: 1 μM SAQ Concentration Without VSP								
16	4.3	4.8	3.9	4.9	0.80	1.3	2.8	0.31
17	5.5	8.8	2.9	3.7	0.78	1.8	5.1	0.27
18	0.67	6.8	0.49	2.8	0.17	2.4	2.8	0.45
19	2.9	9.1	1.1	3.2	0.35	2.2	3.3	0.40
20	8.5	11	3.0	3.8	0.78	3.4	7.2	0.32
21	0.82	3.5	0.55	4.0	0.14	1.7	2.1	0.46
22	0.64	2.5	1.2	1.2	1.0	0.40	1.4	0.22
23	0.56	4.0	0.44	1.2	0.37	1.0	1.5	0.40

Mean ± SD	**3.0 ± 2.9**	**6.4 ± 3.1**	**1.7 ± 1.4[#]**	**3.1 ± 1.3[#]**	**0.55 ± 0.33**	**1.8 ± 0.92**	**3.3 ± 2.0**	**0.35 ± 0.087**

[**]all placentas were perfused with 1 μM SAQ except placenta 1 – 5 which were perfused with 10 μM; m-f and f-m $CL_{u,c,i}$ were compared with a one-tailed Wilcoxon signed rank test: [*]p-value = 0.008, [^]p-value = 0.34, [#]p-value = 0.008; [&]values for placenta 3 were not available because SAQ was inadvertently omitted from this experiment; [$]SAQ was not effluxed in the presence of VSP. N/A = not available.

Table 3.3: Estimates of 11-OH-THC and COOH-THC $CL_{u,mf,c,i}$, $CL_{u,fm,c,i}$, and the ratio of these indexes in the absence of VSP

Placenta ID	$CL_{u,mf,c}$ (mL/min)	$CL_{u,fm,c}$ (mL/min)	$CL_{u,mf,c,i}$	$CL_{u,fm,c,i}$	$CL_{u,c,i}$ ratio
Arm 3: 100 – 250 nM 11-OH-THC[**] Concentration					
16	11	ND	9.8	ND	ND
17	14	9.6	7.1	4.1	1.7
18	4.1	15	3.0	6.0	0.50
19	18	11	6.9	3.7	1.9
20	19	18	6.9	6.1	1.1
21	5.8	7.8	3.9	9.0	0.43
22	1.5	ND	2.8	ND	ND
23	6.3	7.1	5.0	2.1	2.4
Mean ± SD	**11 ± 6.7**	**11 ± 4.2**	**5.5 ± 1.8[*]**	**5.2 ± 2.4[*]**	**1.3 ± 0.78**
Arm 3: 250 nM COOH-THC Concentration					
16	10	7.5	9.0	7.6	1.2
17	17	13	9.0	5.3	1.7
18	8.5	23	6.2	9.5	0.65
19	30	16	11	5.4	2.1
20	17	14	6.1	4.8	1.3
21	10	6.3	6.9	7.3	0.95
22	2.9	6.0	5.5	2.8	2.0
23	8.2	12	6.5	3.7	1.8
Mean ± SD	**13 ± 8.4**	**12 ± 5.7**	**7.6 ± 2.0[^]**	**5.8 ± 2.2[^]**	**1.5 ± 0.52**

[**]All placentas were perfused with 250 nM 11-OH-THC except 16 and 17 which were perfused with 100 nM; m-f and f-m $CL_{u,c,i}$ were compared with a one-tailed Wilcoxon signed rank test: [*]p-value = 0.42, [^]p-value = 0.074; ND = clearance values not determined as the effluent concentrations were below limit of quantification. Mean and SD values do not include placentas that had ND values

3.4.2 THC and SAQ Placental Transport ($CL_{T,placenta}$), Passive Diffusion CL ($CL_{PD,placenta}$) and fraction transported (f_t)

At the 5 μM perfusate concentration and in the absence of VSP, THC's $CL_{T,placenta}$ (4.6 ± 5.0) and $CL_{PD,placenta}$ (7.5 ± 4.7) yielded a f_t of 0.34 ± 0.10 (Table 3.1) and did not change in the presence of VSP (f_t = 0.41 ± 0.050). At the reduced THC perfusate concentration (100 – 250 nM) the estimated f_t of THC remained the same (0.38 ± 0.072) (Table 3.1). The corresponding f_t of SAQ in the absence (Arm 1/Arm 3) and presence of VSP (Arm 2) was 0.31 ± 0.15/0.35 ± 0.087 and 0, respectively (Table 3.2).

3.4.3 THC and SAQ Cotyledon Tissue Concentrations

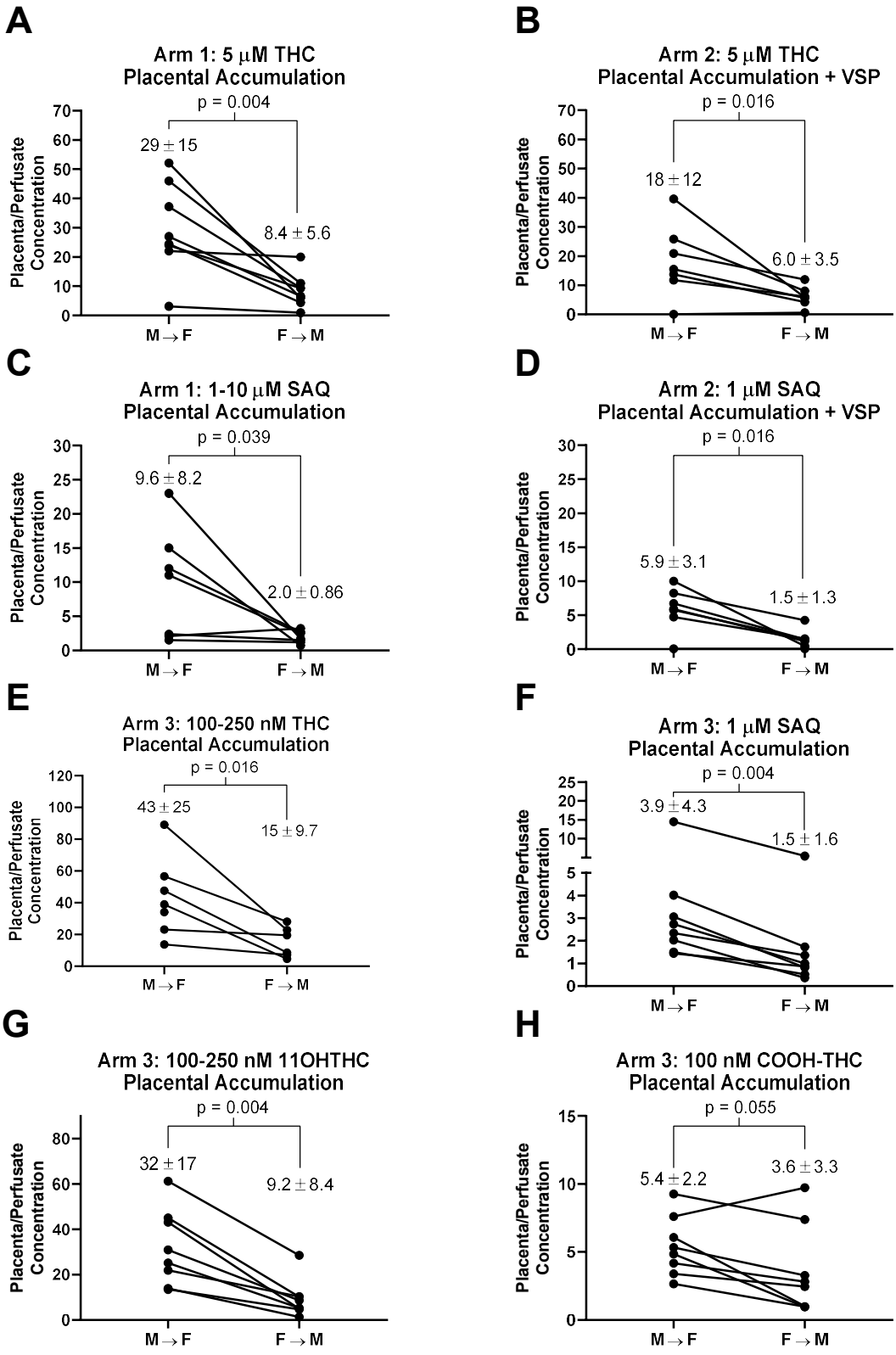

Figure 3.4: After Arm 1 and 2 perfusions, the THC (A, B) and SAQ (C, D) placental accumulation (normalized to the donor perfusate concentration) was significantly higher after the m-f vs. f-m perfusions in the absence or presence of VSP. After Arm 3 perfusions, THC (E), SAQ (F) and 11-OH-THC (G) placental accumulation (normalized to the donor perfusate concentration) was significantly higher after the m-f vs. f-m perfusions while COOH-THC (H) placental accumulation trended towards significance. Cotyledon tissue biopsies were taken post-perfusion from each cotyledon. Placental accumulations were compared with a one-tailed, Wilcoxon signed rank test. Data shown are mean ± SD (n = 7 – 8).

No drug was detected in the fresh placenta tissue samples collected before the perfusions. The placental concentration normalized to the donor perfusate concentration in Arms 1 and 2 of both THC (5 μM) and SAQ in tissue samples collected at the end of each experiment was higher for m-f vs. f-m perfused cotyledons, with and without VSP (Figure 3.4A-D). The cotyledon tissue biopsies from the first 5 placentas were taken directly after the conclusion of the perfusions. However, to confirm that the high amount of THC in the tissue was not due to residual drug-containing perfusate in the tissue the remaining placentas were washed for 10 minutes with drug-free buffer prior to the tissue biopsy sampling. We did not see a significant difference in the THC cotyledon concentrations with or without washing (Mann-Whitney test, p = 0.79 and 0.14 for mf and fm, respectively) and therefore combined the results. Similar data were obtained in the Arm 3 perfusions (Figure 3.4E – H), for all four drugs: THC, 11-OH-THC, COOH-THC, and SAQ.

3.5 Discussion

To reduce inter-placental variability in estimating transplacental drug clearance, two cotyledons from each placenta were perfused on the same day in the m-f and f-m direction, respectively. We included in our perfusates a prototypic P-gp substrate (SAQ) and a passive diffusion marker (AP) and compared transplacental transfer of the drugs in the absence and presence of the pan P-gp, BCRP, and MRP4 inhibitor, VSP. This combination of drugs enabled us to obtain interpretable data on whether THC and its metabolites are effluxed by the placental P-gp/BCRP. The SAQ concentration (10 μM) was chosen (for the first 5 placentas) based on

previous studies that reported an average $CL_{c,i}$ ratio of 0.11[171,172,177,178], and this concentration is below its K_m (~15 μM) for P-gp[179,180] (SAQ is not a substrate of BCRP[181]). Nevertheless, to ensure that P-gp was not saturated, SAQ's concentration was decreased to 1 μM for the remaining 18 placentas because our LC-MS/MS assay had the sensitivity to do so. Based on the observation that the $CL_{u,c,i}$ ratios between the 1 and 10 μM concentrations were not significantly different (Mann-Whitney test, p = 0.11), we combined the results. In Arms 1 and 2, THC was perfused at a targeted 5 μM concentration (actual total and unbound concentration 4.2 ± 1.0 μM and 239 ± 143 nM, respectively). The unbound maximum adult plasma concentration of THC *in vivo* after 5 mg IV, 19 mg inhalational, or 20 mg oral consumption is ~7.6, 2.7, and 0.2 nM, respectively[182]. The concentrations in these initial perfusions were supra-pharmacological to ensure that we could quantify THC in both the maternal and fetal effluents. To verify that THC concentrations in Arm 1 were not saturating transplacental transfer, subsequent perfusions (Arm 3) were conducted at lower concentrations (target 100 – 250 nM, actual total and unbound concentration of 166 ± 63 and 11 ± 4.8 nM, respectively). These unbound maximum THC plasma concentrations are comparable to those after 5 mg THC IV dosing. Our assay sensitivity did not allow lowering the perfusate concentrations further.

Theoretically, a drug such as AP that passively diffuses across the placenta, the $CL_{u,mf,c}$ and $CL_{u,fm,c}$ should not be significantly different. In practice, we observed that AP CLs are often different (Table S3.7), perhaps due to differences in the surface area perfused between the cotyledons. Therefore, it is customary to normalize for this difference by expressing the $CL_{u,mf,c}$ and $CL_{u,fm,c}$ of the drugs of interest (THC, 11-OH-THC, COOH-THC, and SAQ) as $CL_{u,c,i}$ (Eq. 4)[171-173,177].

For drugs actively effluxed by the placenta, the $CL_{u,mf,c,i}$ should be significantly lower than the $CL_{u,fm,c,i}$ and the $CL_{u,c,i}$ ratio should be significantly less than 1. Indeed, this was the case for SAQ and as expected, the addition of VSP equalized the $CL_{u,mf,c,i}$ and $CL_{u,fm,c,i}$ (Figure 3.3C, 3.3D, 3.3F and Table 3.2). These results confirmed both functional and inhibitable P-gp activity

in the *ex vivo* perfused cotyledons. In Arm 1, at 5 μM, THC also exhibited a significantly lower $CL_{u,mf,c,i}$ than its corresponding $CL_{u,fm,c,i}$ and the $CL_{u,c,i}$ ratio was significantly less than 1 (Figure 3.3A and Table 3.1). Analogous to SAQ, these results suggest THC is also effluxed by the human placenta. However, with Arm 2, in contrast to SAQ, the $CL_{u,c,i}$ for THC did not equalize in the presence of VSP (Figure 3.3B). We also found that THC transplacental transfer was not concentration dependent with the $CL_{u,c,i}$ ratios and f_t values that were not significantly different between Arms 1 – 3 (Table 3.1). While the mean THC $CL_{u,c,i}$ values were higher in each direction for Arm 3 than the other arms, this was primarily driven by placenta 16. In addition, the mean values were not significantly different across arms (Kruskal-Wallis test, p = 0.12 and 0.47 for mf and fm, respectively). THC binding to tubing was also examined and we observed negligible loss along maternal and fetal lines that could not account for the above differences (percent drug remaining at cotyledon insertion compared to drug in perfusate reservoir: m = 79%, f = 78%). Unlike THC, 11-OH-THC and COOH-THC did not have significantly different $CL_{u,mf,c,i}$ and $CL_{u,fm,c,i}$ (Figure 3.3G and 3.3H, Table 3.3) and thereby appear to only passively diffuse across the placenta. At first glance, the lack of efflux of COOH-THC seems to contradict our *in vitro* findings, using BCRP overexpressing cells, that COOH-THC is a weak substrate of BCRP[96]. But, when a transporter is overexpressed *in vitro*, transport of a drug can be discerned even if it is a weak substrate of the transporter. However, *in vivo*, due to the lower abundance of the same transporter (e.g. in the placenta), such transport may not be observed. We believe that this is the most likely explanation for the discrepant results.

There are several possible explanations for the observed difference in THC transplacental clearances: 1) THC is effluxed by an apical efflux or basal influx transporter(s) of the syncytiotrophoblast not inhibited by VSP. Indeed the placenta expresses several other drug transporters; basal influx: OAT4, OCT3, and OATP2B1; apical efflux: MRP2/3/4[97]. Of note, OCT3 and OAT4 have been shown to be bi-directional transporters. However, based on the molecular profile of these transporters[183], THC is unlikely to be a substrate, and there is no

evidence to suggest otherwise. 2) THC is transported by P-gp but binds at a transport site unaffected by VSP. P-gp has been shown to have multiple binding sites and does demonstrate substrate-dependent inhibition[184-186]. 3) THC binds and is sequestered within the intervillous space to a greater extent than the fetal (vascular) compartment. The intervillous space is rich with structural components such as marginal sinuses, chorionic villi, and connective tissue where THC can bind, which are lacking on the fetal side[187]. Hence the reduced m-f CL (vs. f-m CL) observed for THC may not result from placental efflux but rather from loss of the drug due to extensive binding of THC along the intervillous space prior to reaching the syncytiotrophoblast where the placental transporters are located. Indeed, we observed a greater accumulation of THC within the placental tissue in the m-f as compared to f-m perfusions, in the presence and absence of VSP and at the higher and lower concentrations (Figure 3.4A, 3.4B, 3.4E). However, this differential binding should theoretically occur when the drug from the f-m perfusions reaches the maternal side as well. Importantly, any potential loss or non-specific binding to tissue should abate once steady-state is reached (i.e. when binding equilibrium is reached). In addition, 11-OH-THC and COOH-THC which also have a high degree of non-specific binding and greater tissue accumulation in the m-f vs. f-m perfusions (Figure 3.4G and 3.4H) similar to THC, displayed no significant difference between $CL_{u,mf,c,i}$ and $CL_{u,fm,c,i}$, which suggests that the tissue binding cannot account for the difference in THC transplacental clearance. Furthermore, we see the same trend in SAQ placental accumulation with and without VSP even though the observed difference in $CL_{u,c,i}$ is abolished by VSP. For these reasons, we consider the differential binding hypothesis to be unlikely. Thus, we conclude that either 1) an unknown apical efflux or basal influx transporter(s), unaffected by VSP, or 2) P-gp, which was not inhibited at THC's active site, effluxes THC as the most plausible explanations. Future experiments that could provide some clarity are: 1) perfuse the placenta with cold (4°C) buffer to reduce transporter activity and therefore confirm that our observations are due to efflux transport of THC; and 2) perfuse the placenta with a cocktail of P-gp/BCRP inhibitors (e.g. VSP,

elacridar, tariquidar, zosuquidar, Ko143) to mitigate the possibility of substrate-dependent inhibition of P-gp by VSP.

To utilize the transplacental CLs of THC to predict the *in vivo* K_p (Eqs. 12 and 13), the placental and fetal CL of THC must be estimated. Since metabolism is the likely pathway for these CLs, we previously determined the depletion of THC in microsomes prepared from human placenta and fetal livers[7]. THC is not significantly depleted (or metabolized) by CYP or UGT enzymes in human placenta of any gestational age[7]. However, THC is significantly depleted by CYP3A7 in the 2nd trimester fetal liver[7]. Therefore, using the extrapolated placenta transport CL and passive diffusion CL from all three arms, in conjunction with the previously calculated fetal metabolism data[7], we estimated the THC K_p (0.23 ± 0.08)[188]. The predicted K_p is not substantially different from and remarkably similar to the previously observed THC human umbilical venous/maternal plasma ratio at term (0.26 ± 0.10)[43]. This congruence supports the utility of this approach to predict *in vivo* human fetal exposure to THC at term. Importantly, THC is bound to albumin and apolipoproteins in the plasma[62], which respectively have higher and lower concentration, at term, in fetal plasma vs. maternal plasma[189]. However, here we have assumed no difference in overall binding of THC between the maternal and fetal compartments. Notably, the observed *in vivo* COOH-THC K_p was 0.24 ± 0.15 and yet we observed no efflux transport of this cannabinoid. This could be explained by potential metabolism in the placenta or fetal organs, which is yet to be investigated.

To predict fetal toxicity from the psychoactive cannabinoids THC/11-OH-THC, in utero exposure, in particular to the fetal CNS, must be determined. The availability of human fetal tissue (for research purposes) is limited to single time-points at pregnancy termination (e.g. 1st and 2nd trimester), insufficient to obtain dynamic, time-dependent, THC/11-OH-THC brain concentrations across gestational ages. However, such concentrations can be predicted using our maternal-fetal PBPK model[149]. To do so, amongst other physiological and drug-dependent parameters, the m-f-PBPK model would need to be populated with gestational-age dependent

THC/11-OH-THC $CL_{T,placenta}$, $CL_{PD,placenta}$, and placental/fetal liver metabolic clearance. While we have estimated the metabolic CLs in the placenta and the fetal liver, due to experimental limitations, THC transplacental clearances from perfusions can only be obtained in term placentas. This obstacle can be overcome if the transporter mediating the efflux of THC is identified. Then, such predictions can be made by scaling for the placenta transporter expression across gestational age as we have done for other drugs[190].

In conclusion, we quantified the transplacental kinetics of THC, 11-OH-THC, and COOH-THC in the *ex vivo* perfused human term placenta. THC appears to be actively effluxed by the human placenta and not inhibitable by a P-gp/BCRP antagonist, VSP, congruent with previous results *in vitro* and *in vivo* in animals in our lab[96]. In contrast, the metabolites 11-OH-THC and COOH-THC passively diffused across the placenta. The *ex vivo* extrapolated THC K_p is in excellent agreement with the observed *in vivo* K_p[43]. Populating a m-f-PBPK model with the placental transfer kinetics estimated here is necessary to dynamically predict fetal THC, 11-OH-THC, and COOH-THC exposure at term. If the transporter(s) responsible for our observations is identified, the efflux can be scaled using the placental transporter abundance at different gestational ages to predict fetal THC exposure throughout pregnancy[97]. This is crucial for predicting the disposition of THC in diverse populations where transport abundance and/or activity may be altered by genetic polymorphisms, physiologic changes, fetal sex or the presence of drug-drug interactions. The m-f-PBPK-predicted pharmacologically relevant fetal plasma and tissue concentrations can then be used to assess (*in vitro* or through animal studies) fetal neurodevelopmental risk after maternal cannabis consumption.

Collaborations: Nicholas Ieronimakis, Emily D. Sheikh, Joshua W. Monson, Sarah E. Ligon, Rebecca L. Talley, Elisabeth M. Dornisch, Kamy J. Howitz, and Jennifer R. Damicis collected placentas and conducted perfusions.

3.6 Supplemental Information

Table S3.1: Demographic Information of the Perfused Placentas

		Arm 1 (5 μM THC Concentration Without VSP) n = 8	Arm 2 (5 μM THC Concentration With VSP, 4 μM) n = 7	Arm 3 (100 – 250 nM THC Concentration Without VSP) n = 8	
Maternal Race	**White**	6 (75%)	6 (86%)	5 (62.5%)	Data are n (%)
	African American	0 (0%)	1 (14%)	1 (12.5%)	
	American Indian	0 (0%)	0 (0%)	0 (0%)	
	Asian or Pacific Islander	1 (12.5%)	0 (0%)	1 (12.5%)	
	Other	1 (12.5%)	0 (0%)	1 (12.5%)	
Baby Sex (male ♂; female ♀)		3 (38%) ♂ 5 (62%) ♀	2 (28%) ♂ 5 (72%) ♀	2 (25%) ♂ 6 (75%) ♀	
Diabetic		0 (0%)	1 (14%)*	0 (0%)	
Tobacco / drug / alcohol use **		None	None	None	
Gravidity		3 ± 1	3 ± 1	3 ± 2	Data are mean ± SD
Parity		2 ± 1	2 ± 0.8	2 ± 1	
Maternal age (years)		30 ± 6.8	28 ± 6.7	31 ± 3.4	
BMI at delivery (kg/m^2)		33 ± 5.0	38 ± 7.7	27 ± 6.3	
Gestational age at delivery (weeks)		39 ± 0.17	39 ± 0.80	39 ± 0.24	
Birth weight (g)		3283 ± 330	3382 ± 473	3529 ± 395	

*Type A1 gestational diabetes. ** Self-reported

All placentas were from C-sections

Table S3.2: LC-MS/MS parameters for Drug Quantification

A. LC gradient program

Time (min)	Flow Rate (mL/min)	A (water with 0.1% formic acid, %)	B (acetonitrile with 0.1% formic acid, %)
0	0.3	90	10
0.5	0.3	90	10
2	0.3	5	95
4	0.3	5	95
4.1	0.3	90	10
4.5	0.3	90	10

B. ESI MS/MS parameters

Compound	Parent Ion (m/z)	Product Ion (m/z)	Declustering Potential (V)	Collision Energy (V)	Collision Cell Exit Potential (V)
THC	315.2	193.3	60	30	10
d3-THC	318.3	196.3	60	30	12
11-OH-THC	331.4	193.3	150	35	15
d3-11-OH-THC	334.4	196.3	150	35	15
COOH-THC	345.3	327.3	150	23	15
d3-COOH-THC	348.3	330.3	150	23	15
SAQ	671.0	128.0	80	70	10
d9-SAQ	680.2	128.0	80	50	10
AP	189.2	77.0	60	30	8
TOL	271.3	155.0	60	30	6

C. APCI MS/MS parameters

Compound	Parent Ion (m/z)	Product Ion (m/z)	Collision Energy (V)
THC	315.3	193.2	22
d3-THC	318.3	196.3	20
11-OH-THC	331.3	193.2	26
d3-11-OH-THC	334.3	196.3	26
COOH-THC	345.3	327.3	20
d3-COOH-THC	348.3	330.3	20
SAQ	671.0	570.0	30
d9-SAQ	680.2	570.0	32
AP	189.2	77.0	22
TOL	271.3	155.0	16

Table S3.3: Fetal Arteriole Pressures (mmHg) Throughout each Perfusion

	Arm 1: 5 μM THC Concentration Without VSP		Arm 2: 5 μM THC Concentration With VSP (4 μM)		Arm 3: 100 – 250 nM THC Concentration Without VSP	
	M*	F**	M#	F##	M^	F^^
Mounting	44 ± 11	49 ± 10	42 ± 10	38 ± 5.3	35 ± 7.1	33 ± 7.4
Acclimation end	38 ± 7.1	40 ± 9.4	32 ± 6.8	34 ± 6.9	30 ± 4.9	30 ± 6.4
0 min	36 ± 7.0	39 ± 9.2	32 ± 5.1	34 ± 6.8	31 ± 3.5	30 ± 5.6
15 min	36 ± 8.2	41 ± 5.8	33 ± 5.8	36 ± 10	32 ± 5.7	30 ± 5.3
30 min	36 ± 6.2	42 ± 6.7	33 ± 6.3	35 ± 10	31 ± 4.9	29 ± 5.6
45 min	36 ± 6.1	42 ± 7.0	33 ± 6.9	37 ± 10	31 ± 4.8	29 ± 5.3
60 min	37 ± 10	42 ± 7.3	34 ± 7.3	36 ± 11	32 ± 5.3	29 ± 5.1
90 min	41 ± 20	43 ± 8.3	34 ± 7.5	34 ± 12	32 ± 6.0	31 ± 6.9
120 min	34 ± 4.8	42 ± 8.8	33 ± 7.2	34 ± 12	32 ± 5.1	30 ± 8.2
150 min	37 ± 4.0	42 ± 9.1	N/A	N/A	N/A	N/A
180 min	38 ± 3.6	42 ± 8.5	N/A	N/A	N/A	N/A
210 min	40 ± 5.4	41 ± 8.8	N/A	N/A	N/A	N/A
240 min	41 ± 8.9	41 ± 9.2	N/A	N/A	N/A	N/A

M and F represent maternal and fetal perfusions, respectively. Values represent mmHg (mean ± SD) recorded from arteriole in-line transducer. Where no values are provided, the perfusions were terminated at 120 min. No significant change in arteriole pressure over the duration of the perfusion was noted for each set of m or f perfusions within each arm: p-value = 0.82^{*}, 0.91^{**}, $0.76^{\#}$, $0.76^{\#\#}$, $0.89^{\wedge}$, $0.66^{\wedge\wedge}$ (Friedman test).

Table S3.4: Estimates of THC $CL_{mf,c}$, $CL_{fm,c}$, and fraction of drug unbound in the maternal ($f_{u,perf,m}$) and fetal ($f_{u,perf,f}$) effluent in the absence and presence of VSP

Placenta ID	$CL_{mf,c}$ (mL/min)	$CL_{fm,c}$ (mL/min)	$f_{u,perf,m}$	$f_{u,perf,f}$
Arm 1: 5 μM THC Concentration Without VSP				
1	0.17	0.63	0.03	0.04
2	0.64	2.4	0.05	0.04
3	1.4	1.4	0.08	0.05*
4	1.6	1.1	0.08	0.05
5	0.58	1.5	0.07	0.06
6	0.27	0.87	0.05	0.05
7	0.47	0.51	0.08	0.04
8	0.47	1.0	0.15	0.03
Mean ± SD	**0.70 ± 0.51**	**1.2 ± 0.59**	**0.08 ± 0.04**	**0.05 ± 0.01**
Arm 2: 5 μM THC Concentration With VSP (4 μM)				
9	0.18	0.58	0.09	0.04
10	0.31	1.8	0.08	0.04
11	0.74	0.17	0.06	0.04
12	0.78	1.4	0.04	0.03
13	0.32	0.44	0.07	0.03
14	0.51	0.26	0.06	0.03
15	0.11	0.67	0.04	0.04
Mean ± SD	**0.42 ± 0.26**	**0.76 ± 0.61**	**0.06 ± 0.02**	**0.04 ± 0.004**
Arm 3: 100 – 250 nM THC Concentration Without VSP**				
16	1.4	3.9	0.03	0.03
17	1.2	2.7	0.05	0.06
18	0.40	2.3	0.11	0.05
19	1.3	1.4	0.07	0.05
20	1.8	3.1	0.05	0.05
21	0.59	0.80	0.09	0.05
22	0.096	1.1	0.05	0.06
23&&**	NA	NA	NA	NA
Mean ± SD	**1.0 ± 0.61**	**2.2 ± 1.1**	**0.07 ± 0.03**	**0.05 ± 0.01**

*Unbound fraction could not be measured, and therefore the mean value was used; **All placentas were perfused with 250 nM THC except 16 and 17 which were perfused with 100 nM; &&values for placenta 23 were not available because THC was inadvertently omitted from this experiment

Table S3.5: Estimates of SAQ $CL_{mf,c}$, $CL_{fm,c}$, and fraction of drug unbound in the maternal ($f_{u,perf,m}$) and fetal ($f_{u,perf,f}$) effluent in the absence and presence of VSP

Placenta ID	$CL_{mf,c}$ (mL/min)	$CL_{fm,c}$ (mL/min)	$f_{u,perf,m}$	$f_{u,perf,f}$
Arm 1: 1 – 10 μM SAQ Without VSP**				
1	0.24	0.94	0.28	0.19
2	0.43	1.0	0.22	0.27
3&	NA	NA	NA	NA
4	1.1	0.80	0.26	0.17*
5	0.51	1.6	0.16*	0.27
6	0.061	0.79	0.08	0.08
7	0.27	0.65	0.06	0.13
8	0.13	0.67	0.06	0.09
Mean ± SD	**0.40 ± 0.36**	**0.92 ± 0.31**	**0.16 ± 0.11**	**0.17 ± 0.08**
Arm 2: 1 μM SAQ With VSP (4 μM)				
9	0.75	0.64	0.20	0.18
10	0.35	1.8	0.18	0.21
11	1.2	0.40	0.08	0.11
12	0.95	1.7	0.12	0.15*
13	0.77	0.34	0.13	0.12
14	1.5	0.29	0.14	0.20
15	0.18	0.55	0.06	0.10
Mean ± SD	**0.81 ± 0.45**	**0.82 ± 0.66**	**0.13 ± 0.05**	**0.15 ± 0.05**
Arm 3: 1 μM SAQ Without VSP				
16	0.37	0.38	0.09	0.08
17	0.33	1.4	0.06	0.16
18	0.11	0.69	0.16	0.10
19	0.21	0.99	0.07	0.11
20	0.63	1.1	0.07	0.10
21	0.093	0.33	0.11	0.10
22	0.087	0.35	0.14	0.14
23	0.13	1.1	0.23	0.27
Mean ± SD	**0.25 ± 0.19**	**0.79 ± 0.40**	**0.12 ± 0.06**	**0.13 ± 0.06**

*Unbound fraction could not be measured, and mean value was used; **all placentas were perfused with 1 μM SAQ except placentas 1 – 5 which were perfused with 10 μM; &values for placenta 3 were not available because SAQ was inadvertently omitted from this experiment

Table S3.6: Estimates of 11-OH-THC and COOH-THC $CL_{mf,c}$, $CL_{fm,c}$, and fraction of drug unbound in the maternal ($f_{u,perf,m}$) and fetal ($f_{u,perf,f}$) effluent in the absence of VSP

Placenta ID	$CL_{mf,c}$ (mL/min)	$CL_{fm,c}$ (mL/min)	$f_{u,perf,m}$	$f_{u,perf,f}$
Arm 3: 100 – 250 nM 11-OH-THC[**] Concentration				
16	1.5	ND	0.14	0.14
17	1.8	1.5	0.13	0.16
18	0.57	2.0	0.14	0.14
19	2.1	1.6	0.11	0.15
20	2.3	2.5	0.12	0.14
21	0.78	0.91	0.14	0.12
22	0.21	ND	0.15	0.16
23	1.3	1.3	0.21	0.19
Mean ± SD	**1.5 ± 0.72**	**1.6 ± 0.55**	**0.14 ± 0.03**	**0.15 ± 0.02**
Arm 3: 250 nM COOH-THC Concentration				
16	1.5	0.99	0.15	0.13
17	2.4	1.8	0.14	0.15
18	1.3	2.9	0.15	0.13
19	3.5	2.4	0.12	0.15
20	2.4	2.0	0.14	0.14
21	1.2	0.79	0.12	0.13
22	0.36	0.78	0.12	0.13
23	1.5	1.9	0.18	0.16
Mean ± SD	**1.8 ± 0.96**	**1.7 ± 0.78**	**0.14 ± 0.02**	**0.14 ± 0.01**

[**]All placentas were perfused with 250 nM 11-OH-THC except 16 and 17 which were perfused with 100 nM; ND = clearance values not determined as concentrations were below limit of quantification. Mean and SD values do not include placentas that had ND values

Table S3.7: Estimates of AP $CL_{mf,c}$, $CL_{fm,c}$, fraction of drug unbound in the maternal ($f_{u,perf,m}$) and fetal ($f_{u,perf,f}$) effluent, $CL_{u,mf,c}$, $CL_{u,fm,c}$, and the ratio of these CLs in the absence and presence of VSP

Placenta ID	$CL_{mf,c}$ (mL/min)	$CL_{fm,c}$ (mL/min)	$f_{u,perf,m}$	$f_{u,perf,f}$	$CL_{u,mf,c}$ (mL/min)	$CL_{u,fm,c}$ (mL/min)	$CL_{u,c}$ ratio
Arm 1: 106 μM AP Without VSP							
1	0.88	1.8	0.99	1.1	0.88	1.7	0.52
2	2.0	3.1	0.98	1.2	2.0	2.6	0.77
3	2.6	3.0	1.0	0.98	2.6	3.1	0.83
4	2.8	2.1	1.1	1.1	2.5	2.0	1.2
5	1.6	2.7	1.0	1.0	1.5	2.6	0.59
6	1.2	1.7	1.0	1.1	1.2	1.6	0.77
7	2.4	1.2	1.0	1.0	2.3	1.1	2.0
8	1.7	1.2	1.1	1.0	1.6	1.2	1.3
Mean ± SD	**1.9 ± 0.69**	**2.1 ± 0.77**	**1.0 ± 0.06**	**1.1 ± 0.06**	**1.8 ± 0.62**	**2.0 ± 0.73**	**1.0 ± 0.51**
Arm 2: 106 μM AP With VSP (4 μM)							
9	1.9	2.2	1.0	1.1	1.8	2.0	0.91
10	1.1	2.2	1.1	1.1	1.0	2.0	0.50
11	2.8	0.9	1.0	1.1	2.8	0.89	3.1
12	2.0	1.9	1.1	1.2	1.8	1.6	1.1
13	1.8	0.96	0.94	1.0	1.9	0.96	2.0
14	2.9	0.87	0.92	1.0	3.2	0.85	3.8
15	0.95	1.2	1.0	0.99	0.92	1.2	0.76
Mean ± SD	**1.9 ± 0.76**	**1.5 ± 0.62**	**1.0 ± 0.07**	**1.1 ± 0.08**	**1.9 ± 0.83**	**1.4 ± 0.51**	**1.7 ± 1.3**
Arm 3: 106 μM AP Without VSP							
16	1.1	1.0	1.0	1.0	1.1	1.0	1.1
17	2.1	2.5	1.1	1.1	1.9	2.3	0.81
18	1.1	2.4	0.79	1.0	1.4	2.4	0.56
19	2.5	2.8	0.95	0.98	2.6	2.9	0.91
20	2.5	2.7	0.90	0.93	2.8	2.9	0.95
21	1.4	0.91	0.92	1.0	1.5	0.87	1.7
22	0.55	2.0	1.0	0.93	0.53	2.1	0.25
23	1.3	3.3	1.1	1.00	1.3	3.3	0.38
Mean ± SD	**1.6 ± 0.72**	**2.2 ± 0.86**	**0.97 ± 0.10**	**0.99 ± 0.048**	**1.6 ± 0.77**	**2.2 ± 0.89**	**0.83 ± 0.46**

Chapter 4: Quantification and Prediction of Human Fetal (-)-Δ^9-tetrahydrocannabinol (THC)/11-OH-THC Exposure Across Gestational Age to Inform Fetal Toxicity of Cannabis

4.1 Abstract

Prenatal cannabis use is associated with neurodevelopmental deficits likely due to exposure to the psychoactive cannabinoids, (-)-Δ^9-tetrahydrocannabinol (THC) and it's metabolite, 11-OH-THC. To determine if these cannabinoids can produce these deficits, preclinical studies that mimic human fetal cannabinoid exposure must be conducted. Therefore, we measured cannabinoid concentrations in trimester 1 (T1), 2 (T2) fetal tissues and/or trimester 3 (T3) maternal (MP) and fetal umbilical venous plasma (UVP). The mean ± SD T3 THC UVP/MP was 0.35 ± 0.13 (n=18); T1 and T2 THC fetal brain/MP was 0.50 ± 0.18 (n=3), 0.45 ± 0.28 (n=14), respectively. To predict fetal cannabinoid exposure at different prenatal cannabis doses (orally or by inhalation), we used a verified maternal-fetal physiologically based pharmacokinetic (m-f-PBPK) model. At a typical inhalational dose of 100 mg THC or oral 10 mg THC, the model-predicted average fetal brain steady-state THC/11-OH-THC concentrations were 37/70 nM and 0.73/8.9 nM, respectively. Our m-f PBPK model can guide future studies to inform risks associated with prenatal cannabis use.

4.2 Introduction

With legalization, cannabis use among pregnant individuals has increased, with consumption detected in over 22.6% of pregnancies in the United States[23]. Such cannabis use raises concern about fetal safety. Indeed, retrospective analyses have found an association between maternal cannabis use and adverse fetal outcomes such as neurodevelopmental deficits, lower birth weight, and growth restriction[5,37,166]. But such retrospective analyses are often confounded by factors such as other substance use (including tobacco, alcohol) or socioeconomic status and variable or self-reported quantification of cannabis use. However, even after correcting for some of these confounding factors, prenatal cannabis use has been linked to lower cognition (e.g. IQ, verbal reasoning, quantitative scores) and increased behavioral problems (e.g. hyperactivity, aggression, inattention)[1-5]. Unfortunately, retrospective

analyses cannot correct for all possible confounding factors. Additionally, for ethical reasons, conducting a randomized controlled prospective study to determine neurodevelopmental outcomes due to prenatal cannabis use is not possible. Therefore, alternative approaches should be explored to determine if cannabis use during pregnancy results in neurodevelopmental deficits in the offspring.

One alternative approach is to conduct *in vivo* toxicity studies in animals that mimic fetal exposure to the compounds causing potential neurodevelopmental deficits from cannabis use. (-)-Δ^9-tetrahydrocannabinol (THC), a major psychoactive constituent of cannabis, is widely believed to be the causative factor. Its primary *in vivo* psychoactive metabolite (±)-11-hydroxy-Δ^9-THC (11-OH-THC) may also contribute. While pregnant animal studies (mostly rodents) exposed to THC or cannabis have been conducted[11,13], they could not mimic the *in vivo* human fetal plasma or fetal brain exposure to THC/11-OH-THC because these critical concentration values are unknown. Therefore, our primary goals were two-fold. First, to quantify the THC/11-OH-THC concentration in 1st and 2nd trimester human fetal brain, liver, kidney, placenta and maternal plasma and in 3rd trimester umbilical venous plasma (UVP), maternal plasma (MP) and placenta from pregnant individuals who had recreationally consumed cannabis prior to pregnancy termination or delivery. Because these are observational studies, the dose of cannabis and the timing of the samples, relative to consumption, is unknown. Therefore, these UVP or fetal tissue concentrations are meaningful only when expressed relative to the MP concentration. While these samples provide a “snapshot” of the fetal cannabinoid concentrations in various tissues or plasma relative to MP at a single time-point, they are not informative of the actual total fetal exposure to cannabinoids, over time, at the recreational doses used. For this, one needs to not only quantify the maximum cannabinoid concentrations (C_{max}) in each fetal tissue/plasma but also the area under the tissue/plasma concentration-time profile (AUC) or the average steady-state cannabinoid tissue/plasma concentration ($C_{ss,avg}$; i.e. AUC/τ; where τ represents the frequency of cannabis consumption). Though such exposure to

THC/11-OH-THC cannot ethically be measured *in vivo*, it can be predicted through a linked parent-metabolite maternal-fetal physiologically based pharmacokinetic (m-f-PBPK) model informed by parameters such as maternal-fetal disposition and placental transfer of THC/11-OH-THC. Therefore, our second goal was to populate our current m-f-PBPK model[149,190-192] with the various maternal-fetal disposition parameters of THC/11-OH-THC after inhalational or oral consumption of cannabis and determine if the predicted fetal tissue/plasma concentrations align with those observed in our first aim. If they do, the model could be used to predict unbound and total fetal plasma and tissue THC/11-OH-THC exposure at different gestational ages as well as different routes of administration and doses of cannabis consumption, assuming the rates of all processes are dose-independent. Also, such predictions could be used to inform the design of *in vivo* toxicity studies after prenatal cannabis administration to animals.

Fetal THC/11-OH-THC exposure is driven by several factors; the first being maternal exposure to cannabinoids which, in turn, is driven by maternal bioavailability and pre-systemic disposition. A second factor is the distributional clearances of the cannabinoids across the placenta via either transport and/or passive diffusion as well as metabolic clearance in the placenta. A third parameter is the irreversible clearance of the cannabinoids by the fetus. All of these disposition parameters need to be incorporated into our m-f-PBPK model to successfully predict the absolute fetal cannabinoid exposure for a given dose and route of consumption by pregnant individuals. We have experimentally determined these disposition parameters by conducting THC/11-OH-THC depletion studies in microsomes derived from human adult liver, intestine, lung, placenta (of different gestational ages), and fetal livers. In the adult liver, THC is almost completely metabolized by hepatic cytochrome P450 (CYP) 2C9 (mostly to the 11-OH-THC)[15]. In the intestine, THC is metabolized by CYP2C9 and 3A enzymes and in the fetal liver by CYP3A7 with no detectable depletion in the adult lung or placenta[7]. Similarly, 11-OH-THC is metabolized in the adult liver and intestine by CYP2C9, CYP3A, and uridine 5'-diphospho-glucuronosyltransferases (UGTs) and by CYP3A7 in the fetal liver[7,15]. Moreover, 11-OH-THC is

also metabolized by the cytosolic aldehyde oxidase and aldehyde dehydrogenase but the fraction metabolized (f_m) via these pathways is unknown[77]. We have also demonstrated and quantified THC (but not 11-OH-THC) transport across the placenta[8] that is not mediated by either P-glycoprotein (P-gp) or Breast Cancer Resistance Protein (BCRP), efflux transporters that are highly expressed in the human placenta[97,193]. The identity of this transporter(s) is unknown and its location could be either on the apical or basal membrane of the syncytiotrophoblast[8].

Several THC PBPK models, including one from our laboratory, are able to simultaneously and accurately predict THC and 11-OH-THC plasma concentrations after intravenous (IV), oral, and inhalational administration[194-198]. However, they have not been employed to predict fetal THC/11-OH-THC exposure, with the necessary fetal/placental disposition parameters incorporated, nor have these model predictions been compared with the observed fetal UVP and tissue "snapshot" cannabinoid concentration data. Thus, our goals were to obtain these "snapshot" data and ascertain if our m-f-PBPK model predictions align with the observed data.

4.3 Materials and Methods

4.3.1 Chemicals and Reagents

(-)-Δ^9-tetrahydrocannabinol (THC), 11-OH-THC, COOH-THC, and d3-THC were purchased from Cayman Chemicals (Ann Arbor, MI). d3-11-OH-THC, d3-COOH-THC, and ethylenediaminetetraacetic acid (EDTA) were purchased from Sigma-Aldrich (St. Louis, MO). Sodium phosphate, sucrose, acetonitrile, hexanes, ethyl acetate, formic acid (liquid chromatography-mass spectrometry (LC-MS/MS grade)), acetic acid (LC-MS/MS grade), silanized glass culture tubes, LC glass inserts, polycarbonate ultracentrifuge tubes, and LC pre-split snap caps were purchased from Fisher Scientific (Hampton, NH).

4.3.2 *In Vivo* Study Design and Procedures

Fetal and maternal samples were collected in a cross-sectional, observational study, divided into two arms based on duration of gestation. The first arm was a first (T1) and second trimester (T2) study conducted at the University of Washington while the second was a third trimester (T3) study (see definition below) conducted at the University of Colorado. Each study was approved by the respective institutional review board. Prior to the study procedures, written informed consent was obtained from each participant. Additionally, each enrolled subject completed a survey to obtain data on substance use during pregnancy, demographics, and reproductive health history. For cannabis use, the information collected was: 1) time since last cannabis consumption 2) method of consumption during last use (oral or inhalation) 3) amount of cannabis consumed during last use and 4) frequency of cannabis use during pregnancy.

For the T1/T2 study, the inclusion criteria were: 1) pregnant person seeking termination; 2) 18 years of age or older; 3) intrauterine pregnancy confirmed with ultrasound; 4) gestational age 8-24 weeks as determined by ultrasound dating; 5) able to speak and read English; 6) have used THC-containing cannabis via smoking or oral ingestion within 48 hours of pregnancy termination; 7) already consented to an abortion procedure via dilation and curettage (D&C) or dilation and evacuation (D&E); 8) have not used other recreational substances (heroin, opiates, benzodiazepines, cocaine, amphetamines/methamphetamines, Adderall, speed, or other substances of abuse) during pregnancy. A urine toxicology test was conducted at the time of the procedure to confirm the self-reported substance use. Prior to termination, subjects routinely received IV sedation for their procedures: benzodiazepines (e.g. midazolam), opioids (e.g. fentanyl), and sedatives (e.g. propofol). Maternal blood (5 mL in ethylenediaminetetraacetic acid (EDTA) tubes), maternal urine, fetal brain, fetal liver, fetal kidney, and placental tissues were collected from each subject, where possible, at the time of termination. Due to the nature of the procedure, it is not possible to collect UV blood. Maternal plasma was harvested and immediately stored in 1 mL aliquots at 4°C. MP, fetal and placenta tissue were collected and

transported to the University of Washington on ice. MP was stored at -80°C immediately upon reaching University of Washington. Fetal tissues (brain, liver, and kidney) were visually identified by an experienced technologist and separated within 2.53 ± 1.26 hours of collection. Placental tissue was separated into 3 different regions (periphery, medial, and near umbilical cord) to include the villi. Once identified and separated, tissues were flash frozen within 1 hour of dissection and immediately stored at -80°C.

For the T3 study, the inclusion criteria were: 1) pregnant person; 2) 18 – 45 years of age; 3) singleton fetus; 4) gestational age ≥16 weeks as determined by last menstrual period and/or early ultrasound; 5) current reported THC-containing cannabis use; 6) able to speak and read English or Spanish; 7) have not used other recreational drugs (alcohol, cocaine, crack, heroin, hallucinogens, inhalants, methamphetamine, prescription pain relievers, or other drugs of abuse) during pregnancy; 8) not coronavirus disease (COVID) positive at delivery. Verbal screening for prenatal cannabis use occurred at the first prenatal visit, 26-28 weeks gestation and at delivery and hospitalization. Subjects were counseled regarding risks associated with perinatal cannabis use and recommended to cease or decrease cannabis use. Samples were collected at the time of delivery. Maternal (5 mL) and umbilical venous blood (3 mL) were simultaneously (or within 30 minutes of each other) collected in EDTA tubes, processed, and stored as in the T1/T2 study. Placental tissue was sampled over 3 different regions (~10 g each; periphery, medial, and near umbilical cord) to include the villi, after removal of the decidua. The tissue was rinsed with saline, flash frozen and stored at -80°C within 1 hour of delivery. Samples were shipped frozen on dry ice to the University of Washington.

4.3.3 Sample Processing and Bioanalyses

Tissue samples (100 – 1000 mg) were homogenized in buffer (1:4 w/v) containing 20 mM sucrose, 50 mM KPi, and 10 mM EDTA with a Bead Ruptor Homogenizer (Omni International, Kennesaw, GA). One mL of plasma or tissue homogenate, in 20 mL silanized glass culture tubes, spiked with 10 µL of acetonitrile containing 2 µM internal standard (d3-THC,

d3-11-OH-THC, and d3-COOHTHC), 100 µL of 1.68% formic acid in water, and 5 mL of 5:1 hexane:ethyl acetate were vigorously agitated on a shaker for 30 min. Then, after centrifugation at 200 x g at room temperature for 10 minutes, the organic supernatant (~5 mL) was transferred into another silanized glass culture tube and evaporated under nitrogen at 40°C. The residue, reconstituted with 100 µL acetonitrile and vortexed for 20 seconds, was transferred to a LC glass insert and stored at -20°C until analysis by LC-MS/MS.

Fraction of THC and 11-OH-THC unbound in fetal plasma ($f_{u,p,fetus}$) was measured in T3 umbilical venous plasma (UVP) samples, as previously described[15]. Briefly, blank UVP was spiked with 500 nM THC or 11-OH-THC yielding an $f_{u,p,fetus}$ value of 0.0071 and 0.0067, respectively (Table S4.1). Using the same approach, we also measured $f_{u,p}$ in our T3 UVP as well as MP.

All plasma and tissue cannabinoid concentrations were quantified by injecting 10 µL of the processed samples onto an Acquity ultra-performance liquid chromatography (UPLC) system (Waters Corporation, Milford, MA) coupled with a Waters Xevo Triple Quadrupole XS in APCI mode (Waters Corporation, Milford, MA). Acquity UPLC bridged ethylene hybrid (BEH) C18 column (1.7 µM 2.1 x 50 mm) attached to a BEH C18 5 mm guard column (Waters Corporation, Milford, MA) was used for chromatographic separation with the mobile phase flow rate of 0.3 mL/min. The mobile phase consisted of acetonitrile and water containing 0.2% acetic acid as the organic and aqueous phases, respectively (see Table S4.9). Integration of the chromatographic peaks was performed using TargetLynx v4.2 (Waters Corporation, Milford, MA). Quality control samples at 0.1, 1, 10 nM concentrations (calibration curve range 0.05 – 10 nM) were within ± 20% of the expected values. Blank human plasma and placenta/fetal tissues, spiked with the above concentrations of cannabinoids, were used as calibrators and processed as per the unknown samples. The lower limit of quantification (LLOQ, defined by a signal to noise ratio > 10), for THC, 11-OH-THC, COOH-THC in MP, UVP, fetal brain and fetal kidney was 0.05, 0.5, and 0.5 nM, respectively and in placenta and fetal liver was 0.1, 1, and 1 nM,

respectively. Samples that were above the highest calibrator concentration were diluted so that they fell within the calibration range.

4.3.4 M-f-PBPK Modeling and Simulations

All non-pregnant (NP) PBPK model simulations including the impact of drug interaction (DDIs) and genetic polymorphism on THC/11-OH-THC pharmacokinetics were conducted in Simcyp V22 (Figure 4.1). The population demographics (age, sex distribution, number of subjects) and dosing regimen (dose amount, dosing time, route of administration) were kept identical to those in the corresponding *in vivo* study.

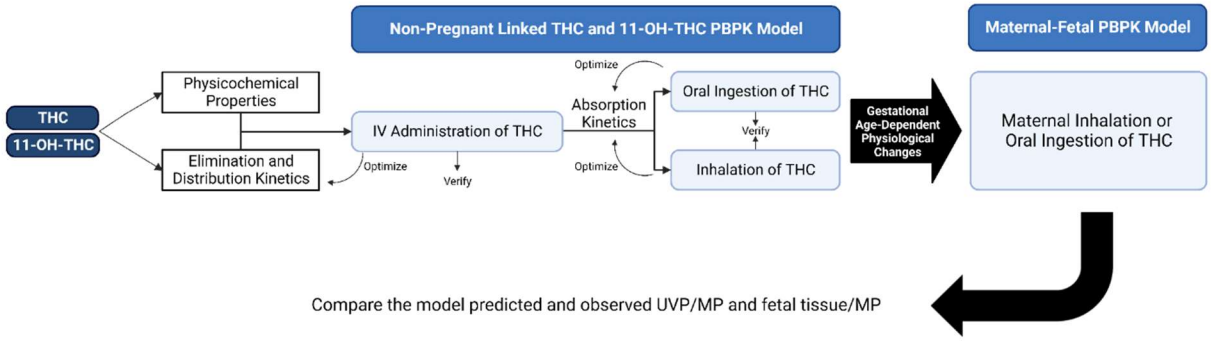

Figure 4.1: Schematic showing THC and 11-OH-THC PBPK model development and verification for inhalational and oral consumption of THC by the non-pregnant population followed by extension to the pregnant population (m-f-PBPK model). First, the model was built in Simcyp V22 for the healthy non-pregnant population by optimizing and verifying the THC elimination and distribution kinetics after intravenous administration. Then, THC absorption kinetics and 11-OH-THC elimination and distribution kinetics were verified after inhalation and oral THC consumption. The THC kinetics in the non-pregnant model were also verified through DDI and pharmacogenetic studies. Then, using our in-house m-f-PBPK model, built in MATLAB Simulink R2023a, which includes the placental and fetal compartments as well as gestational age-dependent physiological changes, the UVP and fetal tissue concentrations were predicted.

As an overview (see details below), the distribution and elimination kinetics of THC, after IV THC administration to non-pregnant adults, were optimized with a training dataset[47] and then verified (see below for criteria) using two independent datasets[46,106]. Then, without changing the systemic disposition of THC, its inhalation and oral absorption kinetics were optimized using the respective training dataset (Inhalation:[47]; Oral:[50]) and then verified using independent datasets (Inhalation:[48]; Oral:[49,51]). To confirm the fraction of THC metabolized by each enzyme

determined *in vitro* (Table S4.1), the observed THC exposure in the presence of DDIs or CYP2C9 genetic polymorphism was predicted and compared to the observed values using the verification criteria described below[28,75,136]. Then, the outputs from these simulations were fed into our previously developed in-house m-f-PBPK model (MATLAB Simulink R2023a), refined by Shum et al.[192], to predict UVP and fetal tissue concentrations as described before[149,191]. This m-f-PBPK model has previously been used (and verified) to predict fetal exposure to drugs that passively diffuse across the placenta or are transported[149,190-192]. This m-f PBPK model includes gestational age-dependent maternal-fetal physiological changes including the gestational-dependent magnitude of induction of maternal hepatic CYP enzymes. Our in-house m-f-PBPK model was used since Simcyp does not have the capability to predict metabolite fetal tissue concentrations and we were interested in the 11-OH-THC fetal brain exposure. Additionally, the NP simulations were verified in MATLAB to confirm that the models were identical between the two software packages. However, we needed to remain with Simcyp for the NP model as our m-f-PBPK model was not built to predict DDIs. COOH-THC exposure was not predicted with either the NP or m-f PBPK model as we do not have the required metabolic kinetic data. Also, since it is not psychoactive, COOH-THC was assumed to be not involved in fetal neurotoxicity.

Non-pregnant PBPK model: The physicochemical properties, distribution parameters, elimination and absorption kinetics for both THC and 11-OH-THC were either estimated by us, derived from the literature or predicted *in silico* (Table S4.1). Tissue to plasma ratio ($K_{p,tissue}$) was determined one of two ways: 1) brain, liver, and kidney K_p was optimized to reflect the *in vivo* $K_{p,tissue}$ observed from human postmortem tissue[53-56,199]; 2) where such data were not available, the Rodgers and Rowland method[200] was used to predict $K_{p,tissue}$. Then, through sensitivity analysis we found that the THC exposure was sensitive to adipose, muscle, and skin K_p and 11-OH-THC exposure was sensitive to muscle K_p. Accordingly, these sensitive K_p values were optimized using the above training datasets to recapitulate the observed concentration-time

profile (IV THC administration only). The hepatic intrinsic clearance (CL_{int}) of THC was estimated using a middle-out approach[201] using the IV training dataset[47]. Briefly, the CL_{int} of THC was back-calculated using the dispersion model. From here, the CL_{int} or maximum rate of metabolism (V_{max}) by each cytochrome P450 (CYP) isoform was estimated based on the measured fraction metabolized (f_m) and Michaelis-Menten constant (K_m) *in vitro*[15]. 11-OH-THC hepatic clearance was estimated using the THC oral training dataset[50] to recapitulate the observed 11-OH-THC AUC to time of infinity (AUC_{inf}). A first order absorption model was used for both inhalation and oral consumption of THC. The fraction absorbed (f_a) after inhalation was estimated using the *in vivo* $AUC_{inhalation}/AUC_{IV}$ and the rate of absorption (k_a) was optimized using the inhalational training dataset[47]. The f_a after oral dosing was estimated from the *in vivo* observed $AUC_{inf,fasted}/AUC_{inf,fed}$ assuming that f_a was 1 in the fed state (high-fat diet), while the k_a and fraction unbound in the gut ($f_{u,gut}$) were optimized using the oral THC training dataset[50]. All parameter optimization (K_p, k_a, $f_{u,gut}$) was done by comparing predicted vs observed concentrations from the above training datasets and using weight least squares to minimize the variance for all the predicted concentrations along the concentration-time profile.

M-f-PBPK model: The model was built to predict exposure between 15-40 GW. Lack of fetal physiological data for <GW15 prevented us from making predictions for T1 fetal exposure. Based on our previous studies, we assumed that hepatic CYP3A was induced 1.99-fold during the second and third trimesters[88,91]. Hepatic CYP2C9 induction of 1.09, 1.16, 1.29, and 1.31-fold at 15, 25, 38, and 40 GW, respectively, was estimated from *in vivo* observed steady-state unbound phenytoin (primarily metabolized in the liver via CYP2C9) concentration across GW[84].

Intrinsic fetal hepatic clearance ($CL_{int,fh}$) across gestational age was estimated using the product of our previously measured $CL_{int,fh}$ (THC: 77.1 mL/min/g liver; 11-OH-THC: 11.3 mL/min/g liver)[7] and the fetal liver weight across gestational age (4.98, 33.0, 112, and 129 g at

15, 25, 38, and 40 GW, respectively)[149]. The fetal liver metabolism was attributed entirely to CYP3A7[7], the abundance of which does not change per gram of liver across gestational age[83].

Intrinsic placental passive diffusion ($CL_{int,PD}$) at term (GW40) was estimated using the previously measured[8], paired, unbound human placental cotyledon clearances ($CL_{u,cotyledon}$) of midazolam, THC, and 11-OH-THC, along with the *in vivo* observed midazolam $CL_{int,PD}$ (Eq. 1).

$$CL_{int,PD,THC\ or\ 11-OH-THC} = \frac{CL_{u,cotyledon,THC\ or\ 11-OH-THC}}{CL_{u,cotyledon,midazolam}} * CL_{int,PD,midazolam} \quad \text{(Eq. 1)}$$

Where midazolam $CL_{int,PD}$ is 500 L/h[191] and $CL_{u,cotyledon,11\text{-}OH\text{-}THC}/CL_{u,cotyledon,midazolam}$ is 0.397, yielding a $CL_{int,PD,11\text{-}OH\text{-}THC}$ of 199 L/h (Table S4.1). As indicated in the introduction, THC is transported across the perfused term human placenta in the fetal-maternal direction, but the location of this transporter(s) is unknown. We found that when THC efflux transport at the apical membrane of the syncytiotrophoblast (apical efflux transport) was assumed, it overpredicted UVP and fetal tissue exposure (Figure S4.4). However, when THC influx transport at the basal membrane of the syncytiotrophoblast (basal influx transport) was assumed, the T3 UVP/MP at GW38 and T2 fetal tissue/MP at GW15 concentration were well-recapitulated (Figure S4.4). Therefore, we assumed that basal influx transporter(s) was responsible for the observed transport. Hence, Eq. 1 yielded $CL_{int,PD,THC}$ of 247 L/h (Table S4.1). Passive diffusion was scaled to earlier GW based on change in placental weight with GW (assuming that surface area for diffusion also changes in proportion with placental weight).

Intrinsic placental transport ($CL_{int,T}$) for THC was estimated at term using the estimated fraction transported (f_t), calculated from the previously published placental perfusion data[8]. The estimated f_t by basal influx transporters was 0.63, resulting in a $CL_{int,T,THC}$ of 420 L/h (Table S4.1). Since the identity of this transporter(s) is unknown, we assumed that its abundance at earlier GW also changed in proportion to placental weight (i.e., the THC f_t remained the same at all GW). If, however, the f_t increases or decreases with gestational age, with our assumption we would be overpredicting and underpredicting the fetal exposure, respectively.

With all the above THC/11-OH-THC parameters populated into the m-f-PBPK model, we predicted their concentrations in MP, UVP, fetal brain, fetal kidney, and fetal liver at GW of 15, 25, 38, and 40 weeks. Simulations were conducted following daily cannabis use as 95% of T2 subjects reported cannabis use at least once per day and 77% of T3 subjects reported cannabis use at least every other day. Unbound concentrations in MP and UVP were calculated as the product of the predicted total concentrations and measured unbound fractions (Table S4.1). Fraction unbound in the adult and fetal plasma were assumed to be constant across gestation. Unbound fetal brain concentrations were assumed to be equivalent to the unbound fetal arterial concentrations (see discussion below). We could not predict placenta concentrations as we needed an accurate estimate of fraction of drug unbound in the placenta tissue ($f_{u,placenta}$). Unfortunately, we did not have good confidence in either measuring or predicting $f_{u,placenta}$.

Model verification: Model predictive performance was evaluated by comparing the predicted drug exposure (NP: area under the concentration-time curve to time of infinity (AUC_{inf}) and C_{max}; Pregnancy: steady-state UVP/MP and fetal tissue/MP concentrations) with the observed *in vivo* data. The model was considered verified if the exposure parameter fell within the 99.998% geometric confidence interval determined based on variability in the corresponding observed exposure data[202]. For the NP model variability, we used the interstudy variability[192] across three independent studies for IV and oral administration (IV:[46,47,106] Oral:[49-51]). For inhalation administration, because inter-study variability, cannot be computed from only two data sets, we used the interindividual variability from the most data-rich study[47]. For the m-f-PBPK model predictions, we used the interindividual variability observed in our *in vivo* data. Our m-f-PBPK model predicted T1 and T2 fetal tissue cannabinoid concentrations devoid of blood while our corresponding observed concentrations included the cannabinoids contained in the blood within the tissues. Therefore, to compare the observed and predicted fetal tissue/MP values, we added to the predicted fetal tissue drug concentration the predicted cannabinoid blood concentrations

using the previously estimated residual blood volume contained within these tissues in neonates (values for fetus are not available) i.e. brain (4.0%), kidney (8.5%), and liver (30%)[203]. For the DDIs and genetic polymorphism effects, the acceptance range of the ratios of THC exposure, with and without the DDI or genetic polymorphism ($AUC_{inf}R$ and $C_{max}R$) was determined based on the magnitude of interaction[28,75,136] and *in vivo* observed intraindividual variability[51,204]. All observed NP concentration-time profiles were quantified using WebPlotDigitizer (version 4.6, https://apps.automeris.io/wpd/), unless the individual concentration-time data were available. All AUC_{inf} calculations for *in vivo* data were estimated using Phoenix WinNonlin version 8.3.4.

4.3.5 Statistical Analysis

Pairwise comparison of MP to UVP, placenta, and fetal tissue in T1, T2, and T3 samples for each subject were conducted using the two-tailed, Wilcoxon signed rank test. For all tests, $p<0.05$ was considered significant.

4.4 Results

4.4.1 Enrollment, Dose Consumed and Time of Sampling from Last Consumption

In the T1/T2 study, 41 participants were enrolled, 1 was disqualified due to a positive urine toxicology test and 40 completed the study (18 T1; 22 T2); in the T3 study, 34 participants enrolled, 8 withdrew and 26 completed the study (see Table S4.2 for demographics). Briefly, gestational age for all participants was 71 ± 8, 105 ± 14, and 267 ± 12 days, for T1, T2 and term, respectively. For last THC consumption prior to termination, in the T1 study 17 reported inhalational THC use while 1 reported oral THC use; in the T2 study all 22 T2 participants reported inhalation use; in the T3 study, 18 reported only inhalation use, 1 reported only oral use, and 7 reported mixed inhalation and oral use.

For the T1/T2 study, the average dose consumed (self-reported per survey) by the participants was 1.3 g cannabis plant (THC dose unknown) by inhalation or 100 mg THC orally (n=1). For T1/T2 subjects, time from last consumption to survey was: <4 hours (n=10); 4-12

hours (n=9); 12-24 hours (n=16); 24-36 hours (n=3); 36-48 hours (n=2). For T1/T2 subjects, on average, there was a delay of 4.74 hours between survey recording and sample collection. For the T3 study, the average dose consumed by the participants was 0.79 g cannabis plant by inhalation (THC dose unknown) or 28 mg THC orally. For T3 subjects, time from last consumption to survey was: 4-12 hours (n=1); 12-24 hours (n=4); 24-36 hours (n=8); 36-48 hours (n=2); 48-72 hours (n=2); >72 hours (n=9). For T3 subjects, on average, there was a delay of 16.1 hours between survey recording and sample collection. Not surprisingly, given that most of the samples were obtained >12 hours after last consumption, there was no apparent association between dosing time and either UVP/MP or fetal brain/MP irrespective of GW. Since THC absorption and THC/11-OH-THC distributional equilibrium between plasma and tissue concentrations was expected to be reached by 12 hours, concentration data from all routes of THC consumption and duration from last consumption were pooled and analyzed as described below.

4.4.2 Observed Fetal UVP/Tissue and Maternal Concentration in Trimester 1, 2, and 3 Pregnancies

The average paired T3 UVP and placental THC and COOH-THC concentrations were significantly lower than the corresponding MP (Figure 4.2, Table 4.1). 11-OH-THC was detectable in many MP samples but only one UVP and placenta sample (Table 4.1). For T1, T2, and T3 subjects, the placenta concentrations did not differ across the sampled regions (data not shown), therefore the average of the three regions is reported. MP and UVP concentration range was within 0.45 – 46 nM and 0.13 – 14 nM for THC, respectively, 0.62 – 26 nM and 5.2 nM for 11-OH-THC, respectively, and 0.98 – 1304 nM and 0.92 – 163 nM for COOH-THC, respectively (Table S4.3). Similarly, the average paired T1 placenta and T2 fetal brain, kidney, and placental tissue THC and COOH-THC concentrations were significantly lower than the corresponding MP (Figure 4.2, Table 4.1). MP and fetal brain concentration range was within 0.52 – 51 nM and 1.0 – 18 nM for THC, respectively (Table S4.4), 0.71 – 45 nM and 13 nM for

11-OH-THC, respectively (Table S4.5), and 1.9 – 334 nM and 2.9 – 35 nM for COOH-THC, respectively (Table S4.6).

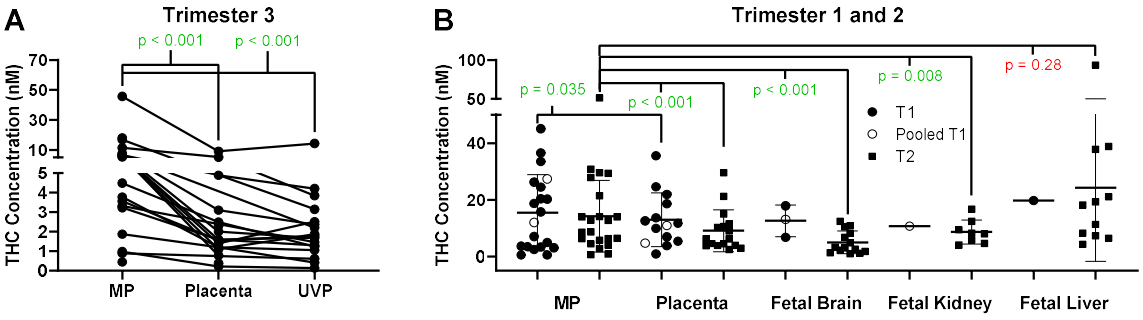

Figure 4.2: Maternal plasma (MP), umbilical venous plasma (UVP), placental and fetal tissue THC concentrations in trimester 1 (T1), 2 (T2), and 3 (T3) pregnancies. (A) The T3 UVP and placenta concentrations within each maternal-fetal dyad were significantly lower than that in the corresponding MP. (B) The T1 placenta and T2 placenta, fetal brain, and fetal kidney concentrations within each maternal-fetal dyad were significantly lower than that in the corresponding MP. The open symbols denote tissues or MP that were pooled (n=3) for analyses due to small volume/size available. All comparisons were made with a two-tailed, Wilcoxon signed rank test.

Table 4.1: Mean T1, T2 and T3 Pregnancy THC, 11-OH-THC, and COOH-THC Concentrations in the Umbilical Venous Plasma, Placenta and Fetal Tissues as well as Their Values Relative to the Corresponding Maternal Plasma Concentration

	THC			11-OH-THC			COOH-THC		
	Trimester 1	Trimester 2	Trimester 3	Trimester 1	Trimester 2	Trimester 3	Trimester 1	Trimester 2	Trimester 3
Maternal Plasma (nM)	15.0 ± 13.9 (n=18)[a]	14.2 ± 12.7 (n=17)[b]	7.90 ± 9.82 (n=21)[c]	6.12 ± 4.38 (n=13)	5.53 ± 3.85 (n=12)	4.81 ± 7.89 (n=10)	124 ± 107 (n=18)[d]	74.9 ± 59.7 (n=18)[e]	108 ± 272 (n=22)[f]
Umbilical Venous Plasma (nM)	---	---	2.55 ± 3.14 (n=18)[c]	---	---	5.20 (n=1)	---	---	23.4 ± 36.9 (n=19)[f]
UVP/MP	---	---	0.35 ± 0.13 (n=18)	---	---	0.20 (n=1)	---	---	0.36 ± 0.18 (n=19)
Fetal Brain (nM)	12.6 ± 5.60 (n=3)	5.01 ± 4.00 (n=14)[b]	---	BLOQ	13.4 (n=1)	---	20.6 ± 5.00 (n=3)	16.8 ± 10.3 (n=9)[e]	---
Fetal Brain/MP	0.50 ± 0.18 (n=3)	0.45 ± 0.28 (n=14)	---	---	0.29 (n=1)	---	0.11 ± 0.03 (n=3)	0.17 ± 0.074 (n=9)	---
Fetal Kidney (nM)	10.7 (n=1)	8.64 ± 4.25 (n=8)[b]	---	5.15 (n=1)	6.80 ± 5.51 (n=6)	---	48.1 (n=1)	27.4 ± 28.6 (n=12)[e]	---
Fetal Kidney/MP	0.89 (n=1)	0.48 ± 0.24 (n=8)	---	1.36 (n=1)	0.68 ± 0.56 (n=6)	---	0.63 (n=1)	0.23 ± 0.14 (n=12)	---
Fetal Liver (nM)	19.7 (n=1)	24.2 ± 25.9 (n=11)	---	BLOQ	14.1 ± 14.5 (n=7)	---	66.7 (n=1)	51.3 ± 44.4 (n=12)[e]	---
Fetal Liver/MP	0.75 (n=1)	1.33 ± 0.71 (n=11)	---	----	1.47 ± 0.99 (n=6)	---	0.39 (n=1)	0.44 ± 0.11 (n=12)	---
Placenta (nM)	13.8 ± 9.93 (n=12)[a]	9.10 ± 7.45 (n=12)[b]	2.37 ± 2.24 (n=18)[c]	5.21 (n=2)	BLOQ	27.0 (n=1)	31.5 ± 23.9 (n=11)[d]	31.7 ± 18.1 (n=8)[e]	21.2 ± 31.8 (n=10)[f]
Placenta/MP	0.96 ± 1.18 (n=12)	0.61 ± 0.29 (n=12)	0.37 ± 0.18 (n=16)	0.66(n=2)	---	1.04 (n=1)	0.22 ± 0.096 (n=11)	0.46 ± 0.63 (n=8)	0.26 ± 0.15 (n=10)

Data presented as Mean ± SD, unless n=1; MP: maternal plasma; UVP: umbilical venous plasma; BLOQ: below limit of quantification; ---: no sample, ratio cannot be calculated; [a,b,c,d,e,f]Fetal UVP or tissue cannabinoid concentrations were significantly different than the corresponding MP concentration ($p<0.05$; two-tailed, Wilcoxon signed rank test).

4.4.3 Non-pregnant PBPK Model Optimization and Verification

For the non-pregnant model, the predicted/observed THC and 11-OH-THC AUC_{inf} and C_{max} fell within the acceptance range for all IV, inhalation and oral datasets as did the ratio of the plasma THC C_{max} and AUC_{inf} in the presence and absence of drug interaction or CYP2C9 genetic polymorphism (Figures S4.1 – 3, Table S4.7).

4.4.4 Comparison of Maternal-Fetal PBPK Model Predicted and Observed Values of UVP/MP and Fetal Tissue/MP Values

Our m-f-PBPK model predictions were in good agreement with the observed "snapshot" T3 UVP/MP (0.31), T2 fetal brain/MP (0.54), T2 fetal kidney/MP (0.73), and T2 fetal liver/MP (1.8) values and fell within the acceptance range (Figure 4.3, Table S4.8). Simulations for the purpose of verification were conducted following daily maternal THC inhalation (100 mg), however these profiles are independent of the consumed dose and route of administration. These predictions were made with two assumptions. First, that the "snapshot" values (observed and predicted) were obtained at 24 hours when distributional equilibrium between plasma and tissue concentrations was expected to be reached (i.e. > 12 hours; see Figure S4.4) and, second, that the fetal-maternal transport of THC was due to an influx transporter located at the basal membrane of the syncytiotrophoblast. In contrast, if THC was assumed to be due to an efflux transporter located at the apical membrane of the syncytiotrophoblast, all ratios were over-predicted (Figure S4.4). Therefore, all the m-f-PBPK model predictions presented below were conducted with the assumption that a basal influx transporter(s) was responsible for the observed THC fetal-maternal $CL_{int,T}$.

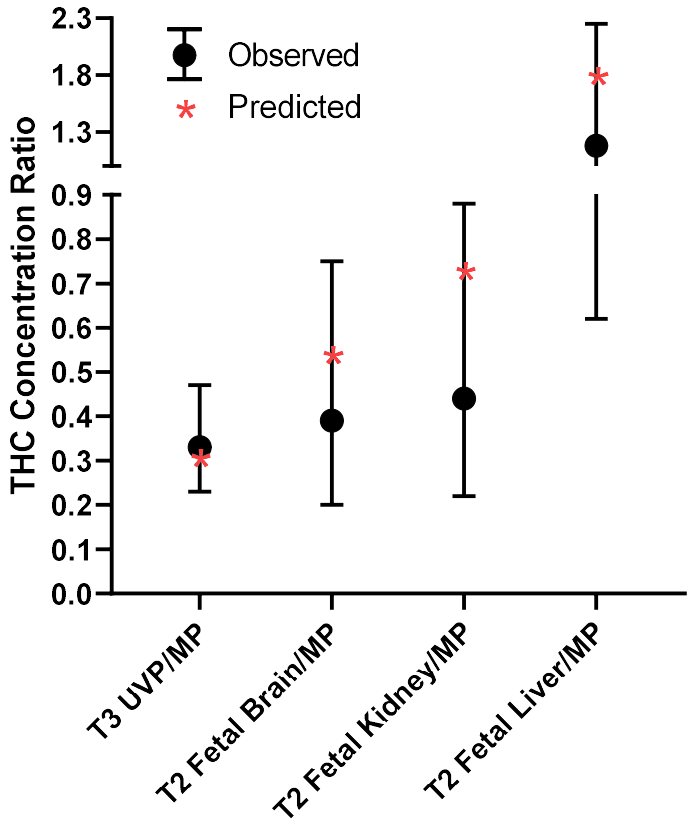

Figure 4.3: m-f-PBPK model "snapshot" predicted vs. observed steady-state THC umbilical venous plasma (UVP) and fetal tissue concentration relative to the corresponding maternal plasma (MP) concentration. The m-f-PBPK model predicted (*) values of trimester 3 (T3; GW38) UVP/MP and trimester 2 (T2; GW15) fetal tissue/MP fell within the acceptance range (horizontal lines; filled circles denote the mean observed value). The m-f-PBPK model predicted values were those at 12 hours post THC consumption (inhalation or oral) when distributional equilibrium between plasma and tissue THC concentration was expected to have been reached (see Figure S4.4).

4.4.5 m-f-PBPK Model Predicted Gestational Age-Dependent Changes in Maternal THC/11-OH-THC Exposure

When compared with the NP population, as gestational age advanced, the steady-state THC and 11-OH-THC MP $C_{ss,avg}$, after THC inhalation, decreased marginally (Table 4.2, Figure 4.4). The effect was modestly larger after oral THC consumption (Table 4.2, Figure 4.4).

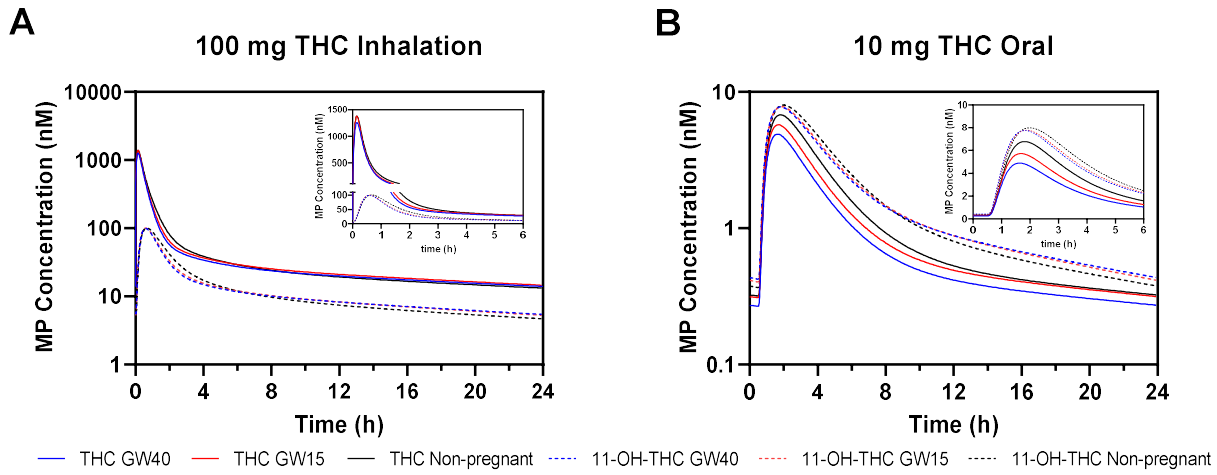

Figure 4.4: m-f-PBPK model predicted non-pregnant and gestational age-dependent THC/11-OH-THC maternal plasma (MP) concentration-time profiles after daily maternal THC inhalation (100 mg) or oral (10 mg) consumption. When compared to the non-pregnant population, as gestational week (GW) advanced from 15 to 40, (A) MP THC $C_{ss,avg}$ and $C_{ss,max,}$ after daily THC (100 mg) inhalation, decreased marginally by 4-11% and 0-7%, respectively; (B) MP THC $C_{ss,avg}$ and $C_{ss,max}$, after daily THC (10 mg) oral consumption, decreased modestly by 15-28% and 16-28%, respectively. Likewise, there was marginal gestational-age dependent decrease (1-5%) in 11-OH-THC MP $C_{ss,avg}$ and $C_{ss,max}$, after both inhalational and oral THC consumption. Insets show data truncated to 6 hours.

4.4.6 m-f-PBPK Model Predicted Gestational Age-Dependent Changes in Fetal Plasma and Brain THC/11-OH-THC Exposure

After THC inhalation, with the increase in GW from 15 to 40, the predicted THC and 11-OH-THC UVP/MP $C_{ss,avg}R$ decreased from 0.46 to 0.29 and from 1.51 to 0.98, respectively. This trend remained for oral THC consumption (Table 4.2). Because the fetal brain K_p was kept constant across gestational age, the change with GW in fetal brain/MP $C_{ss,avg}R$ for both THC and 11-OH-THC mirrored that in UVP/MP $C_{ss,avg}R$ for both inhalational and oral THC consumption (Table 4.2). As expected, the predicted fetal brain/UVP and the fetal brain/MP $C_{ss,avg}R$ were independent of the route of administration. As the THC and 11-OH-THC MP, UVP/MP and fetal brain/MP all decreased with an increase in GW, the maximum predicted steady-state exposure ($C_{ss,avg}$, $C_{ss,max}$, and AUC_{ss}) was at GW15 (Table 4.2, Figure 4.5). For example, at GW15, with a typical inhalation dose of 100 mg THC, the predicted UVP $C_{ss,max}$

were 948 nM THC and 130 nM 11-OH-THC while the corresponding $C_{ss,max}$ in the fetal brain were 880 nM THC and 398 nM 11-OH-THC (Figure 4.6). Similarly, with a typical dose of 10 mg oral THC, the predicted UVP $C_{ss,max}$ were 2.8 nM THC and 12 nM 11-OH-THC while the corresponding $C_{ss,max}$ in the fetal brain were 3.9 nM THC and 38 nM 11-OH-THC (Figure 4.6). The cannabinoid fetal brain/UVP, at a given timepoint, should be similar to the fetal brain K_p and therefore not change based upon the route of administration or amount of dose. The fetal brain/UVP $C_{ss,max}R$ is not independent of the route of consumption as the $C_{ss,max}$ for each route occurred at different timepoints.

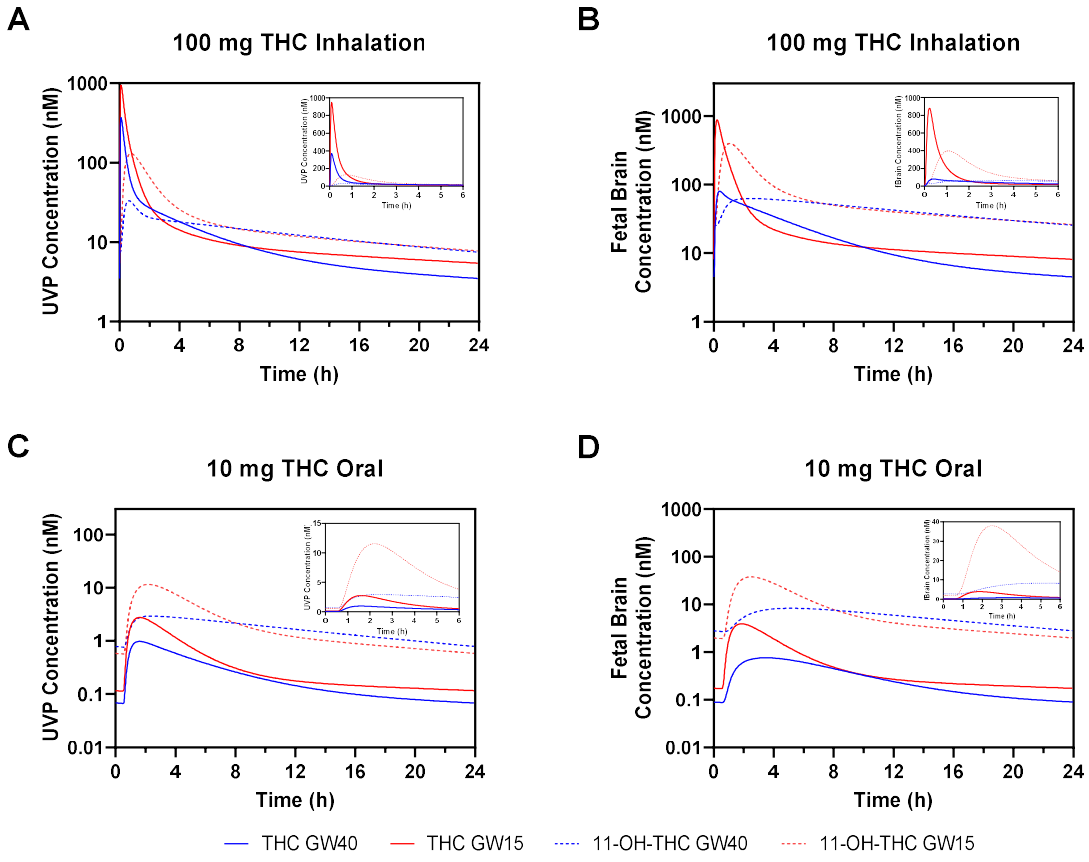

Figure 4.5: m-f-PBPK model predicted gestational age-dependent changes in THC/11-OH-THC umbilical venous plasma (UVP) and fetal brain concentration-time profiles after daily maternal inhalation (100 mg) or oral (10 mg) consumption of THC. The maximum THC and 11-OH-THC exposure ($C_{ss,avg}$ and $C_{ss,max}$) in the (A, C) UVP and (B, D) fetal brain was predicted to be at the earliest gestational week (GW15) for which predictions could be made. This was because the predicted maternal plasma (MP), UVP/MP and fetal brain/MP all decreased with increasing gestational age. Insets show data truncated to 6 hours.

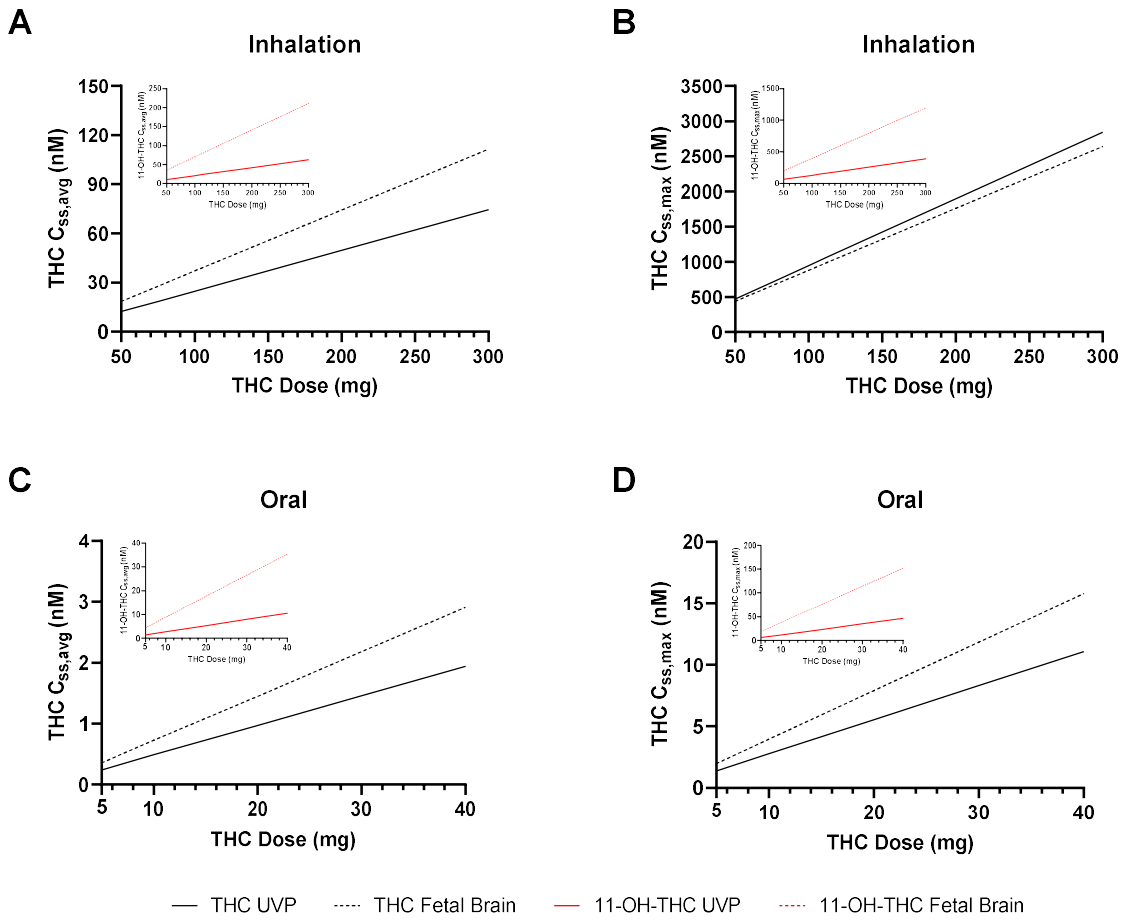

Figure 4.6: m-f-PBPK model predicted dose-dependent average ($C_{ss,avg}$) and maximum ($C_{ss,max}$) steady-state THC and 11-OH-THC concentration in umbilical venous plasma (UVP) and fetal brain after daily maternal inhalation (100 mg) or oral (10 mg) THC consumption at gestational week 15. (A/B) At the typical inhalation THC dose (100 mg), the predicted UVP $C_{ss,avg}$ & C_{max} were 25 & 948 nM THC and 21 & 130 nM 11-OH-THC and for the fetal brain these were 37 & 880 nM THC and 70 & 398 nM 11-OH-THC, respectively. (C/D) At the typical oral THC dose (10 mg), the predicted UVP $C_{ss,avg}$ & $C_{ss,max}$ were 0.49 & 2.8 nM THC and 2.6 & 12 nM 11-OH-THC. For the fetal brain these were 0.73 & 3.9 nM THC and 8.9 & 38 nM 11-OH-THC, respectively. Insets show the 11-OH-THC predicted concentrations.

Table 4.2: m-f-PBPK Model Predicted Dose-Normalized Steady-State Total and Unbound THC and 11-OH-THC Maternal (or Non-pregnant) Plasma, Umbilical Venous Plasma and Fetal Brain Concentrations at 15, 25, and 40 GW of Pregnancy after Daily Inhalation or Oral Cannabis Use

	Inhalation							
	THC				11-OH-THC			
	Non-Pregnant	**GW15**	**GW25**	**GW40**	**Non-Pregnant**	**GW15**	**GW25**	**GW40**
MP or NP $C_{ss,avg}$ (nM/mg dose)	0.57	0.55	0.50	0.51	0.14	0.14	0.14	0.14
MP or NP $C_{ss,avg,u}$ (nM/mg dose)	0.0063	0.0060	0.0055	0.0056	0.0017	0.0017	0.0017	0.0016
MP or NP $C_{ss,max}$ (nM/mg dose)	13.8	13.8	12.8	12.6	1.01	1.00	1.01	0.99
MP or NP $C_{ss,max,u}$ (nM/mg dose)	0.15	0.15	0.14	0.14	0.012	0.012	0.012	0.012
UVP $C_{ss,avg}$ (nM/mg dose)	NA	0.25	0.16	0.14	NA	0.21	0.17	0.13
UVP/MP $C_{ss,avg}R$ (nM/mg dose)	NA	0.46	0.33	0.29	NA	1.51	1.20	0.98
UVP $C_{ss,avg,u}$ (nM/mg dose)	NA	0.0018	0.0012	0.0010	NA	0.0014	0.0011	0.0009
UVP/MP $C_{ss,avg,u}R$ (nM/mg dose)	NA	0.29	0.21	0.18	NA	0.84	0.67	0.55
UVP $C_{ss,max}$ (nM/mg dose)	NA	9.48	3.97	3.70	NA	1.30	0.43	0.33
UVP $C_{ss,max,u}$ (nM/mg dose)	NA	0.067	0.028	0.026	NA	0.0087	0.0029	0.0022
Fetal Brain $C_{ss,avg}$ (nM/mg dose)	NA	0.37	0.23	0.18	NA	0.70	0.55	0.43
Fetal Brain/MP $C_{ss,avg}R$ (nM/mg dose)	NA	0.68	0.46	0.35	NA	5.08	4.00	3.16
Fetal Brain/UVP $C_{ss,avg}R$ (nM/mg dose)	NA	1.50	1.40	1.22	NA	3.36	3.32	3.16
Fetal Brain $C_{ss,avg,u}$ (nM/mg dose)	NA	0.0014	0.0009	0.0007	NA	0.0014	0.0011	0.0008
Fetal Brain/MP $C_{ss,avg,u}R$ (nM/mg dose)	NA	0.24	0.16	0.12	NA	0.81	0.64	0.51
Fetal Brain/UVP $C_{ss,avg,u}R$ (nM/mg dose)	NA	0.81	0.76	0.66	NA	0.96	0.95	0.92
Fetal Brain $C_{ss,max}$ (nM/mg dose)	NA	8.80	1.70	0.81	NA	3.98	1.04	0.63
Fetal Brain $C_{ss,max,u}$ (nM/mg dose)	NA	0.039	0.0077	0.0033	NA	0.0079	0.0020	0.0012

Oral								
	THC				11-OH-THC			
	Non-Pregnant	**GW15**	**GW25**	**GW40**	**Non-Pregnant**	**GW15**	**GW25**	**GW40**
MP or NP $C_{ss,avg}$ (nM/mg dose)	0.13	0.11	0.10	0.093	0.18	0.17	0.17	0.17
MP or NP $C_{ss,avg,u}$ (nM/mg dose)	0.0014	0.0012	0.0011	0.0010	0.0021	0.0021	0.0021	0.0021
MP or NP $C_{ss,max}$ (nM/mg dose)	0.68	0.57	0.55	0.49	0.80	0.78	0.78	0.78
MP or NP $C_{ss,max,u}$ (nM/mg dose)	0.0075	0.0063	0.0060	0.0054	0.0096	0.0093	0.0093	0.0093
UVP $C_{ss,avg}$ (nM/mg dose)	NA	0.049	0.034	0.025	NA	0.26	0.21	0.17
UVP/MP $C_{ss,avg}$R (nM/mg dose)	NA	0.44	0.33	0.27	NA	1.51	1.20	0.98
UVP $C_{ss,avg,u}$ (nM/mg dose)	NA	0.0003	0.0002	0.0002	NA	0.0018	0.0014	0.0011
UVP/MP $C_{ss,avg,u}$R (nM/mg dose)	NA	0.28	0.21	0.18	NA	0.84	0.67	0.55
UVP $C_{ss,max}$ (nM/mg dose)	NA	0.28	0.14	0.10	NA	1.16	0.43	0.29
UVP $C_{ss,max,u}$ (nM/mg dose)	NA	0.0020	0.0010	0.0007	NA	0.0077	0.0029	0.0020
Fetal Brain $C_{ss,avg}$ (nM/mg dose)	NA	0.073	0.048	0.031	NA	0.89	0.69	0.54
Fetal Brain/MP $C_{ss,avg}$R (nM/mg dose)	NA	0.66	0.46	0.33	NA	5.08	4.00	3.16
Fetal Brain/UVP $C_{ss,avg}$R (nM/mg dose)	NA	1.50	1.40	1.22	NA	3.36	3.32	3.16
Fetal Brain $C_{ss,avg,u}$ (nM/mg dose)	NA	0.0003	0.0002	0.0001	NA	0.0017	0.0013	0.0010
Fetal Brain/MP $C_{ss,avg,u}$R (nM/mg dose)	NA	0.23	0.16	0.12	NA	0.81	0.64	0.51
Fetal Brain/UVP $C_{ss,avg,u}$R (nM/mg dose)	NA	0.81	0.76	0.66	NA	0.96	0.95	0.92
Fetal Brain $C_{ss,max}$ (nM/mg dose)	NA	0.39	0.15	0.077	NA	3.80	1.35	0.84
Fetal Brain $C_{ss,max,u}$ (nM/mg dose)	NA	0.0015	0.0006	0.0003	NA	0.0074	0.0026	0.0016

NA: not applicable; MP: maternal plasma; NP: Non-pregnant plasma; UVP: umbilical venous plasma; $C_{ss,avg}$: average steady-state concentration; $C_{ss,avg,u}$: unbound average steady-state concentration; $C_{ss,max}$: maximum steady-state concentration; $C_{ss,max,u}$: unbound maximum steady-state concentration; $C_{ss,avg}$R: ratio of average steady-state concentration; $C_{ss,avg,u}$R: ratio

of unbound average steady-state concentration; $C_{ss,max}R$: ratio of maximum steady-state concentration; $C_{ss,max,u}R$: ratio of unbound maximum steady-state concentration.

4.5 Discussion

To our knowledge, this is the first study to quantify cannabinoid exposure in human MP as well as in UVP or fetal tissues in a large number of T1, T2 and T3 pregnancy subjects (Table 4.1). Additionally, our study is the first to apply our m-f-PBPK model to predict the average and maximum steady-state maternal-fetal cannabinoid exposure after chronic THC consumption via inhalation and oral routes. Such observations and predictions provide an in-depth understanding of fetal cannabinoid exposure, relative to maternal exposure, and how it varies with THC (or cannabis) dose and route of consumption. In addition, these data will guide future studies on the impact of prenatal cannabis use on fetal neurodevelopmental toxicity studies *in vitro* and in preclinical species.

Our observed mean THC paired UVP/MP value at T3 (0.35 ± 0.13; n=18; Table 4.1) was similar to the previously published sparse data by Blackard et al. (0.26 ± 0.10; n=3)[43]. We were able to detect 11-OH-THC in only one UVP sample (Table 4.1) and Blackard et al. did not report this value. The mean observed T3 paired UVP/MP COOH-THC value (0.36 ± 0.18; n=19; Table 4.1) was modestly higher than that reported by Blackard et al. (0.24 ± 0.15; n=10)[43]. The THC UVP/MP $C_{ss,avg,u}R$ is also estimated to be <0.4 given the measured fraction unbound in the adult NP plasma ($f_{u,p}$=0.011) and in fetal plasma ($f_{u,p,fetus}$=0.0071) (Table S4.1). Of note, we measured the MP $f_{u,p}$ (0.013; CV=50%; n=18) and $f_{u,p,fetus}$ (0.0072; CV=88%; n=18) from the *in vivo* T3 samples and these values were almost identical to those listed above. We did not use these values in our m-f-PBPK model as we wanted to use our m-f-PBPK model to make prospective predictions (i.e. without using our own T1/T2/T3 data). These data suggest that fetal liver metabolism and influx transport at the basal membrane of the syncytiotrophoblast work in concert to reduce total (and unbound) fetal exposure to these cannabinoids when compared with maternal exposure. In addition, since the unbound fetal plasma concentrations (specifically

unbound fetal arterial concentration which is <1% of the total fetal plasma concentration) determine the unbound fetal brain concentrations, such protection has the potential to decrease THC fetal neurotoxicity provided the cannabinoids are not actively transported into the brain (see below for further discussion).

In T1 and T2, the observed THC fetal brain/MP values were 0.50 ± 0.18 and 0.45 ± 0.28, respectively (Table 4.1). This lack of change in fetal brain/MP across trimesters is not surprising as the mean difference in gestational age for our T1 and T2 samples was only 5 weeks (Table S4.2). In addition, the fetal brain rapidly develops in utero and the human fetal blood-brain barrier (BBB) develops between GW 8-18[205]. Although the protein expression of P-glycoprotein at the human fetal BBB reaches a maximum in the 3rd trimester[98], THC, 11-OH-THC and COOH-THC are not substrates of human P-gp[8,96]. THC is a lipophilic compound capable of crossing the BBB through transcellular diffusion. Thus, we postulate that THC likely crosses the BBB primarily through passive diffusion and is not effluxed at the fetal BBB. Therefore, the steady-state unbound fetal concentration in the brain interstitial fluid and parenchymal cells should equal that in the fetal circulation (fetal artery). If these assumptions are correct, the absolute unbound steady-state fetal brain concentration will be much lower than the total fetal brain concentration. As discussed above for the T3 fetus, this too should reduce the potential for THC to cause neurotoxicity (see m-f-PBPK model predictions below). The observed THC concentrations in the MP (0.45 – 51 nM), UVP (0.13 – 14 nM), and fetal brain (1.0 – 18 nM), across all gestational ages (Tables S4.3 and S4.4), were far below those previously tested in *in vitro* (2 – 15 μM)[11,12] and fetal mice (dose: 5 mg/kg THC)[13] toxicity studies (unfortunately fetal brain concentrations were not measured in these studies).

The cannabinoid UVP/MP and fetal brain/MP data discussed above are only “snapshots” at a given time and not representative of the steady-state THC exposure (e.g., $C_{ss,max}$ or $C_{ss,avg}$) that is achieved in the various compartments. Since these concentrations cannot be measured *in vivo*, the only recourse is to predict them through m-f-PBPK modeling. This we did after we

verified our THC/11-OH-THC PBPK model for the NP population (Table S4.7, Figures S4.1-3). Since fetal exposure to drugs is driven by maternal exposure, we first predicted the latter.

Maternal exposure of THC was only modestly reduced by gestational age or compared with the NP adults. The reduction in the MP $C_{ss,avg}$ was smaller after inhalational THC (11%) than after oral THC (28%) (Table 4.2, Figure 4.4). This is because, due to its high hepatic extraction, THC's hepatic clearance is blood-flow limited and therefore not expected to change after inhalation THC. Change in hepatic blood flow due to pregnancy is controversial, with some studies reporting no change[206,207]. However, after oral THC consumption, the THC MP $C_{ss,avg}$ was more affected as it is no longer dependent on hepatic blood but is dependent on metabolic clearance. CYP2C9, the major enzyme responsible for clearance of THC is modestly induced in the liver during pregnancy[15,84]. We have shown that induction of CYP3A (an enzyme also important in intestinal THC metabolism) during pregnancy is hepatic, not intestinal, and the magnitude of induction is predicted to be constant throughout pregnancy[91]. Because we couldn't determine the fraction of 11-OH-THC metabolized via various pathways, we did not estimate the pregnancy-induced enzyme induction on its maternal exposure. Moreover, since the maternal pharmacokinetics of these cannabinoids have not been characterized in pregnant people, our predictions could not be verified.

Next, we established that our m-f-PBPK model predictions of THC UVP/MP and fetal tissue/MP concentration values aligned with those in our observational study. For this, we predicted these values post-absorption when distributional equilibrium between plasma and tissue concentrations is expected to be reached, i.e., >12 hours post-consumption, when these values remained relatively constant (Figure 4.3, Figure S4.4). The predicted T3 UVP/MP at GW38 and each of the predicted T2 fetal tissue/MP values at GW15 fell within the acceptance range (Figure 4.3). Therefore, we conclude that the model predicted fetal THC concentrations well and has been verified to the extent possible. Unfortunately, since 11-OH-THC was only

quantifiable in one UVP and fetal brain sample and only a few fetal livers and kidneys (Table S4.3 and S4.5) we could not verify the corresponding predictions for 11-OH-THC.

As unbound MP THC exposure is a driving force for unbound fetal UVP (and systemic) exposure, the decrease in MP THC $C_{ss,avg,u}$ with gestational age reduced the corresponding fetal (UVP) $C_{ss,avg,u}$ (Table 4.2). Due to GW-dependent increases in fetal metabolic CL of THC, the predicted ratios (e.g., UVP/MP $C_{ss,avg,u}R$) decreased with GW (Table 4.1). It is important to note that the fetal THC systemic and UVP plasma concentrations are not equal. As expected, our m-f-PBPK model predictions of the steady-state fetal central venous (or arterial) THC concentrations were modestly lower (19 – 28%) than the corresponding UVP concentrations. This is because all the UV blood draining the placenta does not empty into the fetal central vein; 65% is shunted to the fetal liver[149] where the cannabinoids undergo “first-pass extraction”. For 11-OH-THC, where the first-pass extraction was lower, this difference between fetal central vein or artery vs UV concentrations was less (only 4 – 6%). However, for the purposes of this discussion we have assumed equivalency between the different fetal plasma (UVP, central vein, central artery) steady-state concentrations to allow comparison with the observed UVP/MP data. With that assumption, the THC and 11-OH-THC UVP/MP $C_{ss,avg,u}R$ is influenced by the change in magnitude of $CL_{int,fh}$, $CL_{int,PD}$, and $CL_{int,T}$ (Eq. 2).

$$\frac{UVP\ C_{ss,avg,u}}{MP\ C_{ss,avg,u}} = \frac{(CL_{int,PD})}{(CL_{int,T}+2*CL_{int,fh}+CL_{int,PD})} \quad \text{(Eq. 2)}$$

Each of these three clearance parameters change across gestational age (Table S4.1). However, while the absolute $CL_{int,PD}$ and $CL_{int,T}$ in Eq. 2 increased with gestational age, as indicated earlier (Table S4.1), the ratio of $CL_{int,PD}$ and $CL_{int,T}$ did not change. Therefore, the predicted decrease in cannabinoid UVP/MP $C_{ss,avg,u}R$ with GW was influenced only by the increase in fetal liver metabolic CL and not placental transfer CL (Table 4.2).

As stated previously, the steady-state unbound fetal brain cannabinoid concentrations should be equal to unbound fetal arterial concentrations, with the assumption that both THC and

11-OH-THC passively diffuse across the BBB. Also, we assumed cannabinoid protein binding in the brain to be independent of GW. Consequently, the predicted fetal brain/UVP $C_{ss,avg,u}R$ or fetal brain/UVP $C_{ss,avg}R$ did not change substantially with GW (Table 4.2). The latter is in agreement with our observed data (Table 4.1).

To inform the absolute total and unbound UVP and fetal brain THC/11-OH-THC exposure with GW, we predicted their concentrations when they were expected to be maximum, that is at GW15, the earliest GW for which predictions can be made by our m-f-PBPK model (Table 4.2 and Figure 4.5; exposure at GW25 was in between 15 and 40 and therefore not shown). After a typical daily dose of THC consumed by inhalation (100 mg, range: 50 – 300 mg), the predicted fetal brain THC and 11-OH-THC $C_{ss,avg}$ were 37 (range: 19 – 111 nM) and 70 nM (range: 35 – 211 nM), respectively (Figure 4.6). Similarly, after a typical daily oral consumption of 10 mg THC (range: 5 – 40 mg), the predicted THC and 11-OH-THC $C_{ss,avg}$ in the fetal brain were lower, 0.73 nM (range: 0.36 – 2.9) and 8.9 nM (4.4 – 35 nM), respectively (Figure 4.6). The fetal brain $C_{ss,avg,u}$ is even lower due to extensive binding in the brain. Therefore, after a typical daily dose of 100 mg inhalation THC, the predicted fetal brain $C_{ss,avg,u}$ of THC and 11-OH-THC were 3.9 nM and 0.79 nM, respectively and after a typical daily oral consumption of 10 mg THC, were 0.015 nM and 0.074 nM, respectively. These lower fetal brain steady-state (total and unbound) cannabinoid concentrations after oral vs. inhalation consumption (albeit the oral dose is much lower) could result in lower fetal toxicity. We do not know if the previously observed effects of THC on neurotoxicity *in vitro* (at 2 – 15 μM THC)[11,12] will be consistent when re-conducted at these lower concentrations. Of note, accumulation of THC and 11-OH-THC in the MP, UVP, and fetal brain at steady-state vs. single dose was minimal (<1.07) for once-a-day consumption (Figure S4.5). However, assuming linear pharmacokinetics, the maximum ($C_{max,ss}$) and average ($C_{ss,avg}$) THC and 11-OH-THC concentrations in the UVP and fetal brain for any THC dose (for once-a-day consumption) can

be computed from these data as they should change proportionally with dose. For a different frequency of consumption, our m-f-PBPK model can be used to predict these concentrations.

Our observational study and m-f-PBPK model have some limitations. First, because our *in vivo* study was opportunistic where pregnant individuals were already using cannabis, we did not have definitive information on dose, timing, and frequency of cannabis consumption. Second, we could collect only single timepoint data and therefore obtain only a "snapshot" of cannabinoid exposure. Nevertheless, we were able to interpret the UVP/MP and fetal tissue/MP values (at the times observed), because theoretically and as predicted, they are/should be independent of the dose, timing and frequency, of cannabis use. Third, 11-OH-THC was not quantifiable in the majority of *in vivo* samples and therefore our m-f-PBPK model could not be verified for this psychoactive metabolite. Fourth, due to lack of physiological data at early GW (including abundance of the placental transporter responsible for fetal-maternal efflux of THC), we could not simulate fetal exposure at <GW15. Incorporating these data, when available, into our m-f-PBPK model would allow us to predict cannabinoid exposure throughout gestation. Fifth, we would have preferred to verify our model with THC concentrations collected at multiple times points during the consumption interval. However, this is logistically not possible. Lastly, it is possible that constituents other than THC/11-OH-THC are the cause of the potential neurodevelopmental toxicity of cannabis.

In conclusion, this is the first time that THC, 11-OH-THC, and COOH-THC concentrations in MP, UVP, fetal brain, and placenta tissue have been quantified in a large number of T1, T2 and T3 pregnancies. In addition, this is the first time a verified m-f-PBPK model has been employed to predict UVP and fetal brain (and other fetal tissue) exposure to these cannabinoids on regular consumption of cannabis. Our model predictions are that both UVP and fetal brain exposure to THC was reduced relative to that in the MP at all GW; however, such exposure was greatest at GW15. Influx transport on the basal membrane of the syncytiotrophoblast and fetal liver metabolism acted in concert to reduce fetal exposure to the

cannabinoids and therefore protect the fetus from possible neurodevelopmental toxicity. We propose that future fetal toxicity studies (*in vitro* or *in vivo* in animals) should be conducted to replicate the predicted unbound fetal UVP and fetal brain THC/11-OH-THC concentrations at the typical doses consumed by pregnant people. Our m-f-PBPK model can be used to predict such concentrations for different doses of THC consumed by inhalation or orally. If drug-dependent parameters are known, this model could also predict fetal exposure to other potential neurotoxins.

Collaborations: Lyndsey S. Benson, Erica M. Wymore, Jocelyn E. Phipers, Jennifer C. Dempsey, and Lucinda A. Cort conducted the *in vivo* observational studies and collected all human plasma and tissue samples.

4.6 Supplemental Information

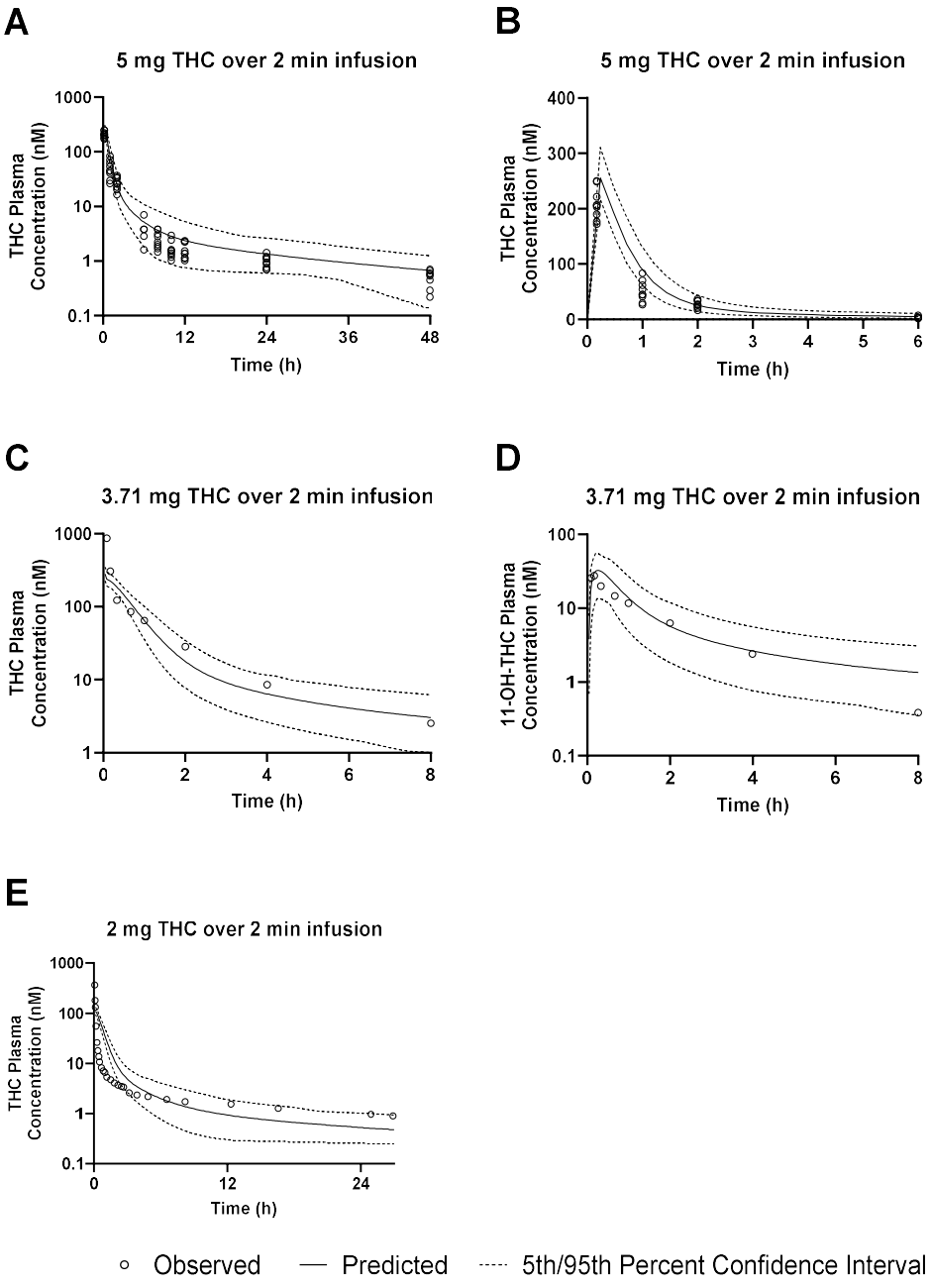

Figure S4.1: Non-pregnant observed and PBPK model predicted THC and 11-OH-THC plasma concentration-time profiles after intravenous THC administration to healthy volunteers. (A, B) The THC systemic disposition parameters were optimized using this training dataset[47]. Panel B shows the data in panel A truncated to 6 hr. (C – E) Then, without changing the values of these parameters, the model was verified with two independent datasets[46,106]. 11-OH-THC plasma concentrations, after THC administration, were measured in only the Naef 2004 study[106]. All predicted/observed THC ratios for AUC_{inf} ($AUC_{inf}R$) and C_{max} ($C_{max}R$) fell within the acceptance range, i.e., 0.67-1.43 and 0.44-1.47, respectively. Data (individual or mean) were digitized using WebPlotDigitizer, version 4.6.

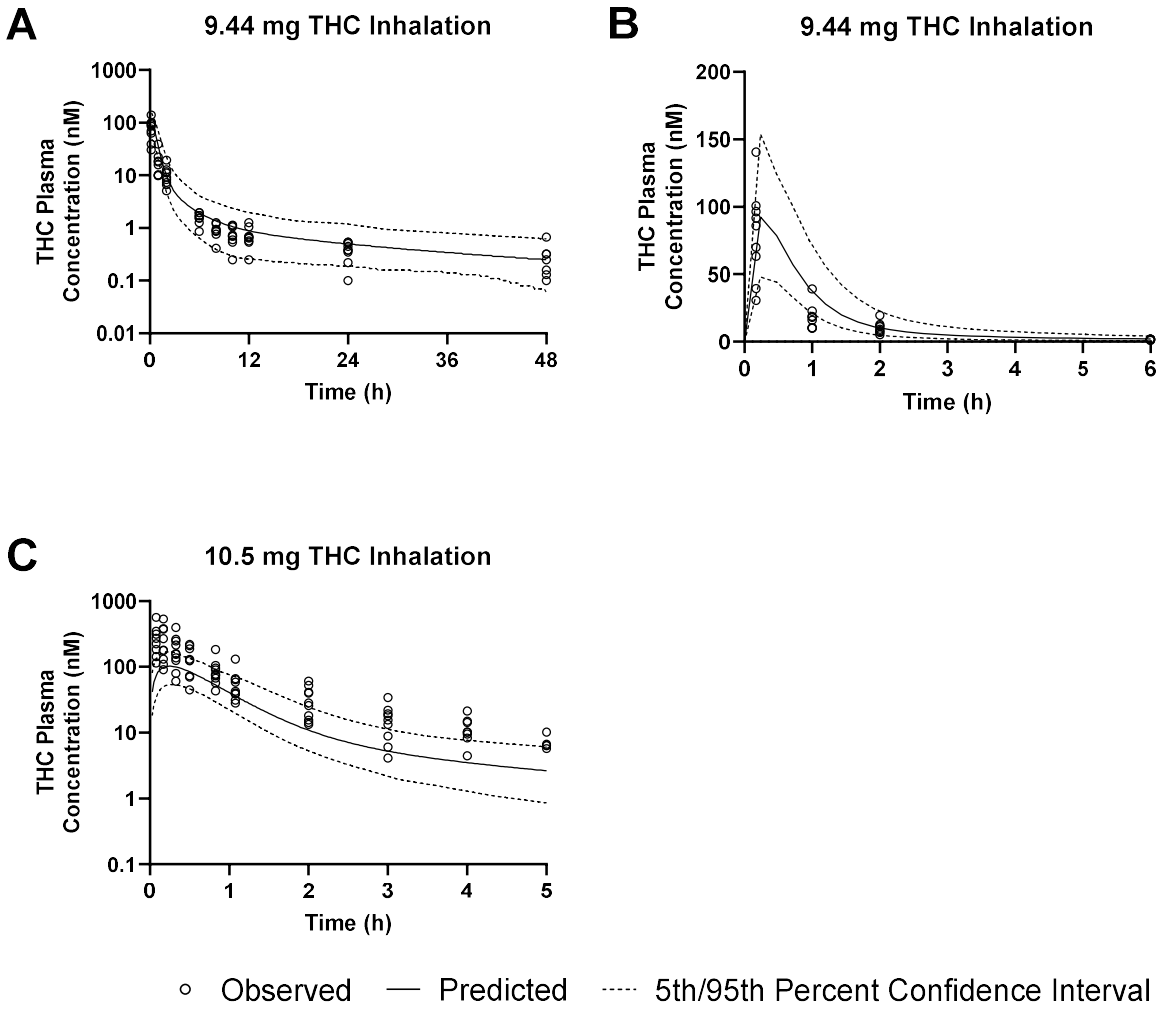

Figure S4.2: Non-pregnant observed and PBPK model predicted THC plasma concentration-time profiles after inhalation THC administration to healthy volunteers. (A, B) The THC inhalation absorption kinetics were optimized using this training dataset[47]. Panel B shows the data in panel A truncated to 6 hr. (C) Then, without changing the THC absorption parameters, the model was verified with an independent dataset[48]. All predicted/observed $AUC_{inf}R$ and $C_{max}R$ fell within the acceptance range, 0.45-1.27 and 0.55-1.10, respectively. 11-OH-THC plasma concentrations were not measured in these studies. Data (individual or mean) were digitized using WebPlotDigitizer, version 4.6.

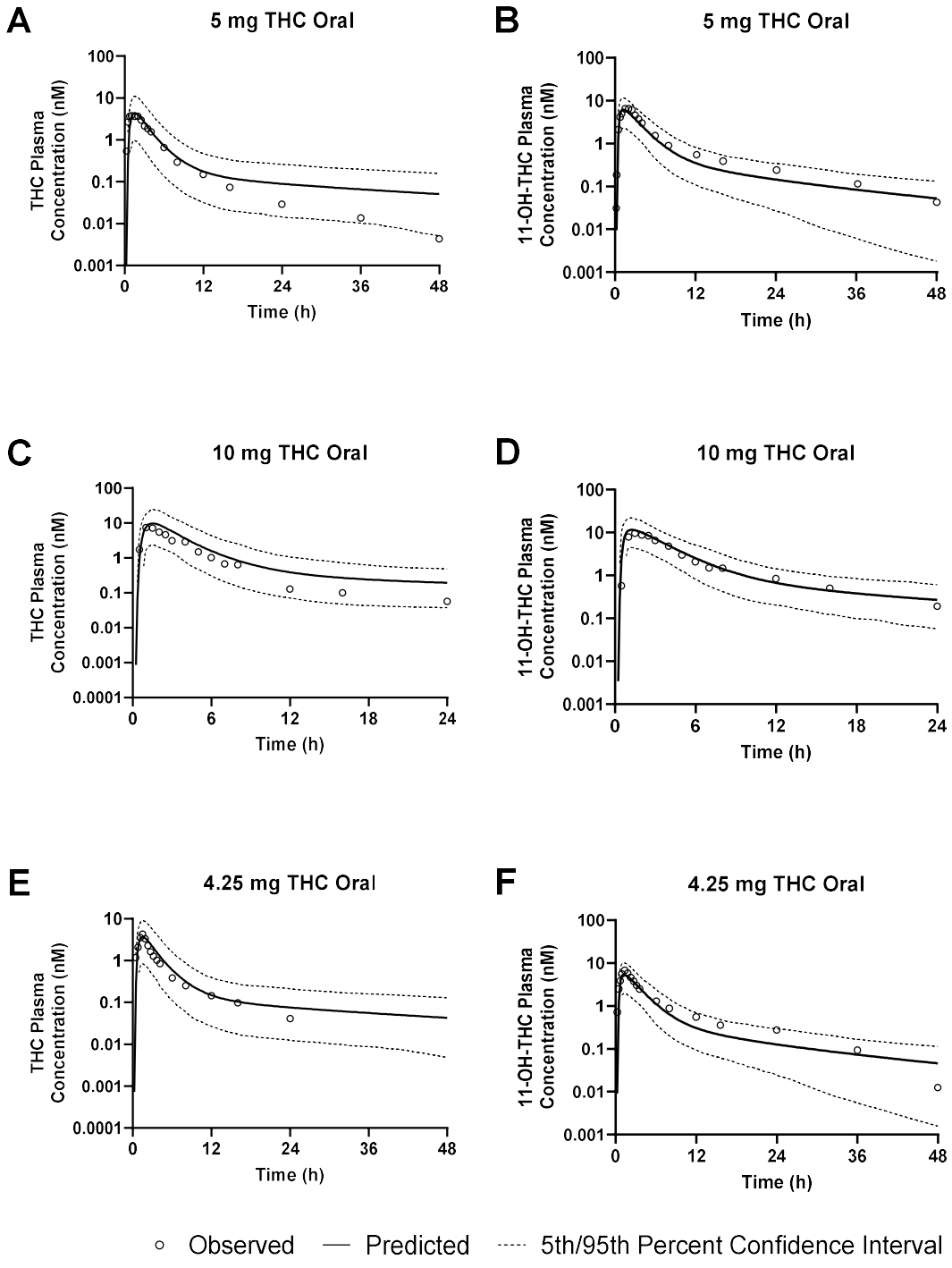

Figure S4.3: Non-pregnant observed and PBPK model predicted THC and 11-OH-THC plasma concentration-time profiles after oral THC administration to healthy volunteers. (A, B) The THC oral absorption kinetics and 11-OH-THC systemic disposition parameters were optimized using this training dataset[50]. (C-F) Then, without changing these parameters, the model was verified with two independent datasets[49,51]. All predicted/observed $AUC_{inf}R$ and $C_{max}R$ fell within the acceptance range, 0.73-1.48 and 0.69-1.41, respectively. Data (individual or mean) were digitized using WebPlotDigitizer, version 4.6.

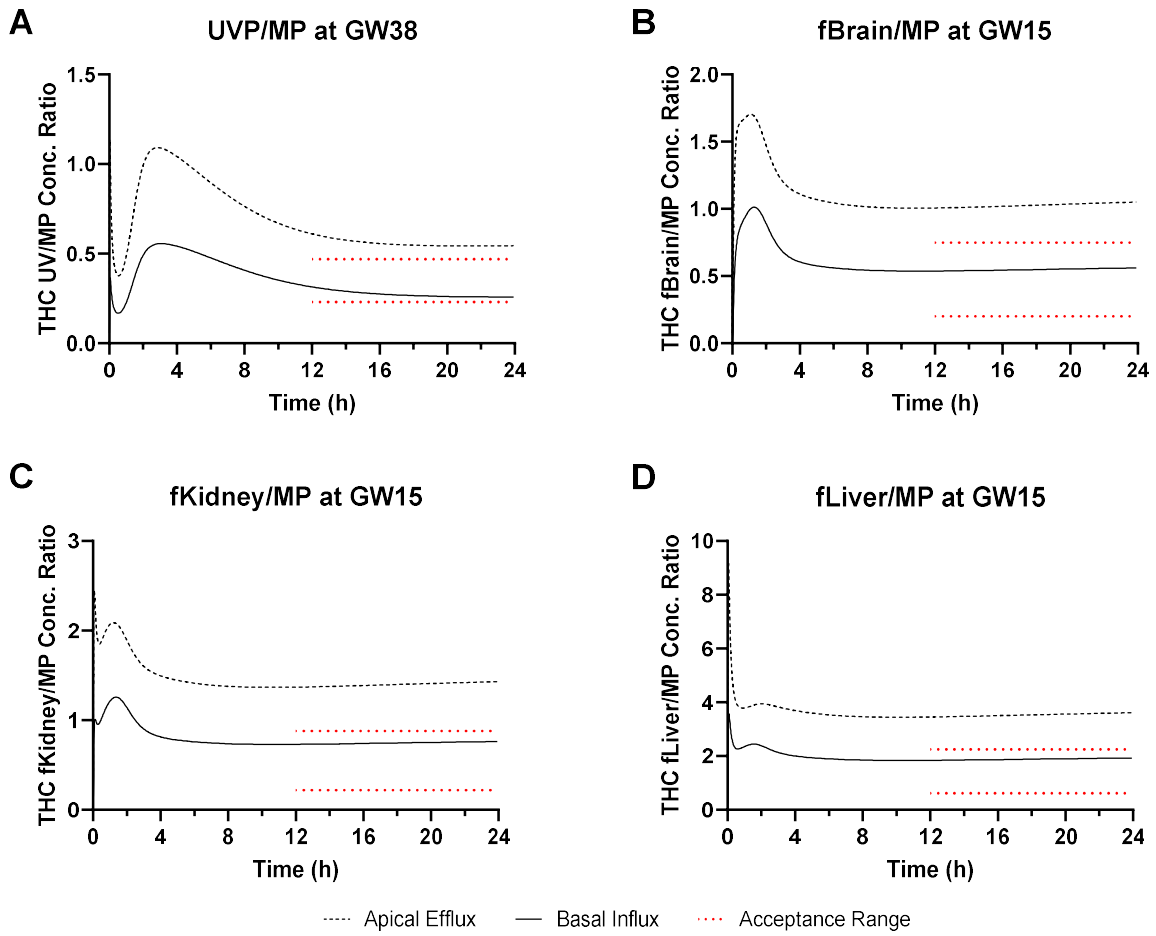

Figure S4.4: m-f-PBPK model predicted steady-state profiles of THC umbilical venous plasma/maternal plasma (UVP/MP) at GW38 as well as fetal tissue/MP (fTissue/MP) at GW15 after daily maternal THC inhalation (100 mg). The m-f-PBPK model predicted profiles were generated with either THC basal influx transport (solid line) or apical efflux transport (dashed line) at the basal and apical membrane of the syncytiotrophoblast, respectively. Only THC basal influx transport predicted trimester 3 (GW38) UVP/MP (A) and trimester 2 (GW15) fetal brain/MP (B), fetal kidney/MP (C), and fetal liver/MP (D) values within the acceptance criteria (red dotted lines) as computed from the *in vivo* observed data. Note, these profiles are independent of the consumed dose and route of administration. The *in vivo* observed data were collected when distribution equilibrium between plasma and tissue THC concentrations was expected to have been reached (i.e. >12 hours). To compare with the observed data, the predicted GW15 fetal tissue concentrations included the THC concentration in the blood within the tissues (see methods).

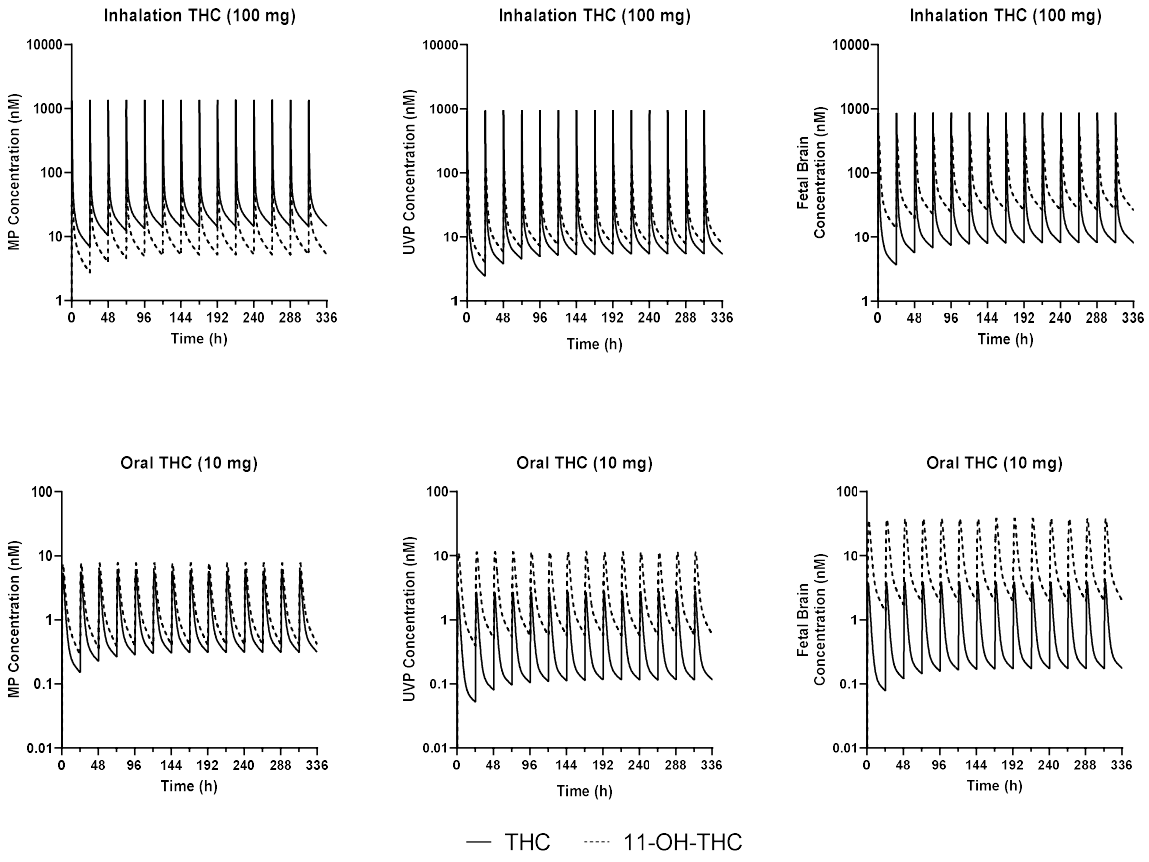

Figure S4.5: M-f-PBPK model predicted THC and 11-OH-THC steady-state plasma concentrations in the MP, UVP and fetal brain after daily consumption of THC (100 mg inhalation or 10 mg oral) at gestational week 15. At steady-state, there was marginal accumulation in the plasma of both THC and 11-OH-THC (<1.1) irrespective of the route of administration. In addition, as expected, the AUC_{ss} and $C_{ss,avg}$ of 11-OH-THC after oral THC consumption was greater than that after inhalation. Consistent with human adult postmortem data, 11-OH-THC fetal brain/UVP concentrations were predicted to be higher than those for THC.

Table S4.1: Drug and System-Dependent Input Parameters for the Non-pregnant and the Maternal-Fetal PBPK Models

Parameter	THC	11-OH-THC	Reference
Physiochemical and Binding			
Molecular Weight (g/mol)	314.15	330.46	ChEMBL
Log P	6.97	6.31	[44]
Ionization Type	Neutral	Neutral	ChEMBL
B/P	0.667	0.625	[45]
$f_{u,p}$	0.011	0.012	[15]
Absorption			
Oral f_a	0.38	N/A	[50]
Oral k_a (1/h)	0.60	N/A	Optimized with [50]
$f_{u,gut}$	0.38	N/A	Optimized with [50]
Q_{gut} (L/h)	16.9	N/A	Simcyp Predicted
Inhalation f_a	0.21	N/A	[47]
Inhalation k_a (1/h)	10.4	N/A	Optimized with [47]
Distribution			
$K_{p,liver}$	51.0	6.51	Optimized with [53,54,56]
$K_{p,kidney}$	2.04	1.47	Optimized with [53,54,56]
$K_{p,brain}$	1.50	3.53	Optimized THC with [53,55,56,199]; 11-OH-THC with [53,56]
$K_{p,muscle}$	0.063	0.001	Optimized with [47]
$K_{p,adipose}$	23.1	Remaining tissue	Optimized with [47]
$K_{p,skin}$	1.59	Remaining tissue	Optimized with [47]
$K_{p,tissue}$ (remaining tissues)	Various	Various	Predicted via Rodgers and Rowland (Simcyp Method 2)
Elimination			
CYP2C9 V_{max} (pmol/min/mg protein)	17.0	N/A	Estimated from [47] and [15] with a middle-out approach
CYP2C9 K_m (nM)	2.91	N/A	[15]
CYP3A CL_{int} (µL/min/mg protein)	578	N/A	Estimated from THC from [47] and [15]
Total Hepatic CL_{int} (µL/min/mg protein)	N/A	3763	Estimated from [50] using a middle-out approach
Pregnancy			
$f_{u,p,fetus}$	0.0071	0.0067	Measured by us
$CL_{int,fh}$ (L/h)	GW15: 23.0 GW25: 153 GW38: 519 GW40: 595	GW15: 3.37 GW25: 22.4 GW38: 76.1 GW40: 87.2	Estimated from [7]
$CL_{int,PD}$ (L/h)	GW15: 43.9 GW25: 110 GW38: 226 GW40: 247	GW15: 35.4 GW25: 88.4 GW38: 182 GW40: 199	Estimated from [8]
$CL_{int,T}$ (L/h) Assuming Influx at the Basal Membrane of the Syncytiotrophoblast	GW15: 74.8 GW25: 187 GW38: 385 GW40: 420	N/A	Estimated from [8]

N/A: not applicable; GW: gestational week; LogP: octanol-water partition coefficient; B/P: blood to plasma ratio; $f_{u,p}$: fraction unbound in the adult non-pregnant plasma; f_a: fraction absorbed; k_a: rate of absorption; $f_{u,gut}$: fraction unbound in the gut; Q_{gut}: blood flow in the gut; K_p: tissue to plasma ratio; CYP: cytochrome P450; V_{max}: maximum rate of metabolism; K_m: Michaelis-Menten constant; CL_{int}: intrinsic clearance; $f_{u,p,fetus}$: fraction unbound in the fetal plasma; $CL_{int,fh}$: intrinsic fetal hepatic clearance; $CL_{int,PD}$: intrinsic placental passive diffusion; $CL_{int,T}$: intrinsic placental transport.

Table S4.2: Demographics of the Subjects who Completed the T1/T2 or the T3 Study

		Trimester 1 n = 18	Trimester 2 n = 22	Trimester 3 n = 26
Maternal Race	**Caucasian**	10 (56%)	17 (77%)	11 (42%)
	African American	2 (11%)	3 (14%)	12 (46%)
	American Indian	1 (5.6%)	0 (0%)	0 (0%)
	Asian or Pacific Islander	2 (11%)	2 (9.1%)	1 (3.8%)
	Hispanic	0 (0%)	0 (0%)	1 (3.8%)
	Other/ Mixed	3 (17%)	0 (0%)	1 (3.8%)
Gestational age at delivery (days)		71 ± 8.0	105 ± 14	267 ± 12
Fetal Sex* (male ♂; female ♀)		7 (35%) ♂ 13 (65%) ♀	16 (73%) ♂ 6 (27%) ♀	Not Collected
Maternal age (years)		29 ± 5.3	26 ± 5.3	26 ± 5.2
Tobacco use within one month of sample collection**		10 (56%)	9 (41%)	7 (27%)

*One T1 subject had triplets and one T2 subject's fetal sex could not be ascertained;
**Self-reported
Data are either n (%) or mean ± SD

Table S4.3: Observed THC, 11-OH-THC, and COOH-THC Concentrations in Maternal Plasma, Umbilical Venous Plasma, and Placenta Tissues during Trimester 3 Pregnancy after Oral or Inhalation Consumption of Cannabis

	Inhalation Consumption	Oral Consumption	MP (nM)	UVP (nM)	UVP/MP	Placenta Mean (nM)	Placenta/ MP	MP (nM)	UVP (nM)	UVP/MP	Placenta Mean (nM)	Placenta/ MP	MP (nM)	UVP (nM)	UVP/MP	Placenta Mean (nM)	Placenta/ MP
			THC					11-OH-THC					COOH-THC				
1	---; > 72 hours	---, ---	BLOQ	BLOQ	---	---	---	BLOQ	BLOQ	---	BLOQ	---	BLOQ	BLOQ	---	BLOQ	---
2	0.75 grams; > 72 hours	---, ---	BLOQ	BLOQ	---	---	---	BLOQ	BLOQ	---	BLOQ	---	BLOQ	BLOQ	---	BLOQ	---
4	0.25 grams; 12-24 hours	---, ---	46	14	0.31	9.2	0.20	26	5.2	0.20	27	1.04	1304	163	0.13	109	0.084
5	0.0625 grams; 12-24 hours	100 mg; > 72 hours	3.8	1.0	0.28	1.2	0.32	BLOQ	BLOQ	---	BLOQ	---	12	5.40	0.45	6.0	0.50
6	0.0625 grams; 24-36 hours	---, ---	7.1	1.7	0.24	2.0	0.28	1.1	BLOQ	---	BLOQ	---	54	18	0.34	9.7	0.18
7	0.125 grams; > 72 hours	10-20 mg; > 72 hours	0.98	0.13	0.14	0.21	0.21	0.62	BLOQ	---	BLOQ	---	6.90	2.90	0.42	2.8	0.41
8	---, > 72 hours	---, ---	5.7	2.5	0.44	1.4	0.24	BLOQ	BLOQ	---	BLOQ	---	52	18	0.35	9.4	0.18
9	0.75 grams; > 72 hours	---, ---	BLOQ	BLOQ	---	---	---	BLOQ	BLOQ	---	BLOQ	---	BLOQ	BLOQ	---	BLOQ	---
10	---; 24-36 hours	---, ---	17	4.2	0.25	4.9	0.29	BLOQ	BLOQ	---	BLOQ	---	108	41	0.38	25	0.23
13	0.5 grams; 24-36 hours	50 mg; > 72 hours	5.9	---	---	0.78	0.13	3.1	---	---	BLOQ	---	33	---	---	4.2	0.13
15	3.5 grams; 36-48 hours	7 mg; 48-72 hours	11	3.9	0.34	5.2	0.46	3.0	BLOQ	---	BLOQ	---	190	40	0.21	---	---
18	0.75 grams; 36-48 hours	---, ---	3.6	1.8	0.50	1.6	0.44	BLOQ	BLOQ	---	BLOQ	---	21	9.0	0.44	BLOQ	---
19	0.25 grams, > 72 hours	---, ---	4.5	1.2	0.27	2.5	0.56	BLOQ	BLOQ	---	BLOQ	---	99	19	0.19	13	0.13
20	0.25 grams, > 72 hours	---, ---	7.7	2.4	0.31	3.1	0.40	0.93	BLOQ	---	BLOQ	---	76	8.2	0.11	BLOQ	---
21	1 gram; 24-36 hours	---, ---	3.2	1.3	0.40	1.6	0.50	0.86	BLOQ	---	BLOQ	---	19	4.3	0.23	9.0	0.48
22	1 gram; 12-24 hours	---, ---	1.9	0.41	0.22	1.2	0.64	BLOQ	BLOQ	---	BLOQ	---	17	5.1	0.30	BLOQ	---
23	0.125 grams; 24-36 hours	---, ---	5.3	1.9	0.35	1.1	0.21	0.85	BLOQ	---	BLOQ	---	16	6.6	0.42	BLOQ	---
24	0.5 grams; 24-36 hours	5 mg; 48-72 hours	BLOQ	BLOQ	---	0.38	---	BLOQ	BLOQ	---	BLOQ	---	0.98	BLOQ	---	BLOQ	---
25	---; 48-72 hours	---, ---	6.3	1.7	0.27	1.6	0.25	BLOQ	BLOQ	---	BLOQ	---	82	38	0.47	24	0.29
27	---; ---	10 mg; > 72 hours	BLOQ	BLOQ	---	2.3	---	BLOQ	BLOQ	---	BLOQ	---	BLOQ	BLOQ	---	BLOQ	---
28	1 gram; 4-12 hours	---, ---	0.90	0.62	0.69	---	---	BLOQ	BLOQ	---	BLOQ	---	9.60	4.6	0.48	BLOQ	---
29	0.3 grams; 12-24 hours	---, ---	0.45	BLOQ	---	---	---	BLOQ	BLOQ	---	BLOQ	---	1.60	0.92	0.58	BLOQ	---
30	3.5 grams; >72 hours	---, ---	6.7	2.2	0.33	---	---	BLOQ	BLOQ	---	BLOQ	---	25	5.4	0.22	BLOQ	---
32	0.125 grams; 24-36 hours	---; 24-36 hours	3.3	1.5	0.44	---	---	BLOQ	BLOQ	---	BLOQ	---	39	9.1	0.23	BLOQ	---
33	2 vape hits; 48-72 hours	10 mg; >72 hours	18	BLOQ	---	---	---	9.4	BLOQ	---	BLOQ	---	150	BLOQ	---	BLOQ	---
34	1 gram; 24-36 hours	---, ---	6.5	3.2	0.49	4.9	0.76	2.2	BLOQ	---	BLOQ	---	53	45	0.85	BLOQ	---
Mean ± SD (%CV)					0.35 ± 0.13 (37)		0.37 ± 0.18 (48)			0.20		1.04			0.36 ± 0.18 (49)		0.26 ± 0.15 (58)

BLOQ: below limit of quantification; ---: no sample/data collected and/or ratio cannot be calculated; Self-reported dosing information is listed for last consumption of THC (amount; time since last consumption) prior to delivery; MP: maternal plasma; UVP: umbilical venous plasma.

Table S4.4: Observed THC Concentrations in Maternal Plasma, Placenta, and Fetal Tissue Obtained during Trimester 1 and 2 Pregnancies after Oral or Inhalation Consumption of Cannabis

Subject	Gestational Age (days)	Dosing	MP (nM)	Fetal Brain (nM)	Fetal Brain/MP	Fetal Kidney (nM)	Fetal Kidney/MP	Fetal Liver (nM)	Fetal Liver/MP	Placenta Mean (nM)	Placenta/MP
Trimester 1											
H28680	67	---; 4-12 hours	3.4							0.89	0.26
H28688	52	1 gram; < 4 hours	19							36	1.9
H28761	72	3.5 grams; < 4 hours	34							6.9	0.21
H28869	59	80 mg THC; < 4 hours	24							25	1.0
H28928	67	3 grams; 36-48 hours	26	18	0.68			20	0.75	19	0.71
H28960	78	0.25 grams; 4-12 hours	16							5.4	0.34
H28972	72	0.5 grams; 12-24 hours	7.0							BLOQ	
H28986	78	1 dab/0.25 grams; 12-24 hours	20							13	0.62
H28987	74	1 joint; 12-24 hours	0.56							BLOQ	
H29026	80	1 gram; 4-12 hours	0.52							BLOQ	
H29045	74	0.1 grams; 4-12 hours	2.5							BLOQ	
H29110	82	2 grams; 36-48 hours	20	6.7	0.33					9.9	0.49
H29122	~77	3 grams; < 4 hours	37							22	0.60
H29141	67	2 grams; 12-24 hours	3.5							BLOQ	
H90004	74	1 gram; 12-24 hours	3.1							14	4.4
H90006	59	100 mg THC oral; 12-24 hours	3.6							BLOQ	
H90015	76	2 grams; 12-24 hours	45							12	0.26
H90020	74	100 mg THC; 4-12 hours	5.0							3.8	0.77
Pool 1			27	13	0.48						
Pool 2			12			11	0.89				
Mean ± SD (%CV)					0.50 ± 0.18 (35)						0.96 ± 1.2 (122)
Trimester 2											
H28718	89	1 gram; 4-12 hours	13							6.2	0.49
H28786	105	1 gram; 12-24 hours	6.4	3.3	0.52	4.0	0.62	11	1.8	4.0	0.62
H28820	94	1 gram; < 4 hours	21							6.2	0.29
H28870	94	0.2 grams; < 4 hours	29							11	0.36
H28894	98	1-2 grams; 4-12 hours	31	6.8	0.22	8.0	0.26	18	0.59	21	0.69
H28896	126	0.20; < 4 hours	0.85	1.0	1.2					BLOQ	
H28913	91	14 mg THC; 12-24 hours	6.2							3.9	0.62
H28983	108	2 units; 24-36 hours	14	4.8	0.34	5.8	0.41	21	1.5	10	0.73
H28998	91	1 gram; 12-24 hours	4.0	1.3	0.33					2.9	0.72
H29046	127	<2 grams; 12-24 hours	4.4	BLOQ						BLOQ	
H29069	110	0.5 grams; 24-36 hours	14	3.0	0.22	4.6	0.33	8.3	0.59	BLOQ	
H29075	115	0.5 grams; 12-24 hours	0.59	BLOQ						BLOQ	
H29128	~112	1 gram; 24-36 hours	28							BLOQ	
H90000	103	1 gram; 4-12 hours	30	10	0.35	9.4	0.32	38	1.3	9.0	0.31
H90003	122	1 gram; < 4 hours	14	8.3	0.59	8.2	0.59	19	1.4	4.5	0.32
H90005	113	---; < 4 hours	5.7	1.8	0.31			4.3	0.75	2.5	0.44
H90010	137	3 mg THC; 12-24 hours	13	11	0.85	12	0.97	39	3.0	15	1.2
H90012	85	0.2 mg THC; < 4 hours	8.7							12	1.3
H90014	105	---; 12-24 hours	2.8	1.2	0.41					BLOQ	
H90016	101	---; 12-24 hours	6.3	2.7	0.42			7.3	1.2	3.8	0.60
H90018	103	0.5 mg THC oil; 4-12 hours	51	12	0.24	17	0.33	94	1.8	30	0.58
H90022	110	3 grams; 12-24 hours	8.6	2.2	0.26			6.5	0.76	4.5	0.53
Mean ± SD (%CV)					0.45 ± 0.28 (63)		0.48 ± 0.24 (50)		1.33 ± 0.71 (54)		0.61 ± 0.29 (47)

BLOQ: below limit of quantification; Blank rows: no sample collected and/or ratio cannot be calculated; Unless otherwise indicated, dosing information is for last consumption of THC by inhalation prior to termination (amount; time since last consumption); MP: maternal plasma.

Table S4.5: Observed 11-OH-THC Concentrations in Maternal Plasma, Placenta, and Fetal Tissue Obtained during Trimester 1 and 2 Pregnancies after Oral or Inhalation Consumption of Cannabis

Subject	MP (nM)	Fetal Brain (nM)	Fetal Brain/MP	Fetal Kidney (nM)	Fetal Kidney/MP	Fetal Liver (nM)	Fetal Liver/MP	Placenta Mean (nM)	Placenta/MP
Trimester 1									
H28680	BLOQ							BLOQ	
H28688	5.4							5.4	1.0
H28761	7.2								
H28869	6.1							BLOQ	
H28928	9.1	BLOQ				BLOQ		BLOQ	
H28960	4.2							BLOQ	
H28972	1.3							BLOQ	
H28986	5.5							BLOQ	
H28987	BLOQ							BLOQ	
H29026	0.71							BLOQ	
H29045	BLOQ							BLOQ	
H29110	9.8	BLOQ						BLOQ	
H29122	10							BLOQ	
H29141	BLOQ							BLOQ	
H90004	1.7							BLOQ	
H90006	2.2							BLOQ	
H90015	16							5.0	0.31
H90020	BLOQ							BLOQ	
Pool 1	8.0	BLOQ							
Pool 2	3.8			5.2	1.4				
Mean ± SD (%CV)									
Trimester 2									
H28718	3.6							BLOQ	
H28786	BLOQ	BLOQ		BLOQ		BLOQ		BLOQ	
H28820	4.8							BLOQ	
H28870	8.3							BLOQ	
H28894	8.4	BLOQ		3.9	0.46	BLOQ		BLOQ	
H28896	BLOQ	BLOQ		BLOQ		BLOQ		BLOQ	
H28913	2.6							BLOQ	
H28983	6.1	BLOQ		BLOQ		9.2	1.5	BLOQ	
H28998	2.3	BLOQ						BLOQ	
H29046	BLOQ	BLOQ						BLOQ	
H29069	BLOQ	BLOQ		BLOQ		5.1		BLOQ	
H29075	BLOQ	BLOQ						BLOQ	
H29128	10							BLOQ	
H90000	14	BLOQ		6.6	0.46	13	0.91	BLOQ	
H90003	9.3	BLOQ		4.1	0.44	7.7	0.82	BLOQ	
H90005	2.7	BLOQ		BLOQ		BLOQ		BLOQ	
H90010	3.5	BLOQ		6.5	1.8	12	3.4	BLOQ	
H90012	4.5							BLOQ	
H90014	0.96	BLOQ		BLOQ		BLOQ		BLOQ	
H90016	1.3	BLOQ		BLOQ		BLOQ		BLOQ	
H90018	45	13	0.29	18	0.39	46	1.0	BLOQ	
H90022	4.4	BLOQ		2.2	0.50	5.0	1.1	BLOQ	
Mean ± SD (%CV)					0.68 ± 0.56 (83)		1.5 ± 0.99 (67)		

BLOQ: below limit of quantification; Blank rows: no sample collected and/or ratio cannot be calculated; MP: maternal plasma.

Table S4.6: Observed COOH-THC Concentrations in Maternal Plasma, Placenta, and Fetal Tissue Obtained during Trimester 1 and 2 Pregnancies after Oral or Inhalation Consumption of Cannabis

Subject	MP (nM)	Fetal Brain (nM)	Fetal Brain/MP	Fetal Kidney (nM)	Fetal Kidney/MP	Fetal Liver (nM)	Fetal Liver/MP	Placenta Mean (nM)	Placenta/MP
H28680	24							6.3	0.26
H28688	134							46	0.35
H28761	295							22	0.075
H28869	68							11	0.16
H28928	171	24	0.14			67	0.39	29	0.17
H28960	88							19	0.22
H28972	25							BLOQ	
H28986	158							41	0.26
H28987	10							BLOQ	
H29026	30							BLOQ	
H29045	16							BLOQ	
H29110	202	15	0.074					21	0.10
H29122	331							BLOQ	
H29141	30							BLOQ	
H90004	242							91	0.38
H90006	58							16	0.27
H90015	278							43	0.16
H90020	65							BLOQ	
Pool 1	189	23	0.12						
Pool 2	76			48	0.63				
Mean ± SD (%CV)			0.11 ± 0.03 (31)						0.22 ± 0.096 (44)
H28718	135							27	0.20
H28786	55	11	0.20	17	0.32	32	0.59	BLOQ	
H28820	53							BLOQ	
H28870	205							30	0.15
H28894	147	17	0.11	29	0.20	72	0.49	23	0.16
H28896	3.1	BLOQ		BLOQ		BLOQ		BLOQ	
H28913	24							BLOQ	
H28983	128	22	0.17	22	0.17	49	0.38	38	0.30
H28998	17	BLOQ						37	2.2
H29046	18	BLOQ						BLOQ	
H29069	84	24	0.28	13	0.15	34	0.41	BLOQ	
H29075	1.9	BLOQ						BLOQ	
H29128	151							BLOQ	
H90000	134	24	0.18	32	0.24	73	0.54	40	0.30
H90003	76	BLOQ		12	0.15	29	0.38	25	0.33
H90005	58	2.9	0.050	7.6	0.13	16	0.27	BLOQ	
H90010	131	BLOQ		80	0.61	80	0.61	74	0.57
H90012	84							15	0.17
H90014	31	6.6	0.21	3.0	0.10	8.0	0.26	7.8	0.25
H90016	37	9.3	0.25	6.9	0.19	17	0.46	BLOQ	
H90018	334	35	0.10	91	0.27	171	0.51	BLOQ	
H90022	81	BLOQ		16	0.19	35	0.42	BLOQ	
Mean ± SD (%CV)			0.17 ± 0.07 (43)		0.23 ± 0.14 (60)		0.44 ± 0.11 (25)		0.46 ± 0.63 (136)

BLOQ: below limit of quantification; Blank rows: no sample collected and/or ratio cannot be calculated; MP: maternal plasma.

Table S4.7: Non-pregnant PBPK Model Predicted and Observed THC and 11-OH-THC Plasma Exposure (AUC_{inf} and C_{max}) after Various Routes of THC Consumption

Intravenous												
	Ohlsson 1982[47]				Hunt and Jones 1980[46]				Naef 2004[106]			
	THC (5 mg)		11-OH-THC		THC (2 mg)		11-OH-THC		THC (3.71 mg)		11-OH-THC	
	C_{max} (nM)	AUC_{inf} (nM*h)	C_{max} (nM)	AUC_{inf} (nM*h)	C_{max} (nM)	AUC_{inf} (nM*h)	C_{max} (nM)	AUC_{inf} (nM*h)	C_{max} (nM)	AUC_{inf} (nM*h)	C_{max} (nM)	AUC_{inf} (nM*h)
Observed	213	256	N/A	N/A	369	112	N/A	N/A	868	293	27.6	41.4
Predicted	312	365	N/A	N/A	204	127	N/A	N/A	378	195	22.9	43.7
P/O	**1.47**	**1.43**	N/A	N/A	**0.55**	**1.13**	N/A	N/A	**0.44**	**0.67**	**0.83**	**1.06**
Acceptance Range	N	N	N/A	N/A	(0.10 – 7.39)	(0.62 – 1.96)	N/A	N/A	(0.08 – 5.82)	(0.44 – 1.40)	N/A	N/A
Inhalation												
	Ohlsson 1982[47]				McBurney 1986[48]							
	THC (9.44 mg)		11-OH-THC		THC (10.5 mg)		11-OH-THC					
	C_{max} (nM)	AUC_{inf} (nM*h)	C_{max} (nM)	AUC_{inf} (nM*h)	C_{max} (nM)	AUC_{inf} (nM*h)	C_{max} (nM)	AUC_{inf} (nM*h)				
Observed	79.9	103	N/A	N/A	271	245	N/A	N/A				
Predicted	88.2	130	N/A	N/A	149	110	N/A	N/A				
P/O	**1.10**	**1.27**	N/A	N/A	**0.55**	**0.45**	N/A	N/A				
Acceptance Range	N	N	N/A	N/A	(0.26 – 0.65)	(0.18 – 0.58)	N/A	N/A				
Oral												
	Oh 2017[50]				Lunn 2019[49]				Parikh 2016[51]			
	THC (5 mg)		11-OH-THC		THC (10 mg)		11-OH-THC		THC (4.25 mg)		11-OH-THC	
	C_{max} (nM)	AUC_{inf} (nM*h)	C_{max} (nM)	AUC_{inf} (nM*h)	C_{max} (nM)	AUC_{inf} (nM*h)	C_{max} (nM)	AUC_{inf} (nM*h)	C_{max} (nM)	AUC_{inf} (nM*h)	C_{max} (nM)	AUC_{inf} (nM*h)
Observed	3.79	15.5	6.49	35.9	7.44	25.6	9.70	46.6	4.26	12.3	6.75	31.7
Predicted	3.59	15.5	4.70	26.3	6.88	29.8	13.7	68.8	2.93	13.1	5.82	29.7
P/O	**0.94**	**1.00**	**0.72**	**0.73**	**0.92**	**1.16**	**1.41**	**1.48**	**0.69**	**1.07**	**0.86**	**0.94**
Acceptance Range	N	N	N	N	(0.73 – 1.72)	(0.88 – 1.41)	(0.74 – 2.38)	(0.77 – 2.47)	(0.54 – 1.28)	(0.78 – 1.25)	(0.45 – 1.45)	(0.48 – 1.54)
Drug-Drug Interactions and Genetic Polymorphism												
	Stott 2013[136]				Sativex: Summary of Product Characteristic[28]				Sachse-Seeboth 2009[75]			
	10.8 mg THC + 400 mg Ketoconazole		11-OH-THC		THC (15 mg)		11-OH-THC		10.8 mg THC + 200 mg BID Fluconazole		11-OH-THC	
	$C_{max}R$	$AUC_{inf}R$	$C_{max}R$	$AUC_{inf}R$	$C_{max}R$	$AUC_{inf}R$	$C_{max}R$	$AUC_{inf}R$	$C_{max}R$	$AUC_{inf}R$	$C_{max}R$	$AUC_{inf}R$
Observed	1.20	1.88	N/A	N/A	1.22	1.32	N/A	N/A	2.33	3.09	N/A	N/A
Predicted	1.71	1.70	N/A	N/A	1.52	1.72	N/A	N/A	2.63	3.56	N/A	N/A
P/O	**1.43**	**0.90**	N/A	N/A	**1.25**	**1.30**	N/A	N/A	**1.13**	**1.15**	N/A	N/A
Acceptance Range	(0.41 – 2.42)	(0.61 – 1.65)	N/A	N/A	(0.41 – 2.41)	(0.67 – 1.50)	N/A	N/A	(0.32 – 1.54)	(0.45 – 1.46)	N/A	N/A

N/A: data not available; N: not applicable as this dataset was used as a training dataset; C_{max}: maximum concentration; AUC_{inf}: area under the plasma concentration-time curve to time infinity; BID: dosed two times per day.

Table S4.8: m-f-PBPK Model Predicted and Observed Umbilical Venous Plasma and Fetal Tissue THC Concentration Relative to Maternal Plasma in Trimester 2 and 3 Pregnancy after Inhalation and Oral Consumption of THC

	Term	Trimester 2		
	UVP/MP	Fetal Brain/MP	Fetal Kidney/MP	Fetal Liver/MP
Observed*	0.33 (38%)	0.39 (63%)	0.44 (49%)	1.18 (54%)
Acceptance Range	(0.23 – 0.47)	(0.20 – 0.75)	(0.22 – 0.88)	(0.62 – 2.25)
Predicted	**0.31**	**0.54**	**0.73**	**1.9**

*Data are Geometric Mean (%CV); MP: maternal plasma; UVP: umbilical venous plasma. The predicted values were at 24 hours; post-absorption when distributional equilibrium between plasma and tissue concentrations is expected to be reached, i.e. >12 hours.

Table S4.9: LC-MS/MS parameters for Drug Quantification

B. LC gradient program

Time (min)	Flow Rate (mL/min)	A (water with 0.2% acetic acid)	B (acetonitrile with 0.2% acetic acid)
0	0.3	90	10
0.5	0.3	90	10
2	0.3	5	95
4	0.3	5	95
4.1	0.3	90	10
4.5	0.3	90	10

B. APCI MS/MS parameters

Compound	Parent Ion (m/z)	Product Ion (m/z)	Collision Energy (V)
THC	315.3	193.2	22
d3-THC	318.3	196.3	20
11-OH-THC	331.3	193.2	26
d3-11-OH-THC	334.3	196.3	26
COOH-THC	345.3	327.3	20
d3-COOH-THC	348.3	330.3	20

Chapter 5: Conclusion

5.1 Major Findings

Prenatal cannabis use is associated with various detrimental fetal outcomes, the foremost concern being neurodevelopmental toxicity[1-5]. Δ^9-tetrahydrocannabinol (THC), the most abundant psychoactive compound in cannabis, is thought to be cause of the potential neurodevelopmental toxicity of prenatal cannabis use[6]. The primary psychoactive metabolite, 11-OH-THC, may also contribute to the toxicity[6]. The observed associations, however, are potentially confounded by concomitant substance abuse, differences in socioeconomic status, and inaccurate (self-reported) cannabis dosing information. A randomized controlled clinical study of the effect of prenatal cannabis use on fetal toxicity is unethical. Therefore, an alternative approach is to conduct preclinical *in vitro* and *in vivo* animal experiments which mimic human fetal THC and 11-OH-THC exposure. But, to do this we must know the average and maximum concentration of the THC and 11-OH-THC that reach the fetal circulation and brain at cannabis doses typically consumed by pregnant individuals. To bridge this gap, we measured cannabinoid concentrations in trimester 1 and 2 fetal tissues and maternal plasma (MP) and in trimester 3 MP and fetal umbilical venous (UVP) plasma. Because the observed *in vivo* concentrations only provided a snapshot of the exposure, we also developed and verified a maternal-fetal physiologically based pharmacokinetic (m-f-PBPK) model to predict total and unbound fetal THC/11-OH-THC concentrations over the entire dosing interval after both inhalation and oral THC consumption. The predicted exposure can then be applied to informative fetal toxicity studies. For model development to proceed, we had to first determine all the potential mechanisms of clearance and distribution that affect THC/11-OH-THC fetal exposure.

To begin, we characterized the drug metabolizing enzymes (DMEs) and quantified the metabolic kinetics by these enzymes for THC/11-OH-THC in the adult intestine, lung, placenta, and fetal liver[7]. As described in Chapter 2, there was no metabolism observed in the lung or placenta microsomes. However, in the intestine, THC was significantly metabolized by CYP2C9

(89%) and CYP3A (11%) while 11-OH-THC was significantly metabolized by CYP3A (51%) and UGT2B7 (25%). The contribution of intestinal metabolism to systemic THC/11-OH-THC clearance is smaller relative to the magnitude of hepatic metabolism. However, we predict that the intestinal metabolism will contribute to F_g' of less than 1, decreasing the overall bioavailability following oral THC consumption. In the fetal liver, both compounds were nearly completely metabolized by CYP3A7. The observed fetal liver metabolism will decrease the fetal exposure relative to maternal exposure causing a decrease in the THC and 11-OH-THC fetal brain concentration. However, the magnitude of decrease is dependent on various other parameters (e.g. placenta passive diffusion and transport; Chapter 3).

Next, we evaluated the transplacental transfer of THC/11-OH-THC/COOH-THC by passive diffusion and active transport[8]. As described in Chapter 3, the metabolites 11-OH-THC and COOH-THC appeared to passively diffuse across the placenta. However, THC was actively transported by an unknown apical efflux or basal influx transporter(s) on the syncytiotrophoblast membrane, unaffected by valspodar (a potent P-gp/BCRP inhibitor). The estimated placental passive diffusion and active transport clearance works in concert with the fetal liver metabolic clearance (above and Chapter 2) to reduce the cannabinoid fetal brain exposure. Then, the estimated THC/11-OH-THC microsomal enzyme and passive diffusion/active transport kinetics were input in our m-f-PBPK model to predict the fetal brain cannabinoid exposure (Chapter 4).

In Chapter 4, we observed that the mean paired UVP/MP value at T3 for THC and COOH-THC was much less than 1 (0.35 ± 0.13 and 0.36 ± 0.18, respectively). The observed THC fetal brain/MP values at T1 and T2 were 0.50 ± 0.18 and 0.45 ± 0.28, respectively. The reduced UVP and fetal brain exposure relative MP aligns with our observed fetal liver metabolism (Chapter 2) and active placenta transport (Chapter 3). Using the observed *in vivo* data we then verified the m-f-PBPK model for THC fetal tissue and UVP/MP. With the verified m-f-PBPK model we simulated the total and unbound THC/11-OH-THC exposure during pregnancy, across gestational age. After a typical daily dose of THC consumed by inhalation

(100 mg), the predicted fetal brain $C_{ss,avg}$ of THC and 11-OH-THC was 37 and 70 nM, respectively. Similarly, after a typical daily oral consumption of 10 mg THC, the predicted $C_{ss,avg}$ of THC and 11-OH-THC in the fetal brain was lower, 0.73 and 8.9 nM, respectively. The fetal brain $C_{ss,avg,u}$ is even lower due to extensive binding in the brain.

5.2 Future Directions and Limitations of Our Studies

We propose that future fetal toxicity studies (*in vitro* or *in vivo* in animals) should replicate the predicted unbound fetal UVP and fetal brain THC/11-OH-THC concentrations at the typical doses consumed by pregnant people. Our verified m-f-PBPK model can be used to predict maternal-fetal exposure to THC/11-OH-THC at various cannabis dose/route/frequency of cannabis used by pregnant people. The range of relevant concentrations needs to encompass the different routes of administration (inhalation and oral), range of dose consumed (inhalation: 50 – 300 mg THC; oral: 5 – 40 mg THC) and frequency across all the gestational ages of pregnancy. This is particularly important as the incidence of prenatal cannabis use is highest in the first trimester[10]. Unfortunately, physiological information (blood flows, tissue weights, etc.) for the fetus at earlier gestational ages (GW<15) is not available to allow such predictions. At these earlier gestational ages, the fetal skin is not keratinized[208] and therefore skin absorption of any cannabinoids present in the amniotic fluid (likely minor) would need to be taken into consideration. Once collected and populated with these “missing” physiological parameters, the m-f-PBPK model will need to be verified by quantifying THC/11-OH-THC concentrations in fetal samples of <15 GW.

The m-f-PBPK model developed as part of this dissertation could only be verified for fetal THC plasma and fetal concentrations relative to corresponding maternal plasma concentration at a single, unknown, timepoint. Because of the nature of our *in vivo* study, we did not have definitive information on dose, timing, and frequency of cannabis consumption and samples could only be collected at one timepoint. Ideally the study would have rigorous dosing

information and the ability to collected samples across the entire concentration-time profile, however this is logistically and ethically challenging and most likely not feasible. On the other hand, a future study with a more sensitive assay could potentially quantify 11-OH-THC in fetal plasma/tissues. We were not able to quantify 11-OH-THC in the majority of samples, preventing us from verifying the 11-OH-THC portion of our m-f-PBPK model. Such verification would enhance the utility of our m-f-PBPK model predictions. Additionally, we have focused on THC/11-OH-THC, but it is possible that constituents other than these compounds are the cause of the potential neurodevelopmental toxicity of cannabis.

There are some gaps in the 11-OH-THC kinetic parameters used to populate our m-f-PBPK model (Chapters 2 and 3). We do not have complete data on 11-OH-THC's metabolic kinetics and fraction metabolized by both microsomal and cytosolic enzymes. This restricted our ability to predict the impact of DDIs and CYP2C9 genetic polymorphism on 11-OH-THC exposure. Without which, we could not estimate how enzyme induction in pregnancy changes maternal plasma 11-OH-THC exposure and thereby fetal exposure. To ascertain the fractional contribution for each enzyme involved in 11-OH-THC metabolism, one would need to conduct depletion studies with plated human hepatocytes, with and without specific inhibitors of each involved enzyme. If sandwich-culture human hepatocytes are used, one could also measure any potential biliary excretion of 11-OH-THC through the bile canaliculi.

In our model, we also used a simplified first-order absorption model after both inhalational and oral consumption of THC. The simplified oral absorption model does not account for blood flow segmentation along the intestinal tract and does not incorporate how the rate of dissolution of THC in the intestine impacts absorption across the gut epithelium. If a model can be developed to include these missing parameters, one could potentially better predict the first-pass metabolism in the gut and could predict the impact of food effect on THC absorption.

From our perfused human term placenta studies, we were able to identify that THC is actively transported at the syncytiotrophoblast membrane[8], most likely basal. However, we were not able to identify the transporter responsible. To do so, one could possibly conduct the perfusions as we had done, but with more selective inhibitors for other known transporters at the syncytiotrophoblast membrane, facing in the fetal to maternal direction. Alternatively, one could employ *in vitro* experiments with placental cell lines such as BeWo to identify potential transporters of which the cannabinoids may be a substrate. In addition, we need to know how the expression and/or activity of the transporter of interest changes across gestational age in order to scale the observed active transporter clearance at term, to earlier gestational ages. We were not able to estimate transport earlier in pregnancy as, due to logistical reasons, the perfusions can only be done with term placentas. Once the transporter is identified one could use quantitative targeted proteomics to measure the expression across the gestational ages of pregnancy. Once these data are collected, and the kinetic parameters estimated, the m-f-PBPK model could be applied with higher confidence to early gestational ages and therefore further inform fetal exposure to THC/11-OH-THC, as well as other biologically active molecules, for future preclinical *in vitro* and *in vivo* studies.

References

1 Day, N. L. *et al.* Effect of prenatal marijuana exposure on the cognitive development of offspring at age three. *Neurotoxicol Teratol* **16**, 169-175, doi:10.1016/0892-0362(94)90114-7 (1994).

2 Goldschmidt, L., Day, N. L. & Richardson, G. A. Effects of prenatal marijuana exposure on child behavior problems at age 10. *Neurotoxicol Teratol* **22**, 325-336, doi:10.1016/s0892-0362(00)00066-0 (2000).

3 Goldschmidt, L., Richardson, G. A., Willford, J. & Day, N. L. Prenatal marijuana exposure and intelligence test performance at age 6. *J Am Acad Child Adolesc Psychiatry* **47**, 254-263, doi:10.1097/CHI.0b013e318160b3f0 (2008).

4 Goldschmidt, L., Richardson, G. A., Willford, J. A., Severtson, S. G. & Day, N. L. School achievement in 14-year-old youths prenatally exposed to marijuana. *Neurotoxicol Teratol* **34**, 161-167, doi:10.1016/j.ntt.2011.08.009 (2012).

5 Paul, S. E. *et al.* Associations Between Prenatal Cannabis Exposure and Childhood Outcomes: Results From the ABCD Study. *JAMA Psychiatry*, doi:10.1001/jamapsychiatry.2020.2902 (2020).

6 Lemberger, L., Martz, R., Rodda, B., Forney, R. & Rowe, H. Comparative pharmacology of Delta9-tetrahydrocannabinol and its metabolite, 11-OH-Delta9-tetrahydrocannabinol. *J Clin Invest* **52**, 2411-2417, doi:10.1172/JCI107431 (1973).

7 Kumar, A. R., Patilea-Vrana, G. I., Anoshchenko, O. & Unadkat, J. D. Characterizing and Quantifying Extrahepatic Metabolism of (-)-Delta(9)-Tetrahydrocannabinol (THC) and Its Psychoactive Metabolite, (+/-)-11-Hydroxy-Delta(9)-THC (11-OH-THC). *Drug Metab Dispos* **50**, 734-740, doi:10.1124/dmd.122.000868 (2022).

8 Kumar, A. R. *et al.* Understanding the Mechanism and Extent of Transplacental Transfer of (-)-∆(9) -Tetrahydrocannabinol (THC) in the Perfused Human Placenta to Predict In Vivo Fetal THC Exposure. *Clin Pharmacol Ther* **114**, 446-458, doi:10.1002/cpt.2964 (2023).

9 Ren, M. *et al.* The origins of cannabis smoking: Chemical residue evidence from the first millennium BCE in the Pamirs. *Sci Adv* **5**, eaaw1391, doi:10.1126/sciadv.aaw1391 (2019).

10 Volkow, N. D., Han, B., Compton, W. M. & McCance-Katz, E. F. Self-reported Medical and Nonmedical Cannabis Use Among Pregnant Women in the United States. *JAMA* **322**, 167-169, doi:10.1001/jama.2019.7982 (2019).

11 Peng, H. *et al.* Effects of prenatal exposure to THC on hippocampal neural development in offspring. *Toxicol Lett* **374**, 48-56, doi:10.1016/j.toxlet.2022.12.007 (2023).

12 Tortoriello, G. *et al.* Miswiring the brain: Delta9-tetrahydrocannabinol disrupts cortical development by inducing an SCG10/stathmin-2 degradation pathway. *EMBO J* **33**, 668-685, doi:10.1002/embj.201386035 (2014).

13 de Salas-Quiroga, A. *et al.* Prenatal exposure to cannabinoids evokes long-lasting functional alterations by targeting CB1 receptors on developing cortical neurons. *Proc Natl Acad Sci U S A* **112**, 13693-13698, doi:10.1073/pnas.1514962112 (2015).

14 Huestis, M. A. & Cone, E. J. Urinary excretion half-life of 11-nor-9-carboxy-delta9-tetrahydrocannabinol in humans. *Ther Drug Monit* **20**, 570-576, doi:10.1097/00007691-199810000-00021 (1998).

15 Patilea-Vrana, G. I. & Unadkat, J. D. Quantifying Hepatic Enzyme Kinetics of (-)-(9)-Tetrahydrocannabinol (THC) and Its Psychoactive Metabolite, 11-OH-THC, through In Vitro Modeling. *Drug Metab Dispos* **47**, 743-752, doi:10.1124/dmd.119.086470 (2019).

16 Patilea-Vrana, G. I., Anoshchenko, O. & Unadkat, J. D. Hepatic Enzymes Relevant to the Disposition of (-)-(9)-Tetrahydrocannabinol (THC) and Its Psychoactive Metabolite, 11-OH-THC. *Drug Metab Dispos* **47**, 249-256, doi:10.1124/dmd.118.085548 (2019).
17 Bonhomme-Faivre, L., Benyamina, A., Reynaud, M., Farinotti, R. & Abbara, C. Disposition of Delta tetrahydrocannabinol in CF1 mice deficient in mdr1a P-glycoprotein. *Addict Biol* **13**, 295-300, doi:10.1111/j.1369-1600.2008.00096.x (2008).
18 Spiro, A. S., Wong, A., Boucher, A. A. & Arnold, J. C. Enhanced brain disposition and effects of Delta9-tetrahydrocannabinol in P-glycoprotein and breast cancer resistance protein knockout mice. *PLoS One* **7**, e35937, doi:10.1371/journal.pone.0035937 (2012).
19 Jeffers, A. M., Glantz, S., Byers, A. & Keyhani, S. Sociodemographic Characteristics Associated With and Prevalence and Frequency of Cannabis Use Among Adults in the US. *JAMA Netw Open* **4**, e2136571, doi:10.1001/jamanetworkopen.2021.36571 (2021).
20 NIDA. *Marijuana and hallucinogen use among young adults reached all time-high in 2021*, <https://nida.nih.gov/news-events/news-releases/2022/08/marijuana-and-hallucinogen-use-among-young-adults-reached-all-time-high-in-2021> (2022).
21 Streck, J. M., Hughes, J. R., Klemperer, E. M., Howard, A. B. & Budney, A. J. Modes of cannabis use: A secondary analysis of an intensive longitudinal natural history study. *Addict Behav* **98**, 106033, doi:10.1016/j.addbeh.2019.106033 (2019).
22 Wadsworth, E., Craft, S., Calder, R. & Hammond, D. Prevalence and use of cannabis products and routes of administration among youth and young adults in Canada and the United States: A systematic review. *Addict Behav* **129**, 107258, doi:10.1016/j.addbeh.2022.107258 (2022).
23 Howard, D. S., Dhanraj, D. N., Devaiah, C. G. & Lambers, D. S. Cannabis Use Based on Urine Drug Screens in Pregnancy and Its Association With Infant Birth Weight. *J Addict Med* **13**, 436-441, doi:10.1097/ADM.0000000000000516 (2019).
24 Vanstone, M. *et al.* Reasons for cannabis use during pregnancy and lactation: a qualitative study. *CMAJ* **193**, E1906-E1914, doi:10.1503/cmaj.211236 (2021).
25 NIDA. *Is Cannabis (Marijuana) Safe to Use While Pregnant or Breastfeeding?*, <https://archives.nida.nih.gov/publications/cannabis-marijuana-safe-to-use-while-pregnant-or-breastfeeding> (2019).
26 Laurence, E. *Your Guide To Cannabis Legalization By State*, <https://www.forbes.com/health/cbd/cannabis-legalization-by-state/> (2023).
27 Pagano, C. *et al.* Cannabinoids: Therapeutic Use in Clinical Practice. *Int J Mol Sci* **23**, doi:10.3390/ijms23063344 (2022).
28 Pharmaceuticals, G. Sativex Oromucosal Spray: Summary of Product Characteristics. (2022).
29 Pharmaceuticals, S. MARINOL (dronabinol) capsules, for oral use. (1985).
30 Pharmaceuticals, S. SYNDROS (dronabinol) oral solution. (1985).
31 Pharmaceuticals, V. CESAMET (nabilone), for oral administration. (1997).
32 Chayasirisobhon, S. The Role of Cannabidiol in Neurological Disorders. *Perm J* **25**, doi:10.7812/TPP/20.156 (2021).
33 Pertwee, R. G. The diverse CB1 and CB2 receptor pharmacology of three plant cannabinoids: delta9-tetrahydrocannabinol, cannabidiol and delta9-tetrahydrocannabivarin. *Br J Pharmacol* **153**, 199-215, doi:10.1038/sj.bjp.0707442 (2008).
34 An, D., Peigneur, S., Hendrickx, L. A. & Tytgat, J. Targeting Cannabinoid Receptors: Current Status and Prospects of Natural Products. *Int J Mol Sci* **21**, doi:10.3390/ijms21145064 (2020).
35 Watanabe, K. *et al.* Comparison of pharmacological effects of tetrahydrocannabinols and their 11-hydroxy-metabolites in mice. *Chem Pharm Bull (Tokyo)* **38**, 2317-2319, doi:10.1248/cpb.38.2317 (1990).

36 Wilson, R. S. & May, E. L. Analgesic properties of the tetrahydrocannabinols, their metabolites, and analogs. *J Med Chem* **18**, 700-703, doi:10.1021/jm00241a012 (1975).
37 El Marroun, H. *et al.* Intrauterine cannabis exposure affects fetal growth trajectories: the Generation R Study. *J Am Acad Child Adolesc Psychiatry* **48**, 1173-1181, doi:10.1097/CHI.0b013e3181bfa8ee (2009).
38 Gunn, J. K. *et al.* Prenatal exposure to cannabis and maternal and child health outcomes: a systematic review and meta-analysis. *BMJ Open* **6**, e009986, doi:10.1136/bmjopen-2015-009986 (2016).
39 Maciel, I. S. *et al.* Perinatal CBD or THC Exposure Results in Lasting Resistance to Fluoxetine in the Forced Swim Test: Reversal by Fatty Acid Amide Hydrolase Inhibition. *Cannabis Cannabinoid Res* **7**, 318-327, doi:10.1089/can.2021.0015 (2022).
40 Baglot, S. L. *et al.* Maternal-fetal transmission of delta-9-tetrahydrocannabinol (THC) and its metabolites following inhalation and injection exposure during pregnancy in rats. *J Neurosci Res* **100**, 713-730, doi:10.1002/jnr.24992 (2022).
41 Khare, M., Taylor, A. H., Konje, J. C. & Bell, S. C. Delta9-tetrahydrocannabinol inhibits cytotrophoblast cell proliferation and modulates gene transcription. *Mol Hum Reprod* **12**, 321-333, doi:10.1093/molehr/gal036 (2006).
42 Bailey, J. R., Cunny, H. C., Paule, M. G. & Slikker, W., Jr. Fetal disposition of delta 9-tetrahydrocannabinol (THC) during late pregnancy in the rhesus monkey. *Toxicol Appl Pharmacol* **90**, 315-321, doi:10.1016/0041-008x(87)90338-3 (1987).
43 Blackard, C. & Tennes, K. Human placental transfer of cannabinoids. *N Engl J Med* **311**, 797, doi:10.1056/NEJM198409203111213 (1984).
44 Thomas, B. F., Compton, D. R. & Martin, B. R. Characterization of the lipophilicity of natural and synthetic analogs of delta 9-tetrahydrocannabinol and its relationship to pharmacological potency. *J Pharmacol Exp Ther* **255**, 624-630 (1990).
45 Giroud, C. *et al.* Delta(9)-THC, 11-OH-Delta(9)-THC and Delta(9)-THCCOOH plasma or serum to whole blood concentrations distribution ratios in blood samples taken from living and dead people. *Forensic Sci Int* **123**, 159-164, doi:10.1016/s0379-0738(01)00538-2 (2001).
46 Hunt, C. A. & Jones, R. T. Tolerance and disposition of tetrahydrocannabinol in man. *J Pharmacol Exp Ther* **215**, 35-44 (1980).
47 Ohlsson, A. *et al.* Single dose kinetics of deuterium labelled delta 1-tetrahydrocannabinol in heavy and light cannabis users. *Biomed Mass Spectrom* **9**, 6-10, doi:10.1002/bms.1200090103 (1982).
48 McBurney, L. J., Bobbie, B. A. & Sepp, L. A. GC/MS and EMIT analyses for delta 9-tetrahydrocannabinol metabolites in plasma and urine of human subjects. *J Anal Toxicol* **10**, 56-64, doi:10.1093/jat/10.2.56 (1986).
49 Lunn, S. *et al.* Human Pharmacokinetic Parameters of Orally Administered Delta(9)-Tetrahydrocannabinol Capsules Are Altered by Fed Versus Fasted Conditions and Sex Differences. *Cannabis Cannabinoid Res* **4**, 255-264, doi:10.1089/can.2019.0037 (2019).
50 Oh, D. A., Parikh, N., Khurana, V., Cognata Smith, C. & Vetticaden, S. Effect of food on the pharmacokinetics of dronabinol oral solution versus dronabinol capsules in healthy volunteers. *Clin Pharmacol* **9**, 9-17, doi:10.2147/CPAA.S119676 (2017).
51 Parikh, N., Kramer, W. G., Khurana, V., Cognata Smith, C. & Vetticaden, S. Bioavailability study of dronabinol oral solution versus dronabinol capsules in healthy volunteers. *Clin Pharmacol* **8**, 155-162, doi:10.2147/CPAA.S115679 (2016).
52 Bansal, S., Maharao, N., Paine, M. F. & Unadkat, J. D. Predicting the Potential for Cannabinoids to Precipitate Pharmacokinetic Drug Interactions via Reversible Inhibition or Inactivation of Major Cytochromes P450. *Drug Metab Dispos* **48**, 1008-1017, doi:10.1124/dmd.120.000073 (2020).

53 Cliburn, K. D., Huestis, M. A., Wagner, J. R. & Kemp, P. M. Cannabinoid distribution in fatally-injured pilots' postmortem fluids and tissues. *Forensic Sci Int* **329**, 111075, doi:10.1016/j.forsciint.2021.111075 (2021).
54 Kemp, P. M., Cardona, P. S., Chaturvedi, A. K. & Soper, J. W. Distribution of ∆(9)-Tetrahydrocannabinol and 11-Nor-9-Carboxy-∆(9)-Tetrahydrocannabinol Acid in Postmortem Biological Fluids and Tissues From Pilots Fatally Injured in Aviation Accidents. *J Forensic Sci* **60**, 942-949, doi:10.1111/1556-4029.12751 (2015).
55 Mura, P., Kintz, P., Dumestre, V., Raul, S. & Hauet, T. THC can be detected in brain while absent in blood. *J Anal Toxicol* **29**, 842-843, doi:10.1093/jat/29.8.842 (2005).
56 Saenz, S. R., Lewis, R. J., Angier, M. K. & Wagner, J. R. Postmortem Fluid and Tissue Concentrations of THC, 11-OH-THC and THC-COOH. *J Anal Toxicol* **41**, 508-516, doi:10.1093/jat/bkx033 (2017).
57 Willinsky, M. D., Kalant, H., Meresz, O., Endrenyi, L. & Woo, N. Distribution and metabolism in vivo of 14C-tetrahydrocannabinol in the rat. *Eur J Pharmacol* **27**, 106-119, doi:10.1016/0014-2999(74)90207-6 (1974).
58 Torrens, A. *et al.* Comparative Pharmacokinetics of Delta(9)-Tetrahydrocannabinol in Adolescent and Adult Male Mice. *J Pharmacol Exp Ther* **374**, 151-160, doi:10.1124/jpet.120.265892 (2020).
59 Schaefer, N. *et al.* Distribution of the (synthetic) cannabinoids JWH-210, RCS-4, as well as ∆9-tetrahydrocannabinol following pulmonary administration to pigs. *Arch Toxicol* **93**, 2211-2218, doi:10.1007/s00204-019-02493-8 (2019).
60 Schaefer, N. *et al.* Simultaneous LC-MS/MS determination of JWH-210, RCS-4, ∆(9)-tetrahydrocannabinol, and their main metabolites in pig and human serum, whole blood, and urine for comparing pharmacokinetic data. *Anal Bioanal Chem* **407**, 3775-3786, doi:10.1007/s00216-015-8605-6 (2015).
61 Lust, C. A. C. *et al.* Short communication: Tissue distribution of major cannabinoids following intraperitoneal injection in male rats. *PLoS One* **17**, e0262633, doi:10.1371/journal.pone.0262633 (2022).
62 Wahlqvist, M., Nilsson, I. M., Sandberg, F. & Agurell, S. Binding of delta-1-tetrahydrocannabinol to human plasma proteins. *Biochem Pharmacol* **19**, 2579-2584, doi:10.1016/0006-2952(70)90007-9 (1970).
63 Klausner, H. A., Wilcox, H. G. & Dingell, J. V. The use of zonal ultracentrifugation in the investigation of the binding of delta9-tetrahydrocannabinol by plasma lipoproteins. *Drug Metab Dispos* **3**, 314-319 (1975).
64 Fanali, G. *et al.* Binding of delta9-tetrahydrocannabinol and diazepam to human serum albumin. *IUBMB Life* **63**, 446-451, doi:10.1002/iub.466 (2011).
65 Yabut, K. C. B. & Isoherranen, N. Impact of Intracellular Lipid Binding Proteins on Endogenous and Xenobiotic Ligand Metabolism and Disposition. *Drug Metab Dispos* **51**, 700-717, doi:10.1124/dmd.122.001010 (2023).
66 Elmes, M. W. *et al.* FABP1 controls hepatic transport and biotransformation of Delta(9)-THC. *Sci Rep* **9**, 7588, doi:10.1038/s41598-019-44108-3 (2019).
67 Elmes, M. W. *et al.* Fatty acid-binding proteins (FABPs) are intracellular carriers for Delta9-tetrahydrocannabinol (THC) and cannabidiol (CBD). *J Biol Chem* **290**, 8711-8721, doi:10.1074/jbc.M114.618447 (2015).
68 Glaz-Sandberg, A. *et al.* Pharmacokinetics of 11-nor-9-carboxy-Delta(9)-tetrahydrocannabinol (CTHC) after intravenous administration of CTHC in healthy human subjects. *Clin Pharmacol Ther* **82**, 63-69, doi:10.1038/sj.clpt.6100199 (2007).
69 Wall, M. E. & Perez-Reyes, M. The metabolism of delta 9-tetrahydrocannabinol and related cannabinoids in man. *J Clin Pharmacol* **21**, 178S-189S, doi:10.1002/j.1552-4604.1981.tb02594.x (1981).

70 Kelly, P. & Jones, R. T. Metabolism of tetrahydrocannabinol in frequent and infrequent marijuana users. *J Anal Toxicol* **16**, 228-235, doi:10.1093/jat/16.4.228 (1992).
71 Wall, M. E., Sadler, B. M., Brine, D., Taylor, H. & Perez-Reyes, M. Metabolism, disposition, and kinetics of delta-9-tetrahydrocannabinol in men and women. *Clin Pharmacol Ther* **34**, 352-363, doi:10.1038/clpt.1983.179 (1983).
72 Huestis, M. A. Pharmacokinetics and metabolism of the plant cannabinoids, delta9-tetrahydrocannabinol, cannabidiol and cannabinol. *Handb Exp Pharmacol*, 657-690, doi:10.1007/3-540-26573-2_23 (2005).
73 Bornheim, L. M. & Correia, M. A. Purification and characterization of the major hepatic cannabinoid hydroxylase in the mouse: a possible member of the cytochrome P-450IIC subfamily. *Mol Pharmacol* **40**, 228-234 (1991).
74 Bland, T. M., Haining, R. L., Tracy, T. S. & Callery, P. S. CYP2C-catalyzed delta9-tetrahydrocannabinol metabolism: kinetics, pharmacogenetics and interaction with phenytoin. *Biochem Pharmacol* **70**, 1096-1103, doi:10.1016/j.bcp.2005.07.007 (2005).
75 Sachse-Seeboth, C. *et al.* Interindividual variation in the pharmacokinetics of Delta9-tetrahydrocannabinol as related to genetic polymorphisms in CYP2C9. *Clin Pharmacol Ther* **85**, 273-276, doi:10.1038/clpt.2008.213 (2009).
76 Stout, S. M. & Cimino, N. M. Exogenous cannabinoids as substrates, inhibitors, and inducers of human drug metabolizing enzymes: a systematic review. *Drug Metab Rev* **46**, 86-95, doi:10.3109/03602532.2013.849268 (2014).
77 Beers, J. L., Authement, A. K., Isoherranen, N. & Jackson, K. D. Cytosolic Enzymes Generate Cannabinoid Metabolites 7-Carboxycannabidiol and 11-Nor-9-carboxytetrahydrocannabinol. *ACS Med Chem Lett* **14**, 614-620, doi:10.1021/acsmedchemlett.3c00017 (2023).
78 Mazur, A. *et al.* Characterization of human hepatic and extrahepatic UDP-glucuronosyltransferase enzymes involved in the metabolism of classic cannabinoids. *Drug Metab Dispos* **37**, 1496-1504, doi:10.1124/dmd.109.026898 (2009).
79 Balhara, A., Kumar, A. R. & Unadkat, J. D. Predicting Human Fetal Drug Exposure Through Maternal-Fetal PBPK Modeling and In Vitro or Ex Vivo Studies. *J Clin Pharmacol* **62 Suppl 1**, S94-S114, doi:10.1002/jcph.2117 (2022).
80 Chan, H. J., Petrossian, K. & Chen, S. Structural and functional characterization of aromatase, estrogen receptor, and their genes in endocrine-responsive and -resistant breast cancer cells. *J Steroid Biochem Mol Biol* **161**, 73-83, doi:10.1016/j.jsbmb.2015.07.018 (2016).
81 Nanovskaya, T. N. *et al.* Methadone metabolism by human placenta. *Biochem Pharmacol* **68**, 583-591, doi:10.1016/j.bcp.2004.04.011 (2004).
82 Zharikova, O. L. *et al.* Identification of the major human hepatic and placental enzymes responsible for the biotransformation of glyburide. *Biochem Pharmacol* **78**, 1483-1490, doi:10.1016/j.bcp.2009.08.003 (2009).
83 Leeder, J. S. *et al.* Variability of CYP3A7 expression in human fetal liver. *J Pharmacol Exp Ther* **314**, 626-635, doi:10.1124/jpet.105.086504 (2005).
84 Tomson, T., Lindbom, U., Ekqvist, B. & Sundqvist, A. Disposition of carbamazepine and phenytoin in pregnancy. *Epilepsia* **35**, 131-135, doi:10.1111/j.1528-1157.1994.tb02922.x (1994).
85 Shi, Z., Yang, W., Goldstein, J. A. & Zhang, S. Y. Med25 is required for estrogen receptor alpha (ERalpha)-mediated regulation of human CYP2C9 expression. *Biochem Pharmacol* **90**, 425-431, doi:10.1016/j.bcp.2014.06.016 (2014).
86 Choi, S. Y., Koh, K. H. & Jeong, H. Isoform-specific regulation of cytochromes P450 expression by estradiol and progesterone. *Drug Metab Dispos* **41**, 263-269, doi:10.1124/dmd.112.046276 (2013).

87 Alshabi, A. *et al.* A cocktail probe approach to evaluate the effect of hormones on the expression and activity of CYP enzymes in human hepatocytes with conditions simulating late stage of pregnancy. *Eur J Clin Pharmacol* **79**, 815-827, doi:10.1007/s00228-023-03489-1 (2023).
88 Hebert, M. F. *et al.* Effects of pregnancy on CYP3A and P-glycoprotein activities as measured by disposition of midazolam and digoxin: a University of Washington specialized center of research study. *Clin Pharmacol Ther* **84**, 248-253, doi:10.1038/clpt.2008.1 (2008).
89 Ke, A. B., Nallani, S. C., Zhao, P., Rostami-Hodjegan, A. & Unadkat, J. D. A PBPK Model to Predict Disposition of CYP3A-Metabolized Drugs in Pregnant Women: Verification and Discerning the Site of CYP3A Induction. *CPT Pharmacometrics Syst Pharmacol* **1**, e3, doi:10.1038/psp.2012.2 (2012).
90 Tracy, T. S. *et al.* Temporal changes in drug metabolism (CYP1A2, CYP2D6 and CYP3A Activity) during pregnancy. *Am J Obstet Gynecol* **192**, 633-639, doi:10.1016/j.ajog.2004.08.030 (2005).
91 Zhang, Z., Farooq, M., Prasad, B., Grepper, S. & Unadkat, J. D. Prediction of gestational age-dependent induction of in vivo hepatic CYP3A activity based on HepaRG cells and human hepatocytes. *Drug Metab Dispos* **43**, 836-842, doi:10.1124/dmd.114.062984 (2015).
92 Papageorgiou, I., Grepper, S. & Unadkat, J. D. Induction of hepatic CYP3A enzymes by pregnancy-related hormones: studies in human hepatocytes and hepatic cell lines. *Drug Metab Dispos* **41**, 281-290, doi:10.1124/dmd.112.049015 (2013).
93 Ohman, I., Luef, G. & Tomson, T. Effects of pregnancy and contraception on lamotrigine disposition: new insights through analysis of lamotrigine metabolites. *Seizure* **17**, 199-202, doi:10.1016/j.seizure.2007.11.017 (2008).
94 Watts, D. H. *et al.* Pharmacokinetic disposition of zidovudine during pregnancy. *J Infect Dis* **163**, 226-232, doi:10.1093/infdis/163.2.226 (1991).
95 Khatri, R. *et al.* Pregnancy-Related Hormones Increase UGT1A1-Mediated Labetalol Metabolism in Human Hepatocytes. *Front Pharmacol* **12**, 655320, doi:10.3389/fphar.2021.655320 (2021).
96 Chen, X., Unadkat, J. D. & Mao, Q. Tetrahydrocannabinol and Its Major Metabolites Are Not (or Are Poor) Substrates or Inhibitors of Human P-Glycoprotein [ATP-Binding Cassette (ABC) B1] and Breast Cancer Resistance Protein (ABCG2). *Drug Metab Dispos* **49**, 910-918, doi:10.1124/dmd.121.000505 (2021).
97 Anoshchenko, O. *et al.* Gestational Age-Dependent Abundance of Human Placental Transporters as Determined by Quantitative Targeted Proteomics. *Drug Metab Dispos* **48**, 735-741, doi:10.1124/dmd.120.000067 (2020).
98 Daood, M., Tsai, C., Ahdab-Barmada, M. & Watchko, J. F. ABC transporter (P-gp/ABCB1, MRP1/ABCC1, BCRP/ABCG2) expression in the developing human CNS. *Neuropediatrics* **39**, 211-218, doi:10.1055/s-0028-1103272 (2008).
99 Hebert, M. F. *et al.* Are we optimizing gestational diabetes treatment with glyburide? The pharmacologic basis for better clinical practice. *Clin Pharmacol Ther* **85**, 607-614, doi:10.1038/clpt.2009.5 (2009).
100 Eyal, S. *et al.* Pharmacokinetics of metformin during pregnancy. *Drug Metab Dispos* **38**, 833-840, doi:10.1124/dmd.109.031245 (2010).
101 Peng, J., Ladumor, M. K. & Unadkat, J. D. Prediction of Pregnancy-Induced Changes in Secretory and Total Renal Clearance of Drugs Transported by Organic Anion Transporters. *Drug Metab Dispos* **49**, 929-937, doi:10.1124/dmd.121.000557 (2021).
102 Lemberger, L., Axelrod, J. & Kopin, I. J. Metabolism and disposition of delta-9-tetrahydrocannabinol in man. *Pharmacol Rev* **23**, 371-380 (1971).

103 Lemberger, L. *et al.* Delta-9-tetrahydrocannabinol. Temporal correlation of the psychologic effects and blood levels after various routes of administration. *N Engl J Med* **286**, 685-688, doi:10.1056/NEJM197203302861303 (1972).
104 Morrison, P. D. *et al.* The acute effects of synthetic intravenous Delta9-tetrahydrocannabinol on psychosis, mood and cognitive functioning. *Psychol Med* **39**, 1607-1616, doi:10.1017/S0033291709005522 (2009).
105 Barkus, E. *et al.* Does intravenous Delta9-tetrahydrocannabinol increase dopamine release? A SPET study. *J Psychopharmacol* **25**, 1462-1468, doi:10.1177/0269881110382465 (2011).
106 Naef, M., Russmann, S., Petersen-Felix, S. & Brenneisen, R. Development and pharmacokinetic characterization of pulmonal and intravenous delta-9-tetrahydrocannabinol (THC) in humans. *J Pharm Sci* **93**, 1176-1184, doi:10.1002/jps.20037 (2004).
107 Ohlsson, A. *et al.* Plasma delta-9 tetrahydrocannabinol concentrations and clinical effects after oral and intravenous administration and smoking. *Clin Pharmacol Ther* **28**, 409-416, doi:10.1038/clpt.1980.181 (1980).
108 Lindgren, J. E., Ohlsson, A., Agurell, S., Hollister, L. & Gillespie, H. Clinical effects and plasma levels of delta 9-tetrahydrocannabinol (delta 9-THC) in heavy and light users of cannabis. *Psychopharmacology (Berl)* **74**, 208-212, doi:10.1007/BF00427095 (1981).
109 Barnett, G., Chiang, C. W., Perez-Reyes, M. & Owens, S. M. Kinetic study of smoking marijuana. *J Pharmacokinet Biopharm* **10**, 495-506, doi:10.1007/BF01059033 (1982).
110 Perez-Reyes, M., Di Guiseppi, S., Davis, K. H., Schindler, V. H. & Cook, C. E. Comparison of effects of marihuana cigarettes to three different potencies. *Clin Pharmacol Ther* **31**, 617-624, doi:10.1038/clpt.1982.86 (1982).
111 Huestis, M. A., Henningfield, J. E. & Cone, E. J. Blood cannabinoids. I. Absorption of THC and formation of 11-OH-THC and THCCOOH during and after smoking marijuana. *J Anal Toxicol* **16**, 276-282, doi:10.1093/jat/16.5.276 (1992).
112 Kauert, G. F., Ramaekers, J. G., Schneider, E., Moeller, M. R. & Toennes, S. W. Pharmacokinetic properties of delta9-tetrahydrocannabinol in serum and oral fluid. *J Anal Toxicol* **31**, 288-293, doi:10.1093/jat/31.5.288 (2007).
113 Toennes, S. W. *et al.* Influence of ethanol on cannabinoid pharmacokinetic parameters in chronic users. *Anal Bioanal Chem* **400**, 145-152, doi:10.1007/s00216-010-4449-2 (2011).
114 Toennes, S. W., Ramaekers, J. G., Theunissen, E. L., Moeller, M. R. & Kauert, G. F. Comparison of cannabinoid pharmacokinetic properties in occasional and heavy users smoking a marijuana or placebo joint. *J Anal Toxicol* **32**, 470-477, doi:10.1093/jat/32.7.470 (2008).
115 Hunault, C. C. *et al.* Delta-9-tetrahydrocannabinol (THC) serum concentrations and pharmacological effects in males after smoking a combination of tobacco and cannabis containing up to 69 mg THC. *Psychopharmacology (Berl)* **201**, 171-181, doi:10.1007/s00213-008-1260-2 (2008).
116 Schwope, D. M., Karschner, E. L., Gorelick, D. A. & Huestis, M. A. Identification of recent cannabis use: whole-blood and plasma free and glucuronidated cannabinoid pharmacokinetics following controlled smoked cannabis administration. *Clin Chem* **57**, 1406-1414, doi:10.1373/clinchem.2011.171777 (2011).
117 Desrosiers, N. A. *et al.* Phase I and II cannabinoid disposition in blood and plasma of occasional and frequent smokers following controlled smoked cannabis. *Clin Chem* **60**, 631-643, doi:10.1373/clinchem.2013.216507 (2014).
118 Brenneisen, R., Meyer, P., Chtioui, H., Saugy, M. & Kamber, M. Plasma and urine profiles of Delta9-tetrahydrocannabinol and its metabolites 11-hydroxy-Delta9-tetrahydrocannabinol and 11-nor-9-carboxy-Delta9-tetrahydrocannabinol after cannabis

smoking by male volunteers to estimate recent consumption by athletes. *Anal Bioanal Chem* **396**, 2493-2502, doi:10.1007/s00216-009-3431-3 (2010).
119 Cami, J., Guerra, D., Ugena, B., Segura, J. & de la Torre, R. Effect of subject expectancy on the THC intoxication and disposition from smoked hashish cigarettes. *Pharmacol Biochem Behav* **40**, 115-119, doi:10.1016/0091-3057(91)90330-5 (1991).
120 Manno, J. E. *et al.* Temporal indication of marijuana use can be estimated from plasma and urine concentrations of delta9-tetrahydrocannabinol, 11-hydroxy-delta9-tetrahydrocannabinol, and 11-nor-delta9-tetrahydrocannabinol-9-carboxylic acid. *J Anal Toxicol* **25**, 538-549, doi:10.1093/jat/25.7.538 (2001).
121 Huestis, M. A. & Cone, E. J. Relationship of Delta 9-tetrahydrocannabinol concentrations in oral fluid and plasma after controlled administration of smoked cannabis. *J Anal Toxicol* **28**, 394-399, doi:10.1093/jat/28.6.394 (2004).
122 Abrams, D. I. *et al.* Vaporization as a smokeless cannabis delivery system: a pilot study. *Clin Pharmacol Ther* **82**, 572-578, doi:10.1038/sj.clpt.6100200 (2007).
123 Eisenberg, E., Ogintz, M. & Almog, S. The pharmacokinetics, efficacy, safety, and ease of use of a novel portable metered-dose cannabis inhaler in patients with chronic neuropathic pain: a phase 1a study. *J Pain Palliat Care Pharmacother* **28**, 216-225, doi:10.3109/15360288.2014.941130 (2014).
124 Lee, D. *et al.* Plasma Cannabinoid Pharmacokinetics After Controlled Smoking and Ad libitum Cannabis Smoking in Chronic Frequent Users. *J Anal Toxicol* **39**, 580-587, doi:10.1093/jat/bkv082 (2015).
125 Marsot, A. *et al.* Comparison of Cannabinoid Concentrations in Plasma, Oral Fluid and Urine in Occasional Cannabis Smokers After Smoking Cannabis Cigarette. *J Pharm Pharm Sci* **19**, 411-422, doi:10.18433/J3F31D (2016).
126 Hartman, R. L. *et al.* Controlled Cannabis Vaporizer Administration: Blood and Plasma Cannabinoids with and without Alcohol. *Clin Chem* **61**, 850-869, doi:10.1373/clinchem.2015.238287 (2015).
127 Pichini, S. *et al.* Delta9-Tetrahydrocannabinol and Cannabidiol Time Courses in the Sera of "Light Cannabis" Smokers: Discriminating Light Cannabis Use from Illegal and Medical Cannabis Use. *Ther Drug Monit* **42**, 151-156, doi:10.1097/FTD.0000000000000683 (2020).
128 Klumpers, L. E. *et al.* Novel Delta(9) -tetrahydrocannabinol formulation Namisol(R) has beneficial pharmacokinetics and promising pharmacodynamic effects. *Br J Clin Pharmacol* **74**, 42-53, doi:10.1111/j.1365-2125.2012.04164.x (2012).
129 Karschner, E. L., Darwin, W. D., Goodwin, R. S., Wright, S. & Huestis, M. A. Plasma cannabinoid pharmacokinetics following controlled oral delta9-tetrahydrocannabinol and oromucosal cannabis extract administration. *Clin Chem* **57**, 66-75, doi:10.1373/clinchem.2010.152439 (2011).
130 Nadulski, T. *et al.* Randomized, double-blind, placebo-controlled study about the effects of cannabidiol (CBD) on the pharmacokinetics of Delta9-tetrahydrocannabinol (THC) after oral application of THC verses standardized cannabis extract. *Ther Drug Monit* **27**, 799-810, doi:10.1097/01.ftd.0000177223.19294.5c (2005).
131 Lile, J. A., Kelly, T. H., Charnigo, R. J., Stinchcomb, A. L. & Hays, L. R. Pharmacokinetic and pharmacodynamic profile of supratherapeutic oral doses of Delta(9) -THC in cannabis users. *J Clin Pharmacol* **53**, 680-690, doi:10.1002/jcph.90 (2013).
132 Agurell, S. *et al.* Interactions of delta 1-tetrahydrocannabinol with cannabinol and cannabidiol following oral administration in man. Assay of cannabinol and cannabidiol by mass fragmentography. *Experientia* **37**, 1090-1092, doi:10.1007/BF02085029 (1981).
133 Eichler, M. *et al.* Heat exposure of Cannabis sativa extracts affects the pharmacokinetic and metabolic profile in healthy male subjects. *Planta Med* **78**, 686-691, doi:10.1055/s-0031-1298334 (2012).

134 Stott, C. G., White, L., Wright, S., Wilbraham, D. & Guy, G. W. A phase I study to assess the effect of food on the single dose bioavailability of the THC/CBD oromucosal spray. *Eur J Clin Pharmacol* **69**, 825-834, doi:10.1007/s00228-012-1393-4 (2013).
135 Stott, C. G., White, L., Wright, S., Wilbraham, D. & Guy, G. W. A phase I study to assess the single and multiple dose pharmacokinetics of THC/CBD oromucosal spray. *Eur J Clin Pharmacol* **69**, 1135-1147, doi:10.1007/s00228-012-1441-0 (2013).
136 Stott, C., White, L., Wright, S., Wilbraham, D. & Guy, G. A Phase I, open-label, randomized, crossover study in three parallel groups to evaluate the effect of Rifampicin, Ketoconazole, and Omeprazole on the pharmacokinetics of THC/CBD oromucosal spray in healthy volunteers. *Springerplus* **2**, 236, doi:10.1186/2193-1801-2-236 (2013).
137 Ahmed, A. I. *et al.* Safety and pharmacokinetics of oral delta-9-tetrahydrocannabinol in healthy older subjects: a randomized controlled trial. *Eur Neuropsychopharmacol* **24**, 1475-1482, doi:10.1016/j.euroneuro.2014.06.007 (2014).
138 Ahmed, A. I. *et al.* Safety, pharmacodynamics, and pharmacokinetics of multiple oral doses of delta-9-tetrahydrocannabinol in older persons with dementia. *Psychopharmacology (Berl)* **232**, 2587-2595, doi:10.1007/s00213-015-3889-y (2015).
139 de Vries, M., Van Rijckevorsel, D. C., Vissers, K. C., Wilder-Smith, O. H. & Van Goor, H. Single dose delta-9-tetrahydrocannabinol in chronic pancreatitis patients: analgesic efficacy, pharmacokinetics and tolerability. *Br J Clin Pharmacol* **81**, 525-537, doi:10.1111/bcp.12811 (2016).
140 Cherniakov, I. *et al.* Piperine-pro-nanolipospheres as a novel oral delivery system of cannabinoids: Pharmacokinetic evaluation in healthy volunteers in comparison to buccal spray administration. *J Control Release* **266**, 1-7, doi:10.1016/j.jconrel.2017.09.011 (2017).
141 Atsmon, J. *et al.* PTL401, a New Formulation Based on Pro-Nano Dispersion Technology, Improves Oral Cannabinoids Bioavailability in Healthy Volunteers. *J Pharm Sci* **107**, 1423-1429, doi:10.1016/j.xphs.2017.12.020 (2018).
142 Pichini, S. *et al.* Fast and sensitive UHPLC-MS/MS analysis of cannabinoids and their acid precursors in pharmaceutical preparations of medical cannabis and their metabolites in conventional and non-conventional biological matrices of treated individual. *Talanta* **209**, 120537, doi:10.1016/j.talanta.2019.120537 (2020).
143 SAMHSA. Key substance use and mental health indicators in the United States: Results from the 2020 National Survey on Drug Use and Health. *Center for Behavioral Health Statistics and Quality, Substance Abuse and Mental Health Services Administration* **HHS Publication No. PEP21-07-01-003, NSDUH Series H-56** (2021).
144 Amin, M. R. & Ali, D. W. Pharmacology of Medical Cannabis. *Adv Exp Med Biol* **1162**, 151-165, doi:10.1007/978-3-030-21737-2_8 (2019).
145 Grotenhermen, F. Pharmacokinetics and pharmacodynamics of cannabinoids. *Clin Pharmacokinet* **42**, 327-360, doi:10.2165/00003088-200342040-00003 (2003).
146 Lucas, C. J., Galettis, P. & Schneider, J. The pharmacokinetics and the pharmacodynamics of cannabinoids. *Br J Clin Pharmacol* **84**, 2477-2482, doi:10.1111/bcp.13710 (2018).
147 Hukkanen, J., Pelkonen, O. & Raunio, H. Expression of xenobiotic-metabolizing enzymes in human pulmonary tissue: possible role in susceptibility for ILD. *Eur Respir J Suppl* **32**, 122s-126s (2001).
148 Drozdzik, M. *et al.* Protein Abundance of Clinically Relevant Drug-Metabolizing Enzymes in the Human Liver and Intestine: A Comparative Analysis in Paired Tissue Specimens. *Clin Pharmacol Ther* **104**, 515-524, doi:10.1002/cpt.967 (2018).
149 Zhang, Z. *et al.* Development of a Novel Maternal-Fetal Physiologically Based Pharmacokinetic Model I: Insights into Factors that Determine Fetal Drug Exposure

through Simulations and Sensitivity Analyses. *Drug Metab Dispos* **45**, 920-938, doi:10.1124/dmd.117.075192 (2017).
150 Hakkola, J., Pelkonen, O., Pasanen, M. & Raunio, H. Xenobiotic-metabolizing cytochrome P450 enzymes in the human feto-placental unit: role in intrauterine toxicity. *Crit Rev Toxicol* **28**, 35-72, doi:10.1080/10408449891344173 (1998).
151 Smith, G. B. *et al.* Human lung microsomal cytochrome P4501A1 (CYP1A1) activities: impact of smoking status and CYP1A1, aryl hydrocarbon receptor, and glutathione S-transferase M1 genetic polymorphisms. *Cancer Epidemiol Biomarkers Prev* **10**, 839-853 (2001).
152 Eagling, V. A., Tjia, J. F. & Back, D. J. Differential selectivity of cytochrome P450 inhibitors against probe substrates in human and rat liver microsomes. *Br J Clin Pharmacol* **45**, 107-114, doi:10.1046/j.1365-2125.1998.00679.x (1998).
153 Khojasteh, S. C., Prabhu, S., Kenny, J. R., Halladay, J. S. & Lu, A. Y. Chemical inhibitors of cytochrome P450 isoforms in human liver microsomes: a re-evaluation of P450 isoform selectivity. *Eur J Drug Metab Pharmacokinet* **36**, 1-16, doi:10.1007/s13318-011-0024-2 (2011).
154 Niwa, T., Shiraga, T. & Takagi, A. Effect of antifungal drugs on cytochrome P450 (CYP) 2C9, CYP2C19, and CYP3A4 activities in human liver microsomes. *Biol Pharm Bull* **28**, 1805-1808, doi:10.1248/bpb.28.1805 (2005).
155 Sai, Y. *et al.* Assessment of specificity of eight chemical inhibitors using cDNA-expressed cytochromes P450. *Xenobiotica* **30**, 327-343, doi:10.1080/004982500237541 (2000).
156 Cho, H. J., Kim, J. E., Kim, D. D. & Yoon, I. S. In vitro-in vivo extrapolation (IVIVE) for predicting human intestinal absorption and first-pass elimination of drugs: principles and applications. *Drug Dev Ind Pharm* **40**, 989-998, doi:10.3109/03639045.2013.831439 (2014).
157 Hatley, O. J., Jones, C. R., Galetin, A. & Rostami-Hodjegan, A. Quantifying gut wall metabolism: methodology matters. *Biopharm Drug Dispos* **38**, 155-160, doi:10.1002/bdd.2062 (2017).
158 Paine, M. F. *et al.* The human intestinal cytochrome P450 "pie". *Drug Metab Dispos* **34**, 880-886, doi:10.1124/dmd.105.008672 (2006).
159 Galetin, A. & Houston, J. B. Intestinal and hepatic metabolic activity of five cytochrome P450 enzymes: impact on prediction of first-pass metabolism. *J Pharmacol Exp Ther* **318**, 1220-1229, doi:10.1124/jpet.106.106013 (2006).
160 Davies, M. *et al.* Evaluation of In Vitro Models for Assessment of Human Intestinal Metabolism in Drug Discovery. *Drug Metab Dispos* **48**, 1169-1182, doi:10.1124/dmd.120.000111 (2020).
161 Wu, B., Kulkarni, K., Basu, S., Zhang, S. & Hu, M. First-pass metabolism via UDP-glucuronosyltransferase: a barrier to oral bioavailability of phenolics. *J Pharm Sci* **100**, 3655-3681, doi:10.1002/jps.22568 (2011).
162 Shimada, T., Yamazaki, H., Mimura, M., Inui, Y. & Guengerich, F. P. Interindividual variations in human liver cytochrome P-450 enzymes involved in the oxidation of drugs, carcinogens and toxic chemicals: studies with liver microsomes of 30 Japanese and 30 Caucasians. *J Pharmacol Exp Ther* **270**, 414-423 (1994).
163 Suter, M. *et al.* In utero tobacco exposure epigenetically modifies placental CYP1A1 expression. *Metabolism* **59**, 1481-1490, doi:10.1016/j.metabol.2010.01.013 (2010).
164 Enlo-Scott, Z., Backstrom, E., Mudway, I. & Forbes, B. Drug metabolism in the lungs: opportunities for optimising inhaled medicines. *Expert Opin Drug Metab Toxicol* **17**, 611-625, doi:10.1080/17425255.2021.1908262 (2021).
165 Mamiya, K. *et al.* The effects of genetic polymorphisms of CYP2C9 and CYP2C19 on phenytoin metabolism in Japanese adult patients with epilepsy: studies in

stereoselective hydroxylation and population pharmacokinetics. *Epilepsia* **39**, 1317-1323, doi:10.1111/j.1528-1157.1998.tb01330.x (1998).
166 Marchand, G. *et al.* Birth Outcomes of Neonates Exposed to Marijuana in Utero: A Systematic Review and Meta-analysis. *JAMA Netw Open* **5**, e2145653, doi:10.1001/jamanetworkopen.2021.45653 (2022).
167 Wang, H. *et al.* Fatty acid amide hydrolase deficiency limits early pregnancy events. *J Clin Invest* **116**, 2122-2131, doi:10.1172/JCI28621 (2006).
168 Villazana-Kretzer, D. L. *et al.* ZIKV can infect human term placentas in the absence of maternal factors. *Commun Biol* **5**, 243, doi:10.1038/s42003-022-03158-6 (2022).
169 Reed, L. C., Estrada, S. M., Walton, R. B., Napolitano, P. G. & Ieronimakis, N. Evaluating maternal hyperglycemic exposure and fetal placental arterial dysfunction in a dual cotyledon, dual perfusion model. *Placenta* **69**, 109-116, doi:10.1016/j.placenta.2018.07.015 (2018).
170 Walton, R. B. *et al.* Evaluation of Sildenafil and Tadalafil for Reversing Constriction of Fetal Arteries in a Human Placenta Perfusion Model. *Hypertension* **72**, 167-176, doi:10.1161/HYPERTENSIONAHA.117.10738 (2018).
171 Rahi, M. *et al.* Influence of adenosine triphosphate and ABCB1 (MDR1) genotype on the P-glycoprotein-dependent transfer of saquinavir in the dually perfused human placenta. *Hum Exp Toxicol* **27**, 65-71, doi:10.1177/0960327108088971 (2008).
172 Molsa, M. *et al.* Functional role of P-glycoprotein in the human blood-placental barrier. *Clin Pharmacol Ther* **78**, 123-131, doi:10.1016/j.clpt.2005.04.014 (2005).
173 Sudhakaran, S. *et al.* Differential bidirectional transfer of indinavir in the isolated perfused human placenta. *Antimicrob Agents Chemother* **49**, 1023-1028, doi:10.1128/AAC.49.3.1023-1028.2005 (2005).
174 Biotechnology, S. SOLVO introducing PSC 833 the specific P-gp inhibitor and new drug transporter services. (2009).
175 Genentech. Invirase (saquinavir mesylate) [package insert]. South San Francisco, CA (2012).
176 Panti, A. A., Ekele, B. A., Nwobodo, E. I. & Yakubu, A. The relationship between the weight of the placenta and birth weight of the neonate in a Nigerian Hospital. *Niger Med J* **53**, 80-84, doi:10.4103/0300-1652.103547 (2012).
177 Rahi, M. M., Heikkinen, T. M., Hakala, K. E. & Laine, K. P. The effect of probenecid and MK-571 on the feto-maternal transfer of saquinavir in dually perfused human term placenta. *Eur J Pharm Sci* **37**, 588-592, doi:10.1016/j.ejps.2009.05.005 (2009).
178 Forestier, F. *et al.* Maternal-fetal transfer of saquinavir studied in the ex vivo placental perfusion model. *Am J Obstet Gynecol* **185**, 178-181, doi:10.1067/mob.2001.113319 (2001).
179 Woodahl, E. L., Yang, Z., Bui, T., Shen, D. D. & Ho, R. J. MDR1 G1199A polymorphism alters permeability of HIV protease inhibitors across P-glycoprotein-expressing epithelial cells. *AIDS* **19**, 1617-1625, doi:10.1097/01.aids.0000183626.74299.77 (2005).
180 Collett, A., Tanianis-Hughes, J., Hallifax, D. & Warhurst, G. Predicting P-glycoprotein effects on oral absorption: correlation of transport in Caco-2 with drug pharmacokinetics in wild-type and mdr1a(-/-) mice in vivo. *Pharm Res* **21**, 819-826, doi:10.1023/b:pham.0000026434.82855.69 (2004).
181 Gupta, A., Zhang, Y., Unadkat, J. D. & Mao, Q. HIV protease inhibitors are inhibitors but not substrates of the human breast cancer resistance protein (BCRP/ABCG2). *J Pharmacol Exp Ther* **310**, 334-341, doi:10.1124/jpet.104.065342 (2004).
182 Hollister, L. E. *et al.* Do plasma concentrations of delta 9-tetrahydrocannabinol reflect the degree of intoxication? *J Clin Pharmacol* **21**, 171S-177S, doi:10.1002/j.1552-4604.1981.tb02593.x (1981).

183 Volk, C. OCTs, OATs, and OCTNs: structure and function of the polyspecific organic ion transporters of the SLC22 family. *Wiley Interdisciplinary Reviews: Membrane Transport and Signaling* **3**, 1-13, doi:https://doi.org/10.1002/wmts.100 (2014).
184 Zolnerciks, J. K., Booth-Genthe, C. L., Gupta, A., Harris, J. & Unadkat, J. D. Substrate- and species-dependent inhibition of P-glycoprotein-mediated transport: implications for predicting in vivo drug interactions. *J Pharm Sci* **100**, 3055-3061, doi:10.1002/jps.22566 (2011).
185 Breuil, L. *et al.* Comparative vulnerability of PET radioligands to partial inhibition of P-glycoprotein at the blood-brain barrier: A criterion of choice? *J Cereb Blood Flow Metab* **42**, 175-185, doi:10.1177/0271678X211045444 (2022).
186 Breuil, L. *et al.* Comparison of the Blood-Brain Barrier Transport and Vulnerability to P-Glycoprotein-Mediated Drug-Drug Interaction of Domperidone versus Metoclopramide Assessed Using In Vitro Assay and PET Imaging. *Pharmaceutics* **14**, 1658 (2022).
187 Jansen, C. *et al.* Development of placental abnormalities in location and anatomy. *Acta Obstet Gynecol Scand* **99**, 983-993, doi:10.1111/aogs.13834 (2020).
188 Balhara, A., Kumar, A. R. & Unadkat, J. D. Predicting Human Fetal Drug Exposure Through Maternal-Fetal PBPK Modeling and In Vitro or Ex Vivo Studies. *J Clin Pharmacol* **62 Suppl 1**, S94-S114, doi:10.1002/jcph.2117 (2022).
189 Kilby, M. D., Neary, R. H., Mackness, M. I. & Durrington, P. N. Fetal and maternal lipoprotein metabolism in human pregnancy complicated by type I diabetes mellitus. *J Clin Endocrinol Metab* **83**, 1736-1741, doi:10.1210/jcem.83.5.4783 (1998).
190 Anoshchenko, O., Storelli, F. & Unadkat, J. D. Successful Prediction of Human Fetal Exposure to P-Glycoprotein Substrate Drugs Using the Proteomics-Informed Relative Expression Factor Approach and PBPK Modeling and Simulation. *Drug Metab Dispos* **49**, 919-928, doi:10.1124/dmd.121.000538 (2021).
191 Zhang, Z. & Unadkat, J. D. Development of a Novel Maternal-Fetal Physiologically Based Pharmacokinetic Model II: Verification of the model for passive placental permeability drugs. *Drug Metab Dispos* **45**, 939-946, doi:10.1124/dmd.116.073957 (2017).
192 Shum, S., Shen, D. D. & Isoherranen, N. Predicting Maternal-Fetal Disposition of Fentanyl Following Intravenous and Epidural Administration Using Physiologically Based Pharmacokinetic Modeling. *Drug Metab Dispos* **49**, 1003-1015, doi:10.1124/dmd.121.000612 (2021).
193 Mathias, A. A., Hitti, J. & Unadkat, J. D. P-glycoprotein and breast cancer resistance protein expression in human placentae of various gestational ages. *Am J Physiol Regul Integr Comp Physiol* **289**, R963-969, doi:10.1152/ajpregu.00173.2005 (2005).
194 Awasthi, R., An, G., Donovan, M. D. & Boles Ponto, L. L. Relating Observed Psychoactive Effects to the Plasma Concentrations of Delta-9-Tetrahydrocannabinol and Its Active Metabolite: An Effect-Compartment Modeling Approach. *J Pharm Sci* **107**, 745-755, doi:10.1016/j.xphs.2017.09.009 (2018).
195 Wolowich, W. R., Greif, R., Kleine-Brueggeney, M., Bernhard, W. & Theiler, L. Minimal Physiologically Based Pharmacokinetic Model of Intravenously and Orally Administered Delta-9-Tetrahydrocannabinol in Healthy Volunteers. *Eur J Drug Metab Pharmacokinet* **44**, 691-711, doi:10.1007/s13318-019-00559-7 (2019).
196 Methaneethorn, J., Poomsaidorn, C., Naosang, K., Kaewworasut, P. & Lohitnavy, M. A Delta(9)-Tetrahydrocannabinol Physiologically-Based Pharmacokinetic Model Development in Humans. *Eur J Drug Metab Pharmacokinet* **45**, 495-511, doi:10.1007/s13318-020-00617-5 (2020).
197 Patilea-Vrana, G. I. & Unadkat, J. D. Development and Verification of a Linked Delta (9)-THC/11-OH-THC Physiologically Based Pharmacokinetic Model in Healthy,

Nonpregnant Population and Extrapolation to Pregnant Women. *Drug Metab Dispos* **49**, 509-520, doi:10.1124/dmd.120.000322 (2021).
198 Zhu, L. *et al.* Physiologically-based pharmacokinetic model for predicting blood and tissue tetrahydrocannabinol concentrations. *Comput Chem Eng* **154**, doi:10.1016/j.compchemeng.2021.107461 (2021).
199 Withey, S. L., Bergman, J., Huestis, M. A., George, S. R. & Madras, B. K. THC and CBD blood and brain concentrations following daily administration to adolescent primates. *Drug Alcohol Depend* **213**, 108129, doi:10.1016/j.drugalcdep.2020.108129 (2020).
200 Rodgers, T. & Rowland, M. Physiologically based pharmacokinetic modelling 2: predicting the tissue distribution of acids, very weak bases, neutrals and zwitterions. *J Pharm Sci* **95**, 1238-1257, doi:10.1002/jps.20502 (2006).
201 Bansal, S., Ladumor, M. K., Paine, M. F. & Unadkat, J. D. A Physiologically-Based Pharmacokinetic Model for Cannabidiol in Healthy Adults, Hepatically-Impaired Adults, and Children. *Drug Metab Dispos* **51**, 743-752, doi:10.1124/dmd.122.001128 (2023).
202 Abduljalil, K., Cain, T., Humphries, H. & Rostami-Hodjegan, A. Deciding on success criteria for predictability of pharmacokinetic parameters from in vitro studies: an analysis based on in vivo observations. *Drug Metab Dispos* **42**, 1478-1484, doi:10.1124/dmd.114.058099 (2014).
203 Wayson, M. B. *et al.* Suggested reference values for regional blood volumes in children and adolescents. *Phys Med Biol* **63**, 155022, doi:10.1088/1361-6560/aad313 (2018).
204 Guest, E. J., Aarons, L., Houston, J. B., Rostami-Hodjegan, A. & Galetin, A. Critique of the two-fold measure of prediction success for ratios: application for the assessment of drug-drug interactions. *Drug Metab Dispos* **39**, 170-173, doi:10.1124/dmd.110.036103 (2011).
205 Goasdoue, K., Miller, S. M., Colditz, P. B. & Bjorkman, S. T. Review: The blood-brain barrier; protecting the developing fetal brain. *Placenta* **54**, 111-116, doi:10.1016/j.placenta.2016.12.005 (2017).
206 Robson, S. C., Mutch, E., Boys, R. J. & Woodhouse, K. W. Apparent liver blood flow during pregnancy: a serial study using indocyanine green clearance. *Br J Obstet Gynaecol* **97**, 720-724, doi:10.1111/j.1471-0528.1990.tb16246.x (1990).
207 Munnell, E. W. & Taylor, H. C. Liver Blood Flow in Pregnancy-Hepatic Vein Catheterization. *J Clin Invest* **26**, 952-956, doi:10.1172/JCI101890 (1947).
208 Ersch, J. & Stallmach, T. Assessing gestational age from histology of fetal skin: an autopsy study of 379 fetuses. *Obstet Gynecol* **94**, 753-757, doi:10.1016/s0029-7844(99)00379-8 (1999).